Quantitative Modeling of the Molecular Mechanism Controlling the Asymmetric Cell Division Cycle in *Caulobacter crescentus*

Shenghua Li

Dissertation submitted to the faculty of the Virginia Polytechnic Institute and State University in partial fulfillment of the requirements for the degree of

Doctor of Philosophy
In
Genetics, Bioinformatics and Computational Biology

John Tyson, Chair
Paul Brazhnik
Bruno Sobral
Zhaomin Yang
Reinhard Laubenbacher

October 24th, 2008
Blacksburg, Virginia

Keywords: Mathematical modeling, *Caulobacter crescentus*, protein network, cell cycle

Quantitative Modeling of the Molecular Mechanism Controlling the Asymmetric Cell Division Cycle in *Caulobacter crescentus*

Shenghua Li

ABSTRACT

Caulobacter crescentus is an important model organism for studying regulation of cell growth, division and differentiation in prokaryotes. *C. crescentus* undergoes asymmetric division producing two progeny cells with identical genome but different developmental programs: the "swarmer" cell is flagellated and motile, and the "stalked" cell is sessile (attached to a surface by its stalk and holdfast). Only stalked cells undergo chromosome replication and cell division. A swarmer cell must shed its flagellum and grow a stalk before it can enter the replication-division cycle. Based on published experimental evidence, we propose a molecular mechanism controlling the cell division cycle in this bacterium. Our quantitative model of the mechanism illustrates detailed temporal dynamics of regulatory proteins and corresponding physiological changes during the process of cell cycle progression and differentiation of wild-type cells (both stalked cells and swarmer cells) and of a number of known and novel mutant strains. Our model presents a unified view of temporal regulation of protein activities during the asymmetric cell division cycle of *C. crescentus* and provides an opportunity to study and analyze the system dynamics of the *Caulobacter* cell cycle (as opposed to the dynamics of individual steps). The model can serve as a starting point for investigating molecular regulations of cell division and differentiation in other genera of alpha-proteobacteria, such as *Brucella* and *Rhizobium*, because recent experimental data suggest that these alpha-proteobacteria share similar genetic mechanisms for cell cycle control.

Acknowledgements

I would like to thank my advisors, Drs. John Tyson and Paul Brazhnik, for introducing me to a research in the field of computational cell biology. I appreciate their continuous guidance, patience, and encouragement.

I am grateful to all my colleagues in Drs. Tyson's and Sobral's labs for working with me, providing supportive audience, correcting my errors and carelessness throughout my research. Moreover, we all enjoyed the wonderful moments spent together all these years in Blacksburg. Thanks as well for helping me to get through the hard times we met in the past years. I would like to express my gratitude to all the members of my dissertation committee for their interest in my project and for guiding me to its completion.

I also want to express my appreciation to John's, Kathy's, and Julu's families for their kind help to me and my wife that let us live more smoothly in this little town and in the US.

Last but not least, I am grateful to the booming Chinese economy, which makes it possible for me to travel and study around this wonderful international world.

This dissertation is dedicated first and foremost to my wife, Aihua Li, and also, to my parents, sisters and brothers. They always asked me over the phone again and again how long I still have to study and when I will finish my degree. I can probably say this time I am finally done.

This dissertation is based on the following written works:

1. Brazhnik, P., Li, S., Sobral, B., and Tyson, J.J. (2007). Computational Model of the Division Cycle of *Caulobacter crescentus*. AIP Conference Proceedings *952*, 219-228.
2. Li, S., Brazhnik, P., Sobral, B., and Tyson, J.J. (2008). A quantitative study of the division cycle of *Caulobacter crescentus* stalked cells. PLoS Comput Biol *4*, e9.
3. Li, S., Brazhnik, P., Sobral, B., and Tyson, J.J. (2008). Temporal Controls of the Asymmetric Cell Division Cycle in Caulobacter crescentus. PLoS Comput Biol, *in submission.*
4. *RESEARCH PROSPECTUS* : Kinetic Analysis of a Mechanism for Cell Division Cycle Regulation in *Caulobacter crescentus*: Quantitative Modeling and its Extension in *Sinorhizobium meliloti.*
5. Grant proposal: Proposal for Cell Cycle Regulation in *Sinorhizobium.* (draft)

and conference and other presentations:

1. Li S., Brazhnik P., Sobral B., Tyson J.J. "Dynamics of Molecular Regulations of the Asymmetric Cell Division Cycle in *Caulobacter crescentus*." *Systems Biology of Human Disease*, Harvard Medical School, Boston, MA (June 12-13, 2008).

2. Li S., Brazhnik P., Sobral B., Tyson J.J. "Temporal control of the asymmetric cell division of *Caulobacter crescentus*." *Frontiers in Applied and Computational Mathematics*, NJIT, NJ (May 19-21, 2008).
3. Li S., Brazhnik P., Sobral B., Tyson J.J. "Integrated dynamics of temporal controls in the cell division cycle of *Caulobacter crescentus*." *Department of Biological Science's Annual Research Day*, Virginia Tech, Blacksburg, VA (February 23, 2008).
4. Li S., Brazhnik P., Sobral B., Tyson J.J. "*In silico* Model of the Division Cycle of *Caulobacter crescentus*." *The 2nd Annual Research Symposium of VBI*, Pembroke, VA (September 22, 2007).
5. Li S., Brazhnik P., Sobral B., Tyson J.J. "Quantitative Modeling of the Asymmetric Cell Division Cycle in *Caulobacter crescentus*." *CSHL Conference on Computational Cell Biology*, Cold Spring Harbor, NY (March 6-9, 2007).
6. Li S., Brazhnik P., Tyson J.J. "Kinetic analysis of the mechanism of the cell division cycle in Caulobacter cresentus." *Joint SMB-SIAM Conference on the LifeSciences*, Raleigh, NC (July 31-August 4, 2006).
7. Li S., Brazhnik P., Sobral B., Tyson J.J. "Mathematical modeling of the cell division cycle in *Caulobacter crescentus*." *22nd Annual Research Symposium and Exposition, GSA*, Virginia Tech, Blacksburg, VA (March 29, 2006).

Table of Contents

List of Figures

List of Tables

Chapter 1. Introduction

1.1. The cell division cycle in *Caulobacter crescentus*

The family of alpha-proteobacteria, which is identified based on 16S rRNA similarity (Williams et al., 2007), is a large and diverse group of Gram-negative microorganisms. These bacteria show huge variability in metabolic capacity, morphology, life cycle and diverse ecological niches (Batut et al., 2004). Many members of the family are economically important mutualistic and pathogenic symbionts, such as *Brucella melitensis*, *Richettsia prowazekii*, *Sinorhizobium meliloti*, etc (Batut et al., 2004; Brun and Shimkets, 2000).

Caulobacter crescentus (Figure 1), which also belongs to the family of alpha-proteobacteria, is a dimorphic bacterium which inhabits freshwater, soils and seawater, where it plays an important role in global carbon cycling by mineralizing dissolved organic materials (Poindexter and Hagenzieker, 1981). Recently the bacterium has been engineered to detect heavy metals in water, which may be promising for its industrial and environmental applications (Hillson et al.). Also, *Caulobacter* has been recently detected as a human pathogen, which makes it directly related to human health (Justesen et al., 2007).

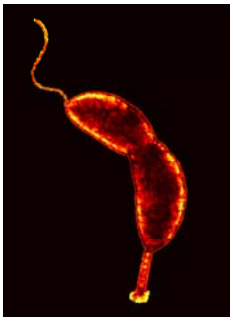

Figure 1. Dividing cell of the *C. crescentus*.
The mother stalked cell is at the bottom, the daughter flagellated cell is at the top. (Transmission electron microscopy **(**TEM) of *C. crescentus* CB15, pseudocolored using NIH Image, courtesy of Dr. Yves Brun at Indiana University).

Among the family of alpha-proteobacteria, *C. crescentus* is easy and relatively safe to manipulate in the laboratory. (Ausmees and Jacobs-Wagner, 2003; Ryan and Shapiro, 2003) Furthermore, its different cell cycle phases can be easily distinguished using microscopy or centrifuge through the different morphologies. Therefore, it has become a model organism to investigate cell cycle regulation in alpha-proteobacteria. Availabity of the genome information (Nierman et al., 2001), microarray data (Laub et al., 2002; Laub et al., 2000) and proteomic data (Grunenfelder et al., 2001) for *Caulobacter* provide a foundation for deciphering molecular mechanisms regulating cellular processes, in particular progression of the bacterium through the division cycle.

In *C. crescentus*, only a cell with a stalk is able to replicate its DNA and divide into two progeny cells (Figure.2). The stalked cell division cycle (~120 min, S phase + G2/M phase) consists of DNA replication, Z-ring assembly in the mid-cell plane, new flagellum production at the opposite-to-the-stalk cell pole of a predivisional cell, and cell division. A swarmer cell, which can swim in the water with its flagellum, grows and differentiates into a stalked cell (~30 min) under favorable nutrient conditions. The swarmer-to-stalked cell differentiation (G1-like phase) includes shedding the flagellum and producing a stalk at the same cell pole. At the end of cell differentiation, DNA replication is also initiated.

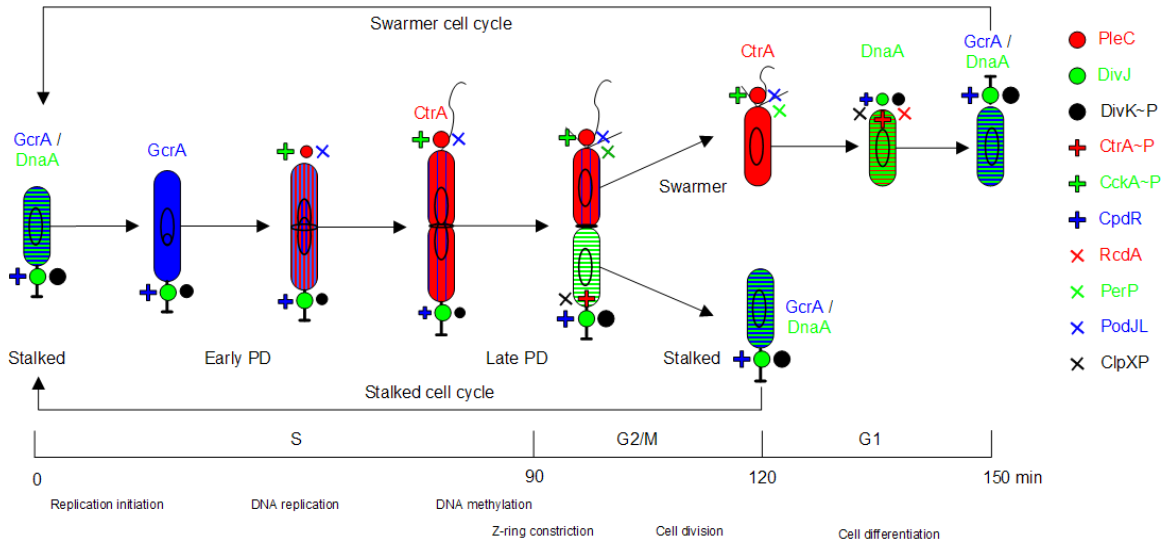

Figure 2. Physiology of the cell division cycle in *C. crescentus*.

The color scheme indicates protein variations through the cell division cycle: GcrA (blue), CtrA (red), DnaA (green). The θ-like structure denotes replicating DNA. The ring in the middle of the cell shows the Z-ring assembly and constriction needed for cell separation (cytokinesis). Protein localization and distribution: the fill-colors indicate elevated concentrations of proteins whose name are written in corresponding colors. Symbols at poles indicate localized proteins, the legend for which is shown on the right.

Of *C. crescentus*'s 3763 protein-coding genes, about 550 are regulated in a cell-cycle-dependent manner (Laub et al., 2000), in large part by three regulatory proteins: CtrA, GcrA and DnaA (red, blue and green color schemes in Figure 2), which together control the expression of about 1/3 cell-cycle regulated genes (Collier et al., 2006; Collier and Shapiro, 2007; Laub et al., 2002; Milo et al., 2002). The three so called "master-regulators" control each other's activities so that the downstream genes they regulate are expressed timely in order to guide the cell through the G1/S transition, DNA replication, cytokinesis and other relevant cellular events (Figure 2).

1.2. Mathematical modeling of cell cycle

The cell division cycle is a complex and dynamical process controlled by the coordinated action of many proteins (and some other physiological events) forming the cell cycle regulatory network (McAdams and Arkin, 1998; Tyson et al., 2001). This biochemical network consists of parallel and consecutive, highly nonlinear processes, comprising positive and negative feedbacks. Verbal, handwaving arguments about simple subnetworks become inefficient or fail when dealing with such complexity. A disciplined mathematical approach empowered by computers (McAdams and Arkin, 1998; Tyson et al., 2001) is the only way to deal rigorously with the complexity of molecular regulatory networks in a cell.

Due to their fundamental importance, the protein interaction networks regulating the cell division cycle have been intensively studied genetically and biochemically. The mechanism of the cell cycle 'engine' is best known for budding yeast and fission yeast. Theoreticians (Chen et al., 2004; Sveiczer et al., 2004) have created comprehensive, quantitative (mathematical) models that reproduce a large amount of experimental data and productively guide further experimental studies (Cross et al., 2002; Cross et al., 2005; Thornton et al., 2004). Considerable progress has also been made in modeling cell cycle controls in frog eggs (Ciliberto et al., 2003; Pomerening et al., 2005; Sha et al., 2003; Sible and Tyson, 2007). Recently, models of mammalian cell cycle controls have been constructed (Novak and Tyson, 2004; Qu et al., 2003; Swat et al., 2004), based on a comparative analysis of the homologous genetic networks operating in yeast cells and mammalian cells (Kohn and Pommier, 2005).

1.3. Why *Caulobacter crescentus*?

Compared to yeast, frog eggs and mammalian cells, progress in understanding cell cycle regulation in bacteria has lagged behind. But recent experimental advances have pinpointed crucial proteins (CtrA, DnaA and GcrA) regulating cell cycle events in the alpha-proteobacterium *Caulobacter crescentus* (Holtzendorff et al., 2006). These advances allow us to propose reasonable mechanisms and mathematical models for the division and differentiation of *Caulobacter* cells.

C. crescentus also became favorable among other prokaryotes due to the following factors:

1) *C. crescentus* plays a fundamental role digesting small pieces of material in water and recycling global carbon (Poindexter and Hagenzieker, 1981).

2) *C. crescentus* can be engineered to detect toxic levels of bioavailable uranium (Hillson et al., 2007).

3) *C. crescentus* infects human as a pathogen which was first discovered from the dialysis of a patient undergoing peritoneal dialysis (Justesen et al., 2007).

4) Since *Caulobacter* shares conserved homologs of cell cycle-related genes and proteins among many species of alpha-proteobacteria (Hallez et al., 2004), the research methods and results from *C. crescentus*, as a model organism for cell cycle control, can be applicable to other more economically important species of alpha-proteobacteria such as *Brucella*, *Rhizobium*, *Rechettisa*, etc.

5) Within the last decades, a lot of genes, involved in the cell cycle control in *C. crescentus* have been identified (Ausmees and Jacobs-Wagner, 2003; Brun and Shimkets,

2000; Ryan and Shapiro, 2003). In addition, high throughput data (genomics (Nierman et al., 2001), microarray data (Laub et al., 2002; Laub et al., 2000) and proteomics data (Grunenfelder et al., 2001)) have become available.

6) The first, quantitative analysis of molecular factors regulating the cell division cycle in *C. crescentus* was published recently by Brazhnik and Tyson (Brazhnik and Tyson, 2006). They proposed a CtrA-based bistable 'switch' to address the dynamics of cell cycle control in *C. crescentus*. That master-regulator 'switch' controlling the level of CtrA protein can be thought of in this case as a simplified version of the CDK/cyclin bistable system driving cell cycle transitions in yeast. (See Section 2.2.1 for a more detailed summary). Since this first proposition, more experimental data related to cell cycle regulation in *C. crescentus* have been released (Biondi et al., 2006; Chen and Stephens, 2007; Collier and Shapiro, 2007; Goley et al., 2007). All these new data make it an opportune time point to use mathematical modeling methods (Sible and Tyson, 2007) to investigate the complexity of temporal dynamics of cell cycle controls in *C. crescentus*, and to interpret relevant physiological events in a unified quantitative scheme.

1.4. What will be found in this thesis?

Using mathematical methods (wiring diagram, ODEs, bifurcation analysis, numerical simulation, etc) (Sible and Tyson, 2007; Tyson et al., 2001), the verbal description of cell cycle regulation in the literature will be summarized and cast into quantitative models, then the dynamics of cell cycle control and other relevant cellular behavior are systematically interpreted within the models. From there, implications and predictions from the models are presented to be able to guide experimental design in *C. crescentus*,

as well as in other species of alpha-proteobacteria. These are the major aspects of this research.

Chapter 2 describes how we build the models based on experimental facts using a bottom-up strategy. Step by step, we develop a model that addresses all the major features of the consensus picture of the cell division cycle of *C. crescentus*. In chapter 3, several improvements of the model are introduced based on newly published experimental data. The newer version offers more details about the underlying regulation for the asymmetric cell division cycle in *C. crescentus.* To accompany the model, an interactive web site and an online simulator are constructed for convenient communication among researchers (presented in chapter 4). Building on our understanding of cell cycle control in *C. crescentus*, in chapter 5 we describe how to extend our investigation to cell cycle control of another species of alpha-proteobacteria, *Sinorhizobium meliloti* (in collaboration with Dr. Sobral's group). Finally, chapter 6 contains some closing comments and conclusions.

Chapter 2. Quantitative modeling of the molecular mechanism regulating the cell division cycle of *C. crescentus*

2.1. A consensus picture of the cell cycle in *C. crescentus*

Essential elements involved in the cell division cycle regulation in *Caulobacter crescentus* are depicted in Figure 3. Specifics of molecular interactions among the genes and proteins in the figure are summarized below.

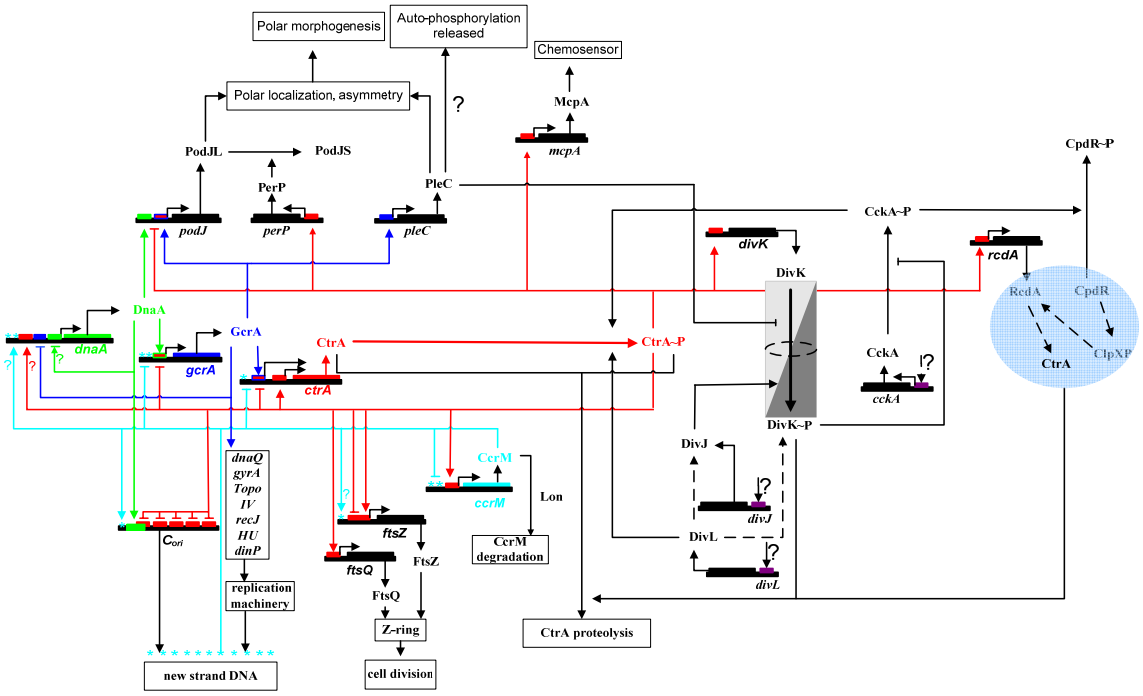

Figure 3. The regulatory network of the cell division cycle control in *C. crescentus*.

2.1.1. CtrA, GcrA and DnaA: master regulatory proteins

C. crescentus has 3,763 protein-encoding genes (Nierman et al., 2001), of which 553 are cell-cycle regulated (Laub et al., 2000). Three master-regulator proteins control directly expressions of about 1/3 of cell-cycle regulated genes in this bacterium (Collier et al., 2006; Collier and Shapiro, 2007; Holtzendorff et al., 2006; Laub et al., 2002; Milo et al., 2002). The transcription factor CtrA directly regulates 95 genes (including *divK, ccrM, gcrA, dnaA, podJ, pleC, ftsZ, ftsQ*) (Domian et al., 1996; Laub et al., 2002), while GcrA controls 49 genes (*ctrA*, *dnaA*, *podJ*, *pleC*, etc) (Holtzendorff et al., 2004; Laub et al., 2002; Laub et al., 2000). The DnaA protein, which is involved in the control of DNA initiation, also functions as a transcription factor to regulate about 40 gene expressions (including *gcrA, pleC, podJ, ftsZ, dnaA itself, etc)* (Collier et al., 2007; Collier and Shapiro, 2007; Hottes et al., 2005).

Variations of CtrA during the cell cycle are elaborately regulated through protein synthesis, phosphorylation and proteolysis (Ausmees and Jacobs-Wagner, 2003; Ryan and Shapiro, 2003). Expression of *ctrA* is under control of two promoters, *ctrA-P1* and *ctrA-P2* (Domian et al., 1996, 1997; Domian et al., 1999). The weaker *ctrA-P1* promoter is activated in the early stalked cell (~35 minutes after the initiation of DNA replication) (Reisenauer and Shapiro, 2002; Stephens et al., 1996) by the GcrA protein (Holtzendorff et al., 2004) and inhibited by high levels of a phosphorylated form of CtrA, CtrA~P (Domian et al., 1999). The stronger *ctrA-P2* promoter is activated later, in predivisional cells, by CtrA~P (Domian et al., 1999). In addition, the *ctrA-P1* promoter is only activated from a new strand of hemimethylated DNA (Domian et al., 1996; Reisenauer

and Shapiro, 2002). The *ctrA-P2* promoter is not active in swarmer cells, even though these cells have high levels of CtrA (Domian et al., 1999). Furthermore, expression from *ctrA-P2* is inhibited in predivisional cells by conditions that inhibit DNA replication (Wortinger et al., 2000). These facts indicate that *ctrA-P2* has regulators for its activity other than CtrA itself (Domian et al., 1999).

CtrA is active when phosphorylated (Jacobs et al., 2003; Quon et al., 1996), a reaction carried out by a histidine kinase, CckA~P (Biondi et al., 2006; Jacobs et al., 2003; Jacobs et al., 1999). The total CckA level is pretty stable throughout the cell cycle (Jacobs et al., 1999). However, CckA is localized and phosphorylated, and CckA~P concentration correlates tightly with CtrA~P (they show a similar pattern of variation during the cell cycle (Jacobs et al., 2003; Jenal, 2000)). In addition, CckA activates CpdR phosphorylation and affects its localization, which indirectly represses CtrA degradation (Biondi et al., 2006; Iniesta et al., 2006). The activity of CckA was recently shown to be downregulated by DivK~P (Biondi et al., 2006; Chen and Stephens, 2007; Ebersbach and Jacobs-Wagner, 2007), thereby linking CtrA phosphorylation and proteolysis pathways. In addition, DivL was shown to be involved in the process of CtrA phosphorylation (Ausmees and Jacobs-Wagner, 2003). Recent data also indicate that DivL may be involved in the phosphorylation of DivK, directly or indirectly (Reisinger et al., 2007).

Proteolysis of CtrA and CtrA~P is significantly accelerated by the phosphorylated form of DivK protein, DivK~P, via the ClpXP protease pathway (Hung and Shapiro, 2002), or with the help of some other (yet unknown) histidine phosphotransferases (Wu et al.,

1999). In terms of the CtrA activity, high DivK~P represses a CckA phosphorylation (Biondi et al., 2006) (so indirectly represses CtrA phosphorylation) and it also accelerates a proteolysis of CtrA (and CtrA~P) (Hung and Shapiro, 2002).

Recently, RcdA and CpdR proteins have been reported to be involved in the ClpXP-dependent CtrA degradation (Chen and Stephens, 2007; Ebersbach and Jacobs-Wagner, 2007). ClpXP is stable throughout the cell cycle (Jenal and Fuchs, 1998) even though its promoter activity varies (Osteras et al., 1999). However, the localization of ClpXP to cell poles is regulated by CpdR. When localized, CpdR recruits ClpX and ClpP directly to proteolyse CtrA (with the help of RcdA protein) (Goley et al., 2007; Iniesta et al., 2006; McGrath et al., 2006). When the proteolysis pathway is activated, the half-life of CtrA/CtrA~P *in vivo* is 5 min or less (Domian et al., 1997).

GcrA is an activator of components of the replisome and of the segregation machinery (Holtzendorff et al., 2004) and also regulates genes like *ctrA, pleC* and *podJ* (Collier et al., 2006; Holtzendorff et al., 2004). The GcrA protein concentration varies through the cell division cycle, peaking early in the cycle in stalked cells and reaching its minimum in a swarmer cell, after cell division. The DNA replication-initiating protein, DnaA, is required for *gcrA* expression (Hottes et al., 2005). In addition, transcription of *gcrA* is repressed by the CtrA protein (Holtzendorff et al., 2004).

The DnaA protein level varies through the cell division cycle in *C. crescentus* (Zweiger and Shapiro, 1994). The half-life time of DnaA is about 60 min throughout the cell cycle.

DnaA expression is inhibited by the GcrA protein (Holtzendorff et al., 2004) and by the gene hemimethylation state when the DNA replicates (Collier et al., 2007). There is also an evidence (McAdams, 2005) that CtrA can upregulate *dnaA*, although available microarray data (Laub et al., 2002) do not provide convincing support for this interaction.

An important function of the DnaA protein in the cell division cycle of *C. crescentus* is to prompt the initiation of DNA replication (Gorbatyuk and Marczynski, 2001, 2005; Marczynski and Shapiro, 2002). The DnaA protein also accelerates the *gcrA* gene expression (Collier et al., 2007) as it can function as a transcription factor. In addition, several early cell cycle gene transcription events require DnaA protein, including *podJ*, *pleC*, *ftsZ*, and even *dnaA* itself (Hottes et al., 2005). Since the *dnaA* gene has two potential DnaA boxes, one located 18bp downstream of the transcription start site, but before the coding sequence, and the other located halfway through the coding sequence (Zweiger and Shapiro, 1994), this indicates that the DnaA protein can potentially regulates its own gene expression.

2.1.2. Polar distribution of DivK and DivK~P

divK transcription is activated by CtrA in late predivisional cells, which results in a slight elevation of the DivK protein, otherwise present throughout the cell cycle at a nearly constant level (Hung and Shapiro, 2002; Jacobs et al., 2001). The total amount of DivK~P, the form which promotes CtrA degradation, does not appear to undergo dramatic changes during the cell cycle. It is 50±20% lower in swarmer cells than in predivisional cells (Jacobs et al., 2001). However, DivK and DivK~P are dynamically

localized during the cell division cycle (Jacobs et al., 2001; Lam et al., 2003; Matroule et al., 2004; McGrath et al., 2004; Skerker and Laub, 2004; Wheeler and Shapiro, 1999). Membrane-bound proteins DivJ and PleC, which localize at stalked and flagellated cell poles respectively, regulate this process (McGrath et al., 2004; Skerker and Laub, 2004) by having opposite effects on DivK phosphorylation. DivJ is a kinase that continuously phosphorylates DivK at the stalked cell pole, and PleC promotes the continuous dephosphorylation of DivK~P at the flagellated cell pole (Matroule et al., 2004 ; McGrath et al., 2004) (See below). Hence, opposing gradients of DivK and DivK~P are established between the two cell poles. Full constriction of the Z-ring disrupts the diffusion of DivK between the two poles (Judd et al., 2003; McGrath et al., 2004). As a result, DivK~P accumulates in the nascent stalked cell compartment and unphosphorylated DivK accumulates in the nascent swarmer cell compartment.

High DivK~P promotes CtrA degradation in the stalked cell compartment (Hung and Shapiro, 2002; Wu et al., 1999), while high CtrA is maintained in the swarmer cell compartment (Ryan et al., 2004). The nonuniform distribution of DivK and DivK~P, and their corresponding effects on CtrA degradation contribute largely to the different developmental programs of swarmer and stalked cells in *C. crescentus*. In addition, recent investigations indicate that CtrA phosphorylation is also at least partially under the control of DivK~P (indirectly via CckA protein, as described in the preceding section), which shows that DivK~P not only controls the stability of CtrA, but also its activity in the cell (Chen and Stephens, 2007; Ebersbach and Jacobs-Wagner, 2007).

2.1.3. PerP, PleC, DivJ and PodJ localization

In *C. crescentus*, many regulatory and structural proteins exhibit asymmetric, often dynamic, localization during the cell cycle (Figure 2). PerP and PodJ (Chen et al., 2006), PleC, DivJ, CckA and DivK~P/DivK (Skerker and Laub, 2004), ClpXP, RcdA, CpdR and CtrA/CtrA~P (Iniesta et al., 2006), they are all involved in the cell cycle regulation at least partially through their different localization schemes during the cell division cycle (Chen and Stephens, 2007; Ebersbach and Jacobs-Wagner, 2007; Goley et al., 2007). However, in this work, we will not explicitly address protein localizations in space but only concentrate on their functional activities contributed to the cell cycle control, assuming they are correctly localized or delocalized in space dimension when needed.

Transcription of *podJ* is upregulated by GcrA and DnaA and downregulated by CtrA. In cells, PodJ has two distinct isoforms: the full-length translation product ($PodJ_L$) and a truncated form ($PodJ_S$). $PodJ_L$ localizes to the incipient swarmer pole, where it helps to recruit factors required for pili biogenesis, including PleC histidine kinase. The periplasmic domain of $PodJ_L$ is degraded by PerP, giving rise to a truncated form ($PodJ_S$). $PodJ_S$ stays attached to the flagellated pole of progeny swarmer cell where it is required for chemotaxis and holdfast formation. During the swarmer-to-stalked cell transition, $PodJ_S$ is cleared and $PodJ_L$ is synthesized and localized again (Hinz et al., 2003). PerP, a periplasmic protease, is required for efficient truncation of $PodJ_L$. Microarray data show that *perP* expression is activated by CtrA (Laub et al., 2002; Laub et al., 2000). In addition, polar PleC activity also affects *perP* expression (Chen et al., 2006).

Therefore, $PodJ_L$, PleC and PerP form a mechanism for regulating the truncation of $PodJ_L$ (Chen et al., 2006). This molecular circuit dynamically regulates temporal distribution of $PodJ_L$ and $PodJ_S$, and the spatial localization of PleC through the cell division cycle.

PleC and DivJ are two distinct proteins for the dephosphorylation and phosphorylation of DivK during the cell cycle. *pleC* expression is activated by GcrA (Holtzendorff et al., 2004). The corresponding protein localizes to the flagellar cell pole once expressed. The localization of PleC is required for its function and $PodJ_L$ affects the PleC localization (Hinz et al., 2003). During the swarmer-to-stalked transition, PleC is released from the cell pole due to the low level of $PodJ_L$ and also by the phosphorylation of itself (Viollier et al., 2002). DivJ is present at low level in a swarmer cell but increases dramatically during the swarmer-to-stalked transition (Wheeler and Shapiro, 1999). Then, it localizes to the stalked cell pole. DivJ's localization helps the phosphorylation of DivK. PleC directly or indirectly regulates the localization of DivJ (Shapiro et al., 2002; Wheeler and Shapiro, 1999). Little is known about the regulatory production and degradation of DivJ in cells.

2.1.4. DNA replication and methylation

DNA replication proceeds in three phases: initiation, elongation and termination. The origin of DNA replication (C_{ori}) in *C. crescentus* has one potential binding site for DnaA, a protein involved in initiating DNA synthesis (Gorbatyuk and Marczynski, 2001). The DnaA binding site partially overlaps with five CtrA binding sites in C_{ori} (Gorbatyuk and Marczynski, 2005; Marczynski and Shapiro, 1992, 2002). Thereby CtrA represses

initiation of DNA replication (Quon et al., 1998). DNA replication is only initiated when DnaA level is high and CtrA level is low. In addition, the origin site has to be fully methylated for DNA replication to re-license the initiation (Reisenauer et al., 1999; Zweiger et al., 1994). These conditions prevail during the swarmer-to-stalked cell transition, and just after division in the stalked cell compartment (Marczynski and Shapiro, 2002). Once initiated, DNA synthesis continues bidirectionally along the circular chromosome, with an average speed of ~20.5 kb/min in minimal broth, finishing in the late predivisional cell (Dingwall and Shapiro, 1989). Elongation of newly replicating DNA strands requires a complex machinery, many components of which are under GcrA control (Holtzendorff et al., 2004).

In *C. crescentus* and other alpha-proteobacteria, CcrM is the methyltransferase that accounts for methylation of newly synthesized DNA strands. *ccrM* transcription is activated by CtrA only from a hemimethylated chromosome for about 20 min, in a late predivisional cell (its expression peaks at ~105 min in the 150 min swarmer cell cycle) (Stephens et al., 1995). Lon protease is required for CcrM degradation (Wright et al., 1996). The half-life of CcrM is less than 10 min *in vivo* (Stephens et al., 1996). Thus, CcrM activity is limited to a short portion of the predivisional cell phase, just before cell division.

Several cell cycle-related genes (*ctrA, gcrA, dnaA, ftsZ and ccrM*) have GANTC methylation sites in their promoters (Collier et al., 2007; Collier et al., 2006; Domian et al., 1996; Reisenauer et al., 1999; Reisenauer and Shapiro, 2002; Zweiger et al., 1994;

Zweiger and Shapiro, 1994). Hence, the expression of these genes is sensitive to the methylation state of the promoter. DNA replication transforms a fully methylated gene (both strands methylated) into a pair of hemimethylated genes (only one strand methylated). At some later time, the unmethylated strands become methylated by the action of CcrM to return the genes to the fully methylated state (Reisenauer et al., 1999). These methylation transitions affect the expression of cell cycle-related genes (Reisenauer et al., 1999). Methylation of C_{ori} is also necessary for initiating a new round of DNA synthesis (Marczynski and Shapiro, 2002). These methylation effects provide a dynamical ratchet feedback from the progression of DNA replication to the cell cycle control system in *C. crescentus.*

2.1.5. Z-ring assembly and constriction

The process of division of a cell in *C. crescentus* is controlled by a number of factors, including DNA replication and segregation, flagellum assembly, and expression of master regulators CtrA and DnaA (Figure 4) (Stephens, 2004; Wagner et al., 2004). The multicomponent Z-ring organelle, which forms and constricts at the mid-cell plane, plays an important role in compartmentation of the predivisional cell and its subsequent division (Brun and Shimkets, 2000). Compartmentation lasts about 15 - 20 min (Judd et al., 2003). After the late predivisional cell is divided into two progeny cells, the Z-ring is disassembled and degraded.

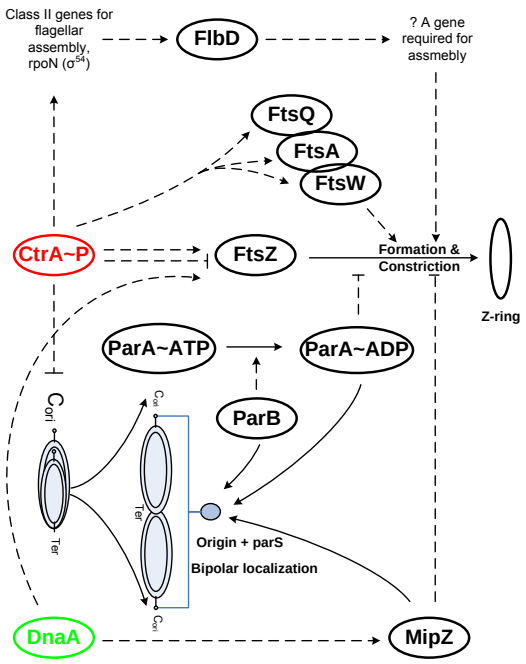

Figure 4. Regulation of the Z-ring assembly in *C. crescentus*.

CtrA regulates transcription of *ftsZ, ftsQ, ftsQ, ftsW*, and some other genes involved in Z-ring assembly and constriction. CtrA represses *ftsZ* transcription in a swarmer cell and in a predivisional cell. It was reported that CtrA is also one of the activators of *ftsZ* expression (Laub et al., 2002). The *ftsZ* gene may also by regulated by DNA methylation since its promoter has a methylation site (Reisenauer et al., 1999; Reisenauer and Shapiro, 2002).

FtsZ is at a maximal level in a predivisional cell that has a visible constriction, and then decreases as CtrA reappears. Following the expression of *ftsZ*, genes *ftsI, ftsW, ftsQ* and *ftsA* are expressed accordingly to help the Z-ring assembly and constriction. CtrA activates *ftsQ, ftsA* and *ftsW* transcriptions. The *ftsQ* gene is expressed only after CtrA-

mediated activation in a late predivisional cell (Wortinger et al., 2000). The FtsQ protein localizes predominantly to the mid-cell plane of the predivisional cell, consistently with the appearance of the Z-ring (Martin et al., 2004; Ohta et al., 1997). The FtsA protein exhibits a time course similar to the one observed for FtsQ (Martin et al., 2004).

CtrA also activates class II genes for flagellum assembly, including σ^{54} (Iniesta et al., 2006; Wagner et al., 2004). In turn, FlbD is activated by σ^{54}, which lead to the activation of a gene required for optimal FtsZ ring assembly.

A segment of DNA sequence, *parS*, locates close to the origin of replication. ParB binds to *parS* and colocalizes with the origin of replication at the flagellated pole in swarmer cells (Bartosik and Jagura-Burdzy, 2005; Bignell and Thomas, 2001). Soon after the initiation of DNA replication, one copy of the origin of replication moves to the opposite pole of cell and then ParB exhibits a bipolar localization pattern. ParA also exhibits a bipolar localization pattern in the predivisional cell and might form a complex with ParB at the origin. Both ParA and ParB proteins maintain constant levels during the cell cycle, even though their gene expressions vary (Mohl and Gober, 1997). Nucleotide exchange between ParA-ATP and ParA-ADP is regulated by ParB (Easter and Gober, 2002). Increasing of ParA-ADP in the cell inhibits cell Z-ring assembly and cell division (Easter and Gober, 2002). It is proposed that a fraction of ParA-ADP would act to inhibit division by preventing assembly of the Z-ring directly or indirectly (Mohl et al., 2001). Overexpression of *parA* and *parB* inhibits cell division and leads to a chromosome

partitioning defect, and depletion of *parB* prevents Z-ring assembly and blocks the initiation of cell division (Mohl et al., 2001; Mohl and Gober, 1997).

Recently, in *C. crescentus*, MipZ has been recognized as having a function similar to the MinCDE system in *E.coli* for repressing the Z-ring assembly and constriction in the middle cell plane (Margolin, 2006; Thanbichler and Shapiro, 2006). MipZ, activated by DnaA (Collier et al., 2007; Thanbichler and Shapiro, 2006), is also involved into the communication between ParB and Z-ring assembly and constriction (Goley et al., 2007).

Z-ring constriction blocks the flux of DivK and DivK~P between flagellated and stalked cell poles (McAdams and Shapiro, 2003). Meanwhile, Z-ring constriction also separates localized proteins (PerP, $PodJ_L$, PleC, DivJ and CckA) only to be functional to separated cell compartments, in contrast with their universal functions to the whole cell in predivisional cell stage (See Section 2.1.3). Therefore, Z-ring constriction has influences, directly or indirectly, on these protein variations and distributions.

2.2. A minimal model

2.2.1. The CtrA-based bistable switch

In (Brazhnik and Tyson, 2006), the core of the model was conjectured as a CtrA-based master regulator switch that drives the cell division cycle in *C. crescentus* (Figure 5).

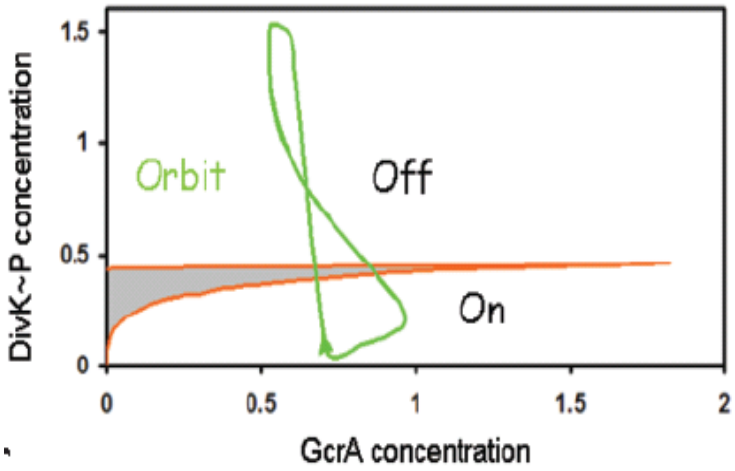

Figure 5. Two-parameter bifurcation diagram demonstrating CtrA-based bistable switch in *C. crescentus.* (This figure is from (Brazhnik and Tyson, 2006), courtesy of *Cell Cycle* Journal and Dr. Paul Brazhnik at Virginia Tech).

During the stalked cell cycle, CtrA alternates between a state of low concentration (at the beginning of the cycle at a stalked cell or early predivisional cell stage, "off" state) and a state of high concentration (at a late predivisional cell stage before division, "on" state) (Brazhnik and Tyson, 2006). These two states can be thought of as quasi-steady states of CtrA abundance, where the rate of production of CtrA is balanced by its rate of degradation. GcrA and DivK~P work together (as a combination of high DivK~P/low GcrA or low DivK~P/high GcrA) to push the transition of CtrA between the low steady

state (low CtrA concentration, "Off") and the high steady state (high CtrA concentration, "On"). The CtrA bistability region separating these two states in the [GcrA], [DivK~P] plane is shown as a wedge-shaped region; CtrA exhibits three steady state values, two stable and one unstable, inside the wedge in Figure 5. As a simulated stalked cell proceeds through the cell division cycle, it crosses back and forth across the wedge (green line is a parametric plot of [GcrA](t) and [DivK~P](t)), switching first from low-to-high [CtrA] to initiate the division process, and then from high-to-low [CtrA], when the Z-ring closed at the end of the cycle.

Under this mechanism, the CtrA-bistable switch model fits well the available patterns of protein variations (Brazhnik and Tyson, 2006). Therefore, in this research, the above mechanism is used as the fundamental regulatory circuit, upon which the more realistic models are built.

2.2.2. Separation of CtrA and CtrA~P in the minimal model

The minimal model did not represent explicitly the process of CtrA activation by phosphorylation. It just assumed that CtrA is always rapidly phosphorylated and kept track only of the active form of CtrA (Brazhnik and Tyson, 2006). As a result of this simplification, the model fails to describe correctly mutants engineered to express *ctrA* constitutively (the only copy of *ctrA* gene is on pJS14), which have been shown to progress through the cell cycle quite normally (Domian et al., 1997). When overexpressed from a high copy number plasmid, cells are viable (slightly filamentous) in strain UJ199 and UJ200 (both are ClpXP mutants, but under the permissive conditions)

(Jenal and Fuchs, 1998). These facts suggest that CtrA phosphorylation is a significant process to control the activity of CtrA. Correspondingly, GcrA might not be that essential in the control of CtrA activity (via the control of CtrA production). To address this, we added the process of CtrA phosphorylation into the minimal model. CckA was added into the model as the kinase that converts CtrA into CtrA~P (See equations in Table S1).

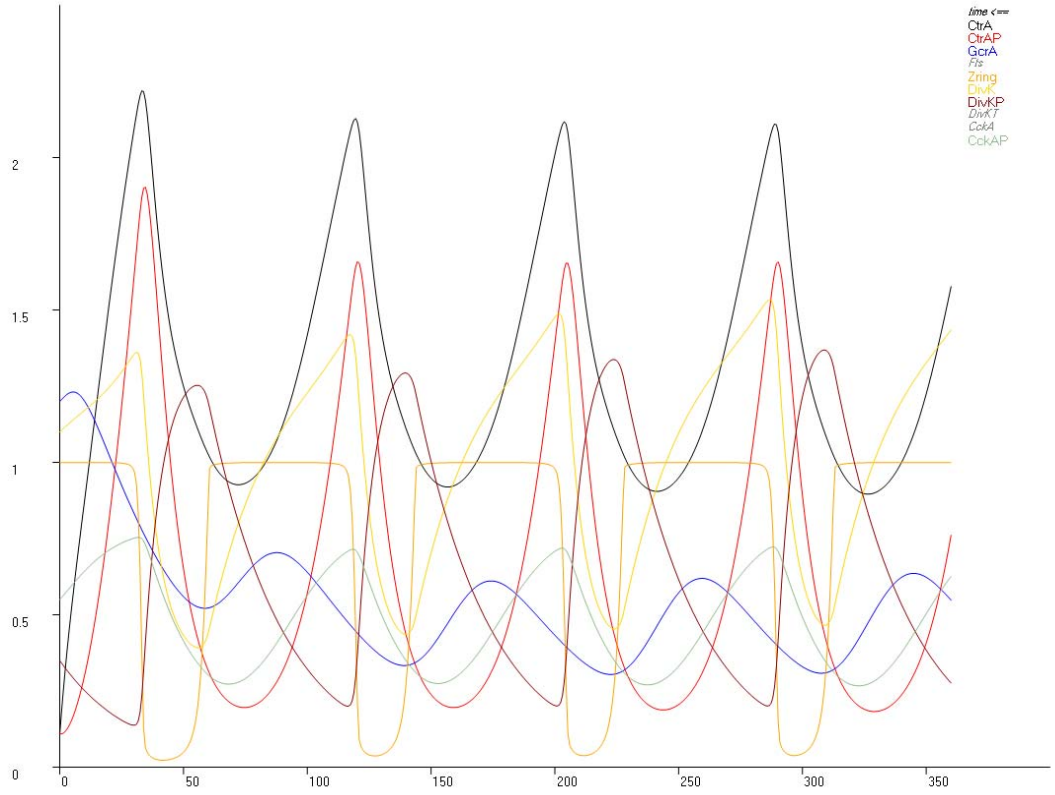

Figure 6. Simulated variations of protein concentrations for the case of constitutive expression of CtrA. The model is implemented, simulated and plotted using Osill8 (http://sourceforge.net/projects/oscill8). (Thank Dr. Emery Conrad for coding this software and helping us in using it.)

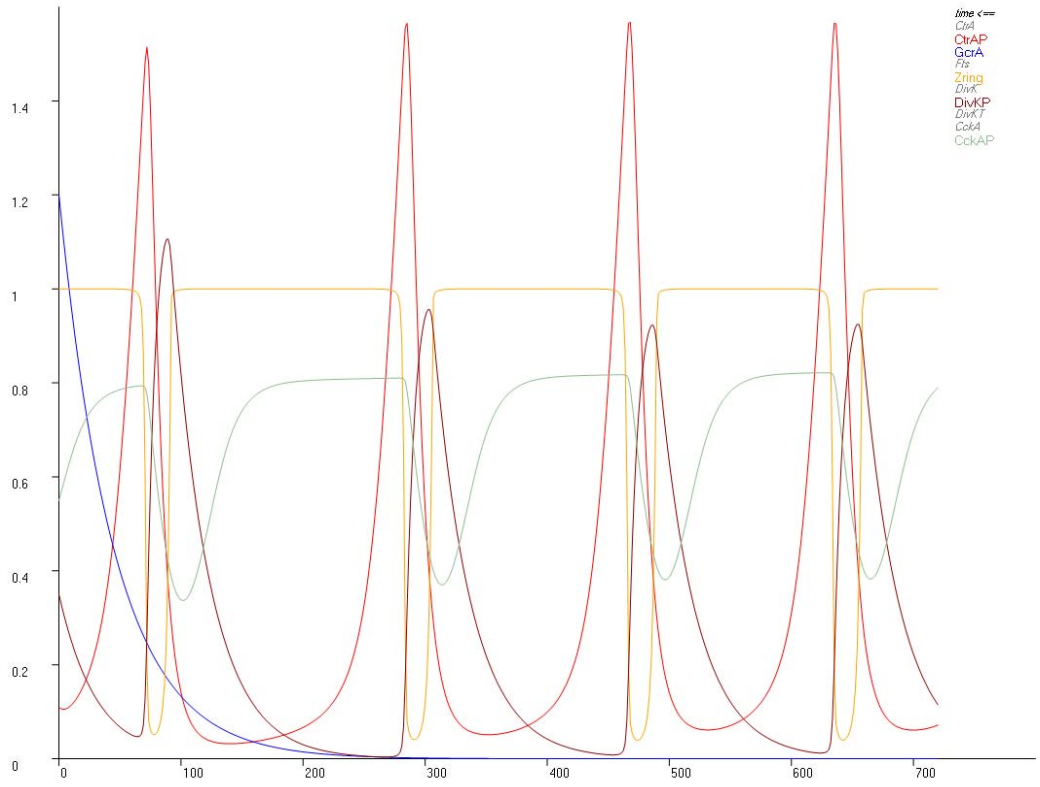

Figure 7. Simulated variations of protein concentrations for the *ΔgcrA* mutant.

The model is implemented, simulated and plotted using Osill8 (http://sourceforge.net/projects/oscill8).

Numerical simulations of both *ctrA* constitutive expression (Figure 6) and *ΔgcrA* (Figure 7) mutants show that protein variations are very similar to those observed for a normal cell cycle, except that the period of the *ΔgcrA* mutant is delayed. Thus the CtrA~P-based bistable switch still works well in this scenario (Figure 8) as well. Constitutively expressed CtrA can lead to normal cell cycle because the CtrA balance in the cell is robustly regulated by both the protein production and degradation. The efficient degradation mechanism dominates after the cell division (even if *ctrA* is constitutively expressed), which overrides the protein production. As a result, CtrA~P will transit from high steady state (high concentration of CtrA~P) to low steady state (low concentration

of CtrA~P). That indicates, within the CtrA~P-based bistable switch model, DivK~P is a dominant factor compared to GcrA. It is obvious that if *ctrA* expression is too high, the cell cycle could be aberrant, as both experimental observations (Jenal and Fuchs, 1998) and our model show.

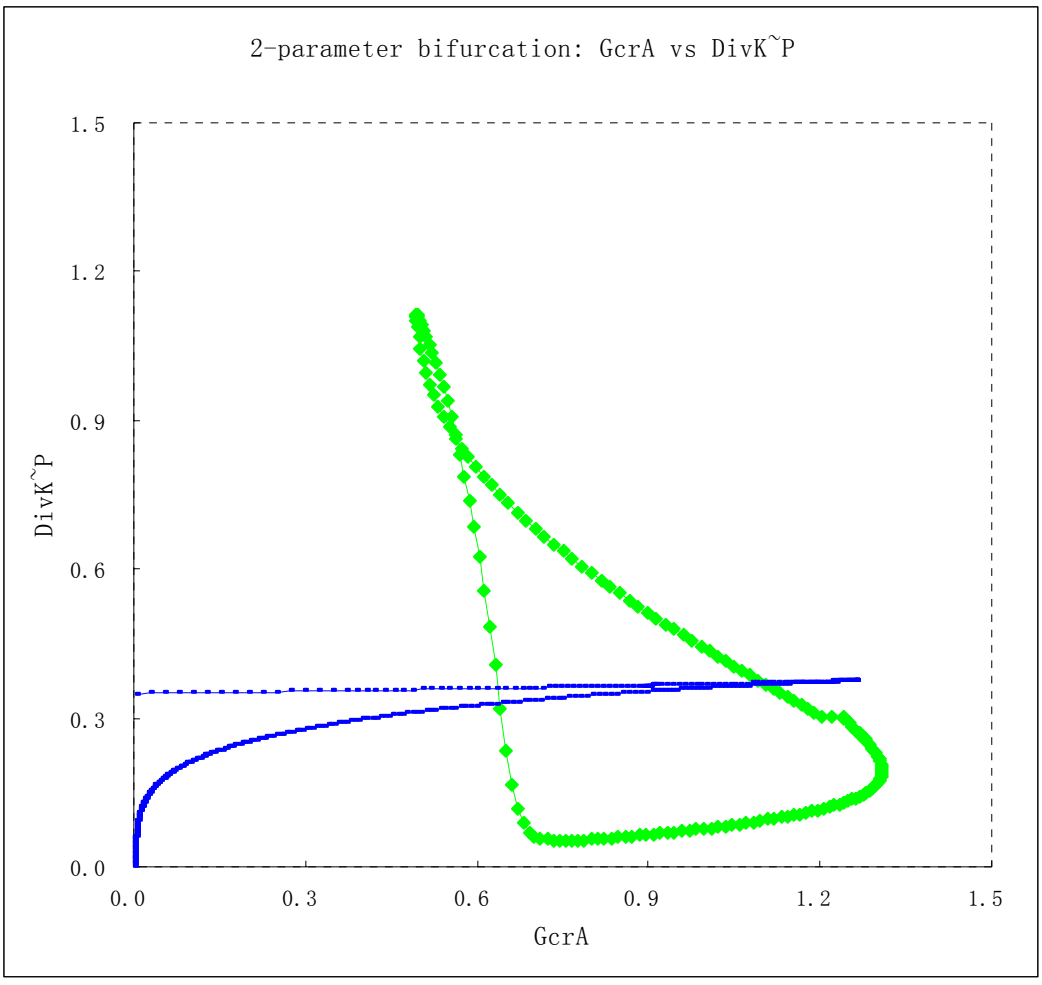

Figure 8. Two-parameter bifurcation diagram: GcrA vs DivK~P.

The green curve is the orbit of wild-type normal cell cycle. The model is implemented and simulated using Osill8 (http://sourceforge.net/projects/oscill8). The data are plotted using Microsoft Excel.

It is important to note here that the simulation of *ΔgcrA* mutant with this model is not consistent with the experimentally observed lethal phenotype (Holtzendorff et al., 2004) .

One possible interpretation of this discrepancy is that in living cells GcrA is also involved into other cell cycle-related pathways (not modeled here) besides CtrA production (Holtzendorff et al., 2004). Therefore, in experimental observations, depletion of GcrA leads to cell lethality in 6 hrs (Holtzendorff et al., 2004), while our mode is not designed to capture this.

The above analysis shows that the CtrA-bistable switch mechanism proposed in (Brazhnik and Tyson, 2006) holds when the CtrA activation step is modeled explicitly (CtrA and CtrA~P are represented separately). In summary, the assumption of lumping CtrA and CtrA~P together introduced in the minimal model is reasonable as a starting point to begin with. Therefore, we hold this assumption in our next step of modeling and use CtrA as a simplified representative of an active species for the CtrA protein (Section 2.3 and 2.4). Later on, we will release this assumption in an improved version (Chapter 3) by including more detailed representation of regulations of the conversion between CtrA and CtrA~P.

2.3. DNA replication controlled model for the stalked cell cycle

To understand the molecular logic behind the cell cycle regulation of a mother cell (stalked cell), the minimal model (Brazhnik and Tyson, 2006) was expanded to capture the processes of DNA replication, DNA methylation, and the effect of the DNA replication initiation protein DnaA. All these features are critical for the control of the cell division cycle of a stalked cell.

The consensus picture (Figure 3) was simplified into the wiring diagram (Figure 9) by taking only the relevant molecular interactions for the stalked cell cycle control and expressing them at protein and physiological levels. Then this wiring diagram was converted into a set of rate equations describing the temporal dynamics of the model focusing on the stalked cell cycle.

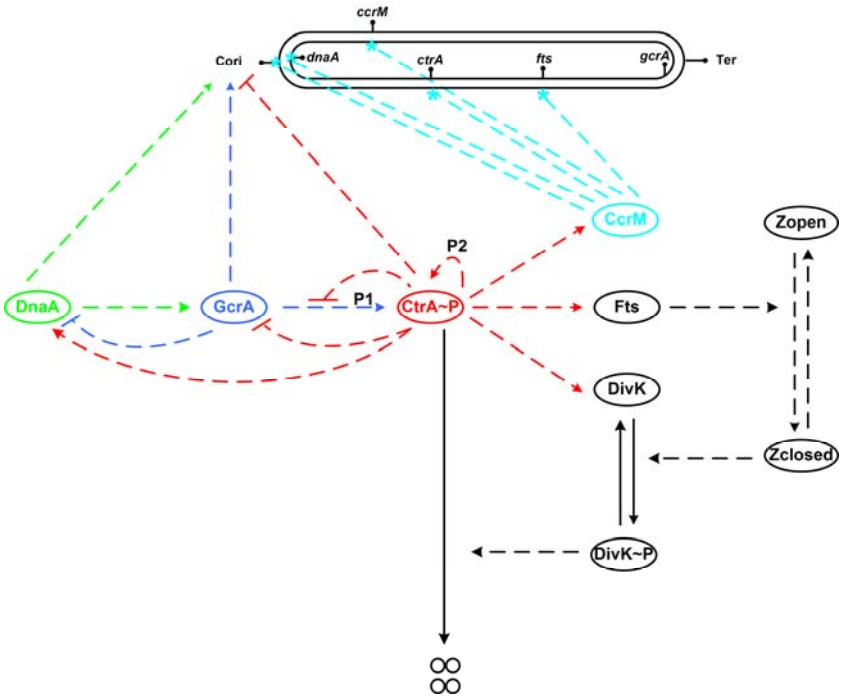

Figure 9. The wiring diagram of the stalked cell cycle model.

Ovals denote protein components. Dashed lines are interactions (activation or repression) between proteins (via their underlying genetic network). Solid lines denote the mass action reactions. 4 circles at the bottom represent products of the CtrA degradation. Degradation of other proteins is not explicitly denoted. The top oval represents a chromosome in the cell with marked relative gene locations.

2.3.1. Assumptions of the model

At this stage, we have limited the scope of our model only to focus on the stalked cell cycle (S phase + G2/M phase) based on the following modeling assumptions:

1. The rise of DivK~P in stalked compartments, after constriction of the Z-ring, is a necessary but not sufficient condition for CtrA degradation. In this version, we use DivK~P as a signal for starting rapid degradation of CtrA. In other words, DivK~P determines 'when' the degradation of CtrA is turned on, but the 'how' (the machinery that degrades CtrA, involving RcdA, CpdR, and ClpXP) is assumed to be there when needed and is not modeled at present.

2. During the division cycle of wild-type cells, the levels of CtrA and CtrA~P rise and fall together (Ausmees and Jacobs-Wagner, 2003; Ryan and Shapiro, 2003), so we can keep track of CtrA synthesis and degradation only, assuming that CtrA~P is a fixed fraction of total CtrA. It is known that DivK~P promotes the proteolysis of CtrA~P and negatively regulates CckA activity, thereby reducing phosphorylation of CtrA (see the consensus picture section). Hence, DivK~P works to eliminate CtrA~P activity by two independent pathways. We lump these two effects together as a single DivK~P-promoted reaction for removing active CtrA.

3. DnaA production is regulated by several factors. However, DnaA protein concentration varies very little during the *C. crescentus* cell cycle (Zweiger and Shapiro, 1994). Although we include relevant regulatory signals in the model, they

do not affect much the dynamics of a stalked cell because DnaA level is nearly constant throughout the cell cycle due to DnaA's long half-life (Collier et al., 2006).

4. Initiation of DNA replication is triggered by the combined conditions of low CtrA, high DnaA, and fully methylated DNA origin site. In addition, initiation requires sufficient replication machinery, which is correlated to a high level of GcrA. We combine these regulatory effects into a single term. We assume that once initiation of DNA replication is successful, DNA elongation starts immediately. Elongation of new DNA strands is linear in time until it finishes, based on experimental data indicating that the speed of DNA replication in *C. crescentus* is almost constant (Dingwall and Shapiro, 1989).

5. Full constriction of the Z-ring requires accumulation and activation of a number of proteins, including FtsZ, FtsQ, FtsA and FtsW, some of which are stimulated by CtrA. To simplify the model, we use Fts as a combined component to relay the signal from CtrA to Z-ring constriction. The transition from Z-ring open (= 1) to fully constricted (= 0) is modeled as a Goldbeter-Koshland ultrasensitive switch (Goldbeter and Koshland, 1981).

6. The effects of the DNA methylation on gene expressions are included in our model because these effects mediate important feedback loops between DNA synthesis and the master regulatory proteins. In the model, the genes *ccrM*, *dnaA*, *ctrA* and *fts* (as a

representative of *fts* series genes), as well as the origin of DNA replication are regulated by methylation.

7. *ccrM* transcription is tightly regulated by the CtrA protein, but accumulation of the CcrM protein shows a noticeable delay from the transcriptional activation of its gene (Grunenfelder et al., 2001), resulting in delayed activation of the DNA methylation (Stephens et al., 1995). This delay is mimicked in our model by an intermediate variable I in the CtrA-to-CcrM pathway.

2.3.2. Components of the model

As a result, the model includes:

- Seven proteins: DnaA, GcrA, CtrA, CcrM, DivK (inactive), and DivK~P (phosphorylated, active form), and a 'representative' Fts protein
- Two phenomenological variables, Z (the state of closure of the septal Z-ring) and I (introducing a delay between activation of *ccrM* transcription and later activation of CcrM protein production)
- The progression of DNA replication (including initiation, elongation and termination) and its methylation (including probabilities of hemimethylation of *ccrM*, *ctrA*, *dnaA* and *fts* genes, and of the replication origin site, C_{ori})

Accordingly, the mathematical model consists of 16 nonlinear differential equations presented in Table S2, including 28 kinetic constants (*k*'s), 13 binding constants (*J*'s) and 4 thresholds (θ's). Our choice of parameter values is given in Table S3.

2.3.3. Numerical simulations of the model

With the equations and parameter values described above, this model was scripted and simulated for the wild-type cells with the initial conditions (Table S4) chosen to represent the beginning of a stalked cell cycle in a wild-type cell.

1. The model accurately describes protein expression patterns during the division cycle of wild-type cells.

Figure 10 illustrates how scaled protein concentrations and other variables of the model change during repetitive cycling of a stalked cell. The duration of a wild-type stalked-cell division cycle in our simulations is 120 min (~90 min for S phase and ~30 min for G2/M phase), as typically observed in experiments (Ausmees and Jacobs-Wagner, 2003; Judd et al., 2003; Ryan and Shapiro, 2003).

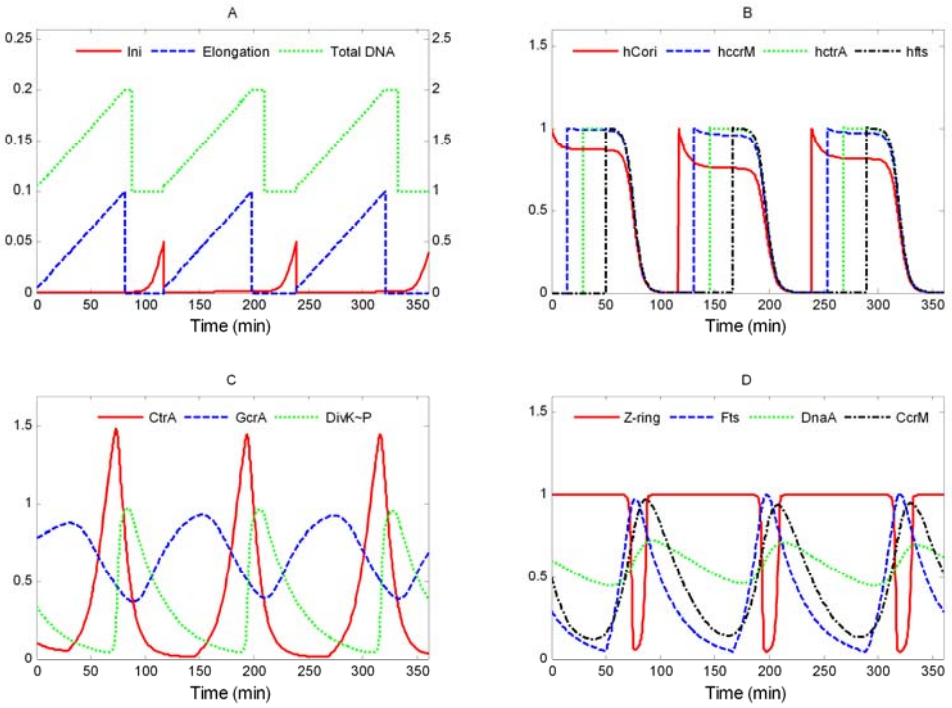

Figure 10. Simulated protein variations for the wild-type stalked cell cycle model.

The main physiological events of the division cycle can be traced back to characteristic signatures of protein expression. The division cycle starts with initiation of DNA replication (Figure 10A) from a fully methylated origin site by elevated DnaA, when CtrA is low and GcrA is sufficiently high (to induce production of required components of the replication machinery) (Figure 10C, D). Immediately after DNA replication starts, C_{ori} is hemimethylated.

As DNA synthesis progresses, certain genetic loci become hemimethylated in order along the chromosome (Figure 10B). Consequently, the regulatory proteins are produced and reach their peak concentrations sequentially. By contrast, *dnaA* expression is activated by the full methylation (Collier et al., 2007), so its expression rate declines immediately after

the DNA replication start. The effect of methylation on the *dnaA* expression is minor compared to the regulatory signals coming from GcrA and CtrA. When the replication fork passes the *ccrM* locus, the gene becomes available for transcription but is not immediately expressed because the CtrA level is low. In a predivisional cell, at ~35 min after start of DNA replication, the replication fork passes the *ctrA* gene (Figure 10B) and its expression is immediately activated by GcrA (Figure 10C) and then further upregulated by CtrA itself. Later on, when the CtrA level becomes high, expression of the *ccrM* gene and later hemimethylated *fts* genes (at ~ 65 minutes), are expressed by the activation from high level CtrA (Figure 10D).

High CtrA level downregulates *gcrA* expression. When DNA replication is finished, the new DNA strands are methylated by elevated CcrM in about 20 min. The DNA methylation shuts down production of CtrA, CcrM and Fts proteins. Meanwhile, elevated Fts proteins promote Z-ring assembly and constriction (Figure 10D), which separates the predivisional cell into two compartments, thereby restricting access of DivK and DivK~P to only one of the old poles of the cell. As a result, in the stalked cell compartment, most DivK is converted into DivK~P, accelerating CtrA proteolysis there (Figure 10C). In a nascent stalked cell, low CtrA concentration releases *gcrA* expression, and GcrA protein level rises. Then, low CtrA, high GcrA and high DnaA drive the nascent stalked cell into a new round of DNA synthesis from the fully methylated chromosome. These computed properties of the model agree reasonably well with what is known (or expected) about cell cycle progression in *C. crescentus*.

2. The model accurately represents observed experimental data during the division cycle of wild-type cells.

In Figure 11 we compare our simulation with experimental data. The data, collected from literature, were obtained by different research groups with various experimental techniques. Based on a visual comparison, we conclude that our model is in a reasonable agreement with experimental observations.

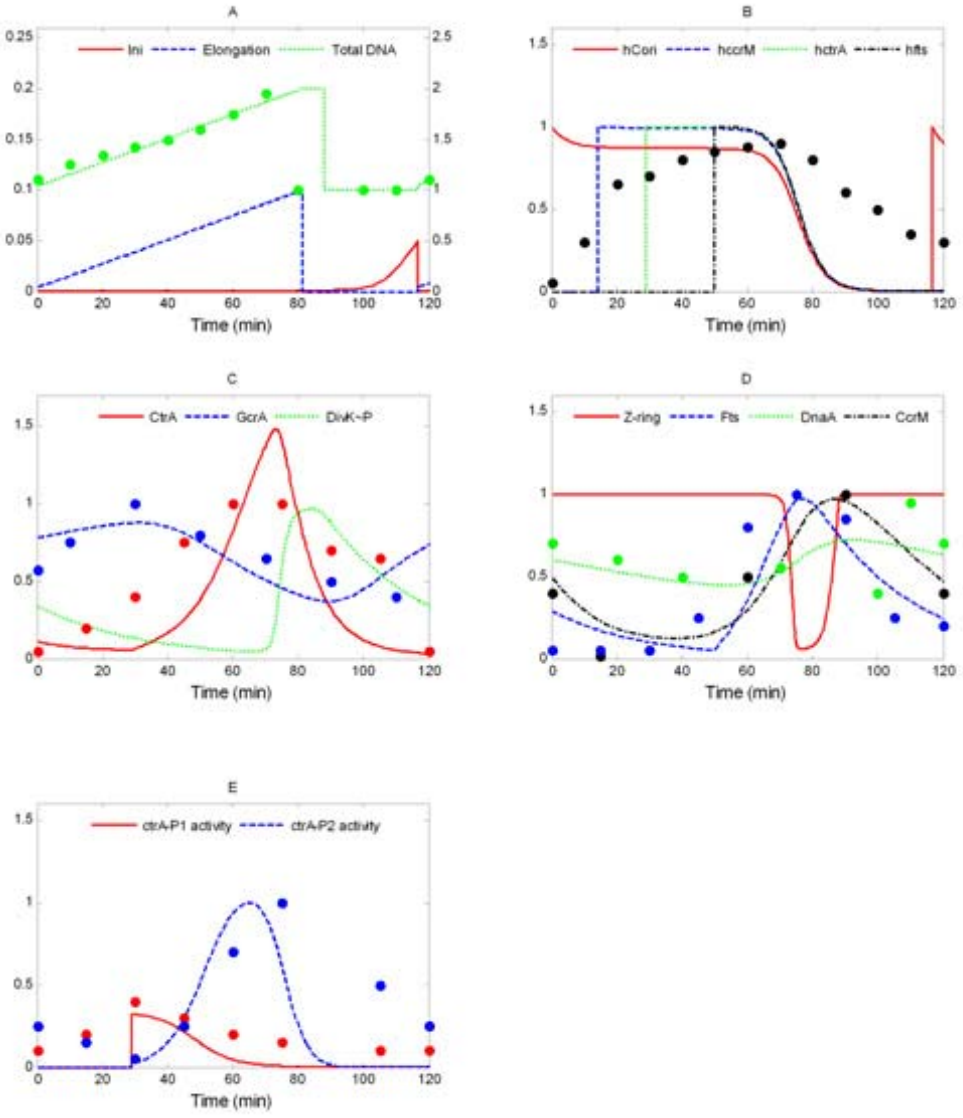

Figure 11. Comparison of simulated protein time profiles and DNA accumulation (curves) with experimental data (circles).

(A) The simulated total DNA (green), Elongation (blue) and Initiation (red) variables. The experimental data for total DNA are taken from Figure 4 in (Dingwall and Shapiro, 1989). (B) Curves are simulated probabilities of hemimethylated states of C_{ori} and three genes. The appearance of hemimethylated gene sites in our simulation reflects the nearly linear growth of overall DNA-hemimethylation observed experimentally (data points (black) from Figure 3 in (Stephens et al., 1996)). The peak of hemimethylation

(~75 min) in our simulation agrees well with experimental observation. (C) Time courses of GcrA (blue) and CtrA (red) are compared against experimental data from Figure 3 in (Holtzendorff et al., 2004) and Figure 1 in (Grunenfelder et al., 2001), respectively. Fluctuations of DivK~P (green) are discussed in the text. (D) The generalized Fts protein time course (blue) is compared to the measured profile of FtsQ from Figure 2 in (Martin et al., 2004). Our simulation of Z-ring constriction (red curve) is consistent with the ~20 min closure time reported in (Judd et al., 2003), Figure 2. CcrM (black) accumulates to high level only in the late predivisional cell, in agreement with the data (black) in (Grunenfelder et al., 2001), Figure 2. DnaA data (green) from Figure 5 in (Zweiger and Shapiro, 1994) do not show significant variations during the stalked cell cycle, consistent with our simulation (green curve). (E) The relative activities of *ctrA* promoters, *ctrA-P1* (red) and *ctrA-P2* (blue), as reported in Figure 4A in (Reisenauer and Shapiro, 2002), compares well with our simulation (red and blue curves).

3. The model was validated by the phenotypes of known mutant strains and predicts phenotypes of several novel mutants.

Phenotypes of mutants provide crucial hints for deciphering the biochemical circuitry of a cell. The simulations performed with the model of the stalked cell division cycle are in agreement with observed phenotypes of over 20 different mutants and predict phenotypes of several novel mutants that have not been described yet in the literature.

To simulate these mutants, parameter values have been changed according to the descriptions of experiments in the literature (Table S6).

The simulated mutants are:

ΔctraA-P1, ΔctraA-P2, ΔctrA, ctrA401^{ts}, *ctrA*^{op},*ctrA* $^{+}$ + P_{xylX} – *ctrAΔ3, ΔgcrA, ΔdnaA,* rescue of *ΔdnaA, ΔftsQ, ΔftsZ, ΔdivK, divK341*^{cs}, rescue of *divK341*^{cs}, *divK*$_{D53A}$, *divK*$_{E9A}$, *divK*$_{D10A}$, *divK*^{op}, *ΔccrM, ccrM*^{op}, *Lon* deletion mutant, *dnaE*^{ts}, *ΔdnaC, gcrA*^{op}, *dnaA*^{op}.

For known phenotypes of known mutants, our model simulations were in agreement with experimental observations. Therefore, our modeling process was validated by the phenotypes of these mutants, as well as by the experimental data of wild-type cells as described in the preceding section. In addition, this model also predicted measurable phenotypes of several novel mutants, including *ΔctraA-P2*, *gcrA*^{op}, and *dnaA*^{op}. These predictable phenotypes can be used to guide future experimental designs.

Details of description of these mutants and their simulation results are available online at http://mpf.biol.vt.edu/research/Caulobacter/pp/mutant_list.php. The list available online makes it easier to follow up by both mathematical modelers and experimental biologists. (See Chapter 4 for details about the web site)

2.3.4. Summary for this section

With this model, we have captured the essential physiological events accompanying the stalked cell cycle progression in *C. crescentus*, including DNA replication, DNA methylation and its effect on the gene expressions, the DnaA influence on the initiation of DNA replication, and the Z-ring assembly and constriction involvement in cytokinesis. Including these important features in our model, we achieved the following key points through our modeling process:

- This model presents a quantitative consensus picture of the stalked cell cycle control in *C. crescentus*.
- Based on the model, cell cycle phenotypes of wild-type cells and mutants were correctly illustrated and interpreted in details through the regulatory dynamics of protein variations.
- Phenotypes of several novel mutants have been predicted with our model, which can be used for further experimental verification of our understanding of the molecular circuitry regulating cell division cycle in *C. crescentus*.
- Put the comparatively detailed regulations of cell cycle in *C. crescentus*, this realistic model confirmed the proposed CtrA-bistable switch (Brazhnik and Tyson, 2006).
- The model and the simulation results (including simulations of mutants) are available online (http://mpf.biol.vt.edu/research/Caulobacter/pp/), which can be a good reference source for experimental biologists.
- The above described results have been reported in a peer reviewed article (Li et al., 2008)

2.4. How stalked and swarmer cell cycles are coordinately regulated in an asymmetric way but share the same underlying CtrA-based bistable switch mechanism

The aforementioned model proved its value in accounting for the temporal dynamics of the stalked cell cycle, which includes S phase and G2/M phase (See Figure 1) only. However, the asymmetric cell division cycle in *C. crescentus* includes another developmental cycle: the swarmer cell cycle. Compared to a stalked cell cycle, a swarmer cell cycle includes a G1-like phase, where the nascent swarmer cell finishes the swarmer-to-stalked differentiation to get ready for entering the stalked cell cycle. Protein variations in this phase start with what the nascent swarmer cell gets at cell division, through the loss of its flagellum and creating of a stalk, to finish with protein concentrations characteristic of a nascent stalked cell.

Therefore, how does the distribution of proteins at cell division to influence the fates of nascent cells to stalked or swarmer morphology? How can the swarmer-to-stalked transition phase (cell differentiation phase, G1-like phase) be integrated into the model of the stalked cell division cycle to describe the swarmer cell cycle as well? To answer these questions, we extend the preceding model into a complete scheme which includes both the swarmer and stalked cell cycles.

At the protein level, the progeny swarmer and stalked cells differs from each other by the DivK/DivK~P distribution, what results in maintaining a high level of CtrA concentration in the nascent swarmer cell (See section 2.1.2) but a low level of CtrA in the nascent

stalked cell. The DivK/DivK~P distribution is regulated by PleC/DivJ (see section 2.1.3 for details). Very little is known of how PleC/DivJ is regulated during the swarmer-to-stalked cell transition; there is evidence that proper DivJ localization (necessary for its function) is affected by PleC (Shapiro et al., 2002; Wheeler and Shapiro, 1999). From this point, PleC and DivJ are added in our model (Figure 12) with a simplified assumption described below.

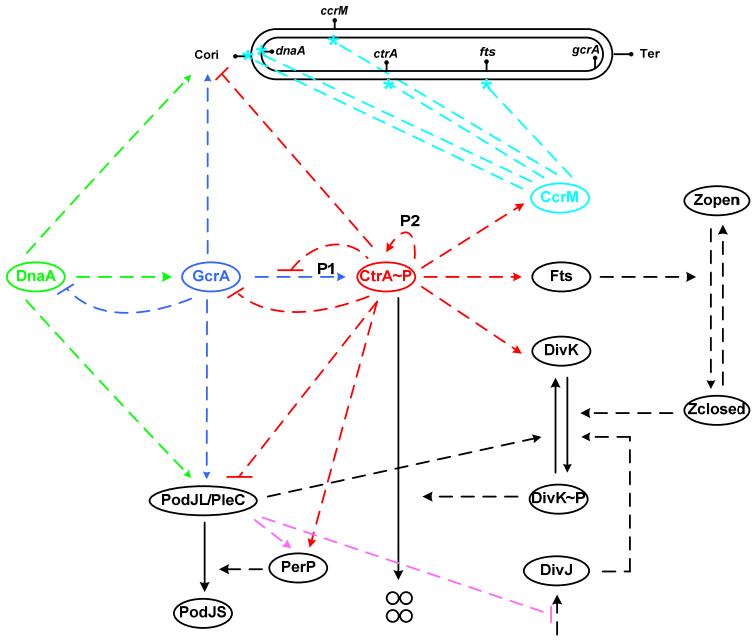

Figure 12. Wiring diagram of the swarmer cell division cycle model.

Notations are as in Figure 9. Pink lines represent physical processes (localization) where the functions of the proteins are influenced.

2.4.1. Assumptions of the model

In addition to the assumptions used for the stalked cell cycle model in the previous section (section 2.3.1), here additional assumptions and simplifications used during the modeling process are summarized below.

1. Localized DivJ and PleC phosphorylate and dephosphorylate DivK respectively. This is now included explicitly in the model. The phosphorylation state of DivK defines, after the Z-ring constriction, the level of CtrA in the cell, which is a determinant of the morphology of the progeny cell in our model. Other proteins involved in CtrA proteolysis are not included explicitly in our model but are assumed to be there when needed.

2. During the swarmer-to-stalked transition, *divJ* is expressed abruptly and persists until cell division (Wheeler and Shapiro, 1999). Proper localization of DivJ is required for its normal function, and its localization is regulated, at least partially, by PleC (Jacobs et al., 2001), presumably by a competition for localization sites (Wheeler and Shapiro, 1999). SpmX is also involved in the process of DivJ localization and activation (Radhakrishnan et al., 2008). Both these effect are simplified and captured implicitly in our model through the regulated expression of PleC ($PodJ_L$ variable, see below).

   PleC production and localization are upregulated by $PodJ_L$, the full-length translational product of the *podJ* gene. Transcription of *podJ* is upregulated by GcrA and DnaA, and downregulated by CtrA (Chen et al., 2006). PleC expression is also activated by GcrA (Holtzendorff et al., 2004). In order to avoid overwhelming of the model with details, we combine $PodJ_L$ and PleC in a single state variable [$PodJ_L$] (Figure 12).

3. Upon differentiation of a swarmer cell into a stalked cell, $PodJ_L$ is synthesized and subsequentially localized to the pole opposite the stalk. In the late predivisional cell, $PodJ_L$ is processed into a short form $PodJ_S$ with the help of PerP, which truncates the periplasmic domain of $PodJ_L$ (Chen et al., 2006). The timing of this event is regulated by CtrA which upregulates PerP (Chen et al., 2006). These regulations are explicitly represented in our model. $PodJ_S$ remains localized at the flagellar pole after cell division and is degraded during the swarmer to stalked cell transition. In this version of the model we do not keep track of $PodJ_S$.

4. $PodJ_L$/PleC, PerP and DivJ are active when localized to flagellar or stalked cell poles. To track this appropriately, we added to equations for these components the "separation factor" ($H = 0$ or 1) which depends on the choice of the cell morphology being tracked.

2.4.2. Components included in the model

In summary, the model includes:

- All the components of the stalked cell cycle model.
- PerP, $PodJ_L$/PleC (lumped together), DivJ.
- A separation factor H: for the stalked cell cycle $H = 0$; for the swarmer cell cycle $H = 1$.

The mathematical model consists of 19 nonlinear differential equations presented in Table S6, including 40 kinetic constants (*k*'s), 23 binding constants (*J*'s) and 4 thresholds (θ's). Our choice of parameter values is given in Table S7.

2.4.3. Numerical simulations of the model

Similar to the stalked cell cycle model, this model was simulated for wild-type cells, with the initial conditions in Table S7 taken to represent the beginning of a stalked cell cycle in a wild-type cell.

1. The model accurately describes protein variation patterns during the division cycle of wild-type cells for both swarmer and stalked cell cycle.

Figure 13 illustrates how scaled protein concentrations and other variables of the model change during repetitive cycling (Figure 13, top, 3 periods) of a swarmer cell. The duration of a wild-type swarmer cell division cycle is 150 min (~30 min for G1-like phase, ~90 min for S phase and ~30 min for G2/M phase) in our simulations, as typically observed in experiments (Ausmees and Jacobs-Wagner, 2003; Judd et al., 2003; Ryan and Shapiro, 2003). Correspondingly, the stalked cell cycle lasts ~120 min in our simulation (around 4 periods are shown at the bottom of Figure 13), which is in agreement with the simulation results presented in Section 2.3.

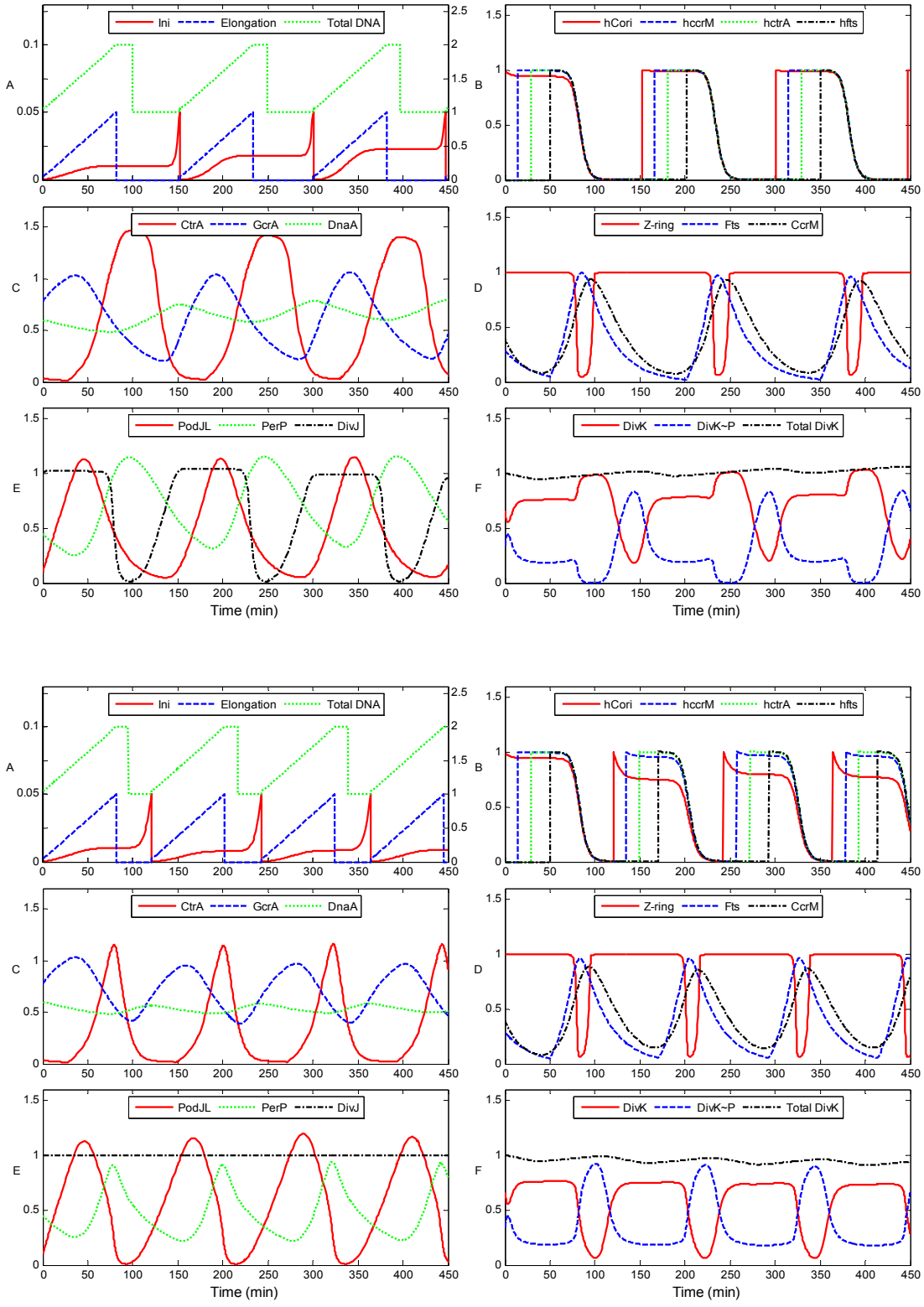

Figure 13. Simulated variations of model state variables (top 6 panels, swarmer cell cycle, bottom 6 panels, stalked cell cycle) during the wild-type *C.crescentus* cell cycle.

The experimental data points collected from literature were reasonably fitted well by this model (data not shown), as well the timings of major physiological events. In addition, with this new model, the morphology of the nascent cell (swarmer or stalked) after division can be specified by the choice of H ($H = 0$ for swarmer cell and $H = 1$ for stalked cell). Therefore, the two developmental programs in *C. crescentus*, along with necessary cell cycle controls and cellular physiologies now are captured in our model.

2. The model agrees with phenotypes of known mutant strains.

Similar to the stalked cell cycle model, the model of the swarmer cell division cycle presented here reproduces results for those mutants described earlier (Section 2.3.3). In addition, this model is suitable for validating against swarmer-cell-specific mutants, two of which are specifically described below.

***ΔperP* mutant**

When *perP* is deleted (*ΔperP* mutant), $PodJ_L$ accumulates in cells (Chen et al., 2006). These mutant cells can finish a cell division cycle (Chen et al., 2006). In our simulation (Figure 14), another cell cycle is observed, as expected, after *perP* is deleted (Figure 14B). $PodJ_L$ variations are also consistent with experimental observations. Our simulation also predicts that after completion of the cycle during which the mutation is introduced, the cell will stop cycling because the elevated level of $PodJ_L$ accelerates dephosphorylation of DivK. With little DivK~P CtrA is hard to wipe out and initiation of DNA replication cannot restart.

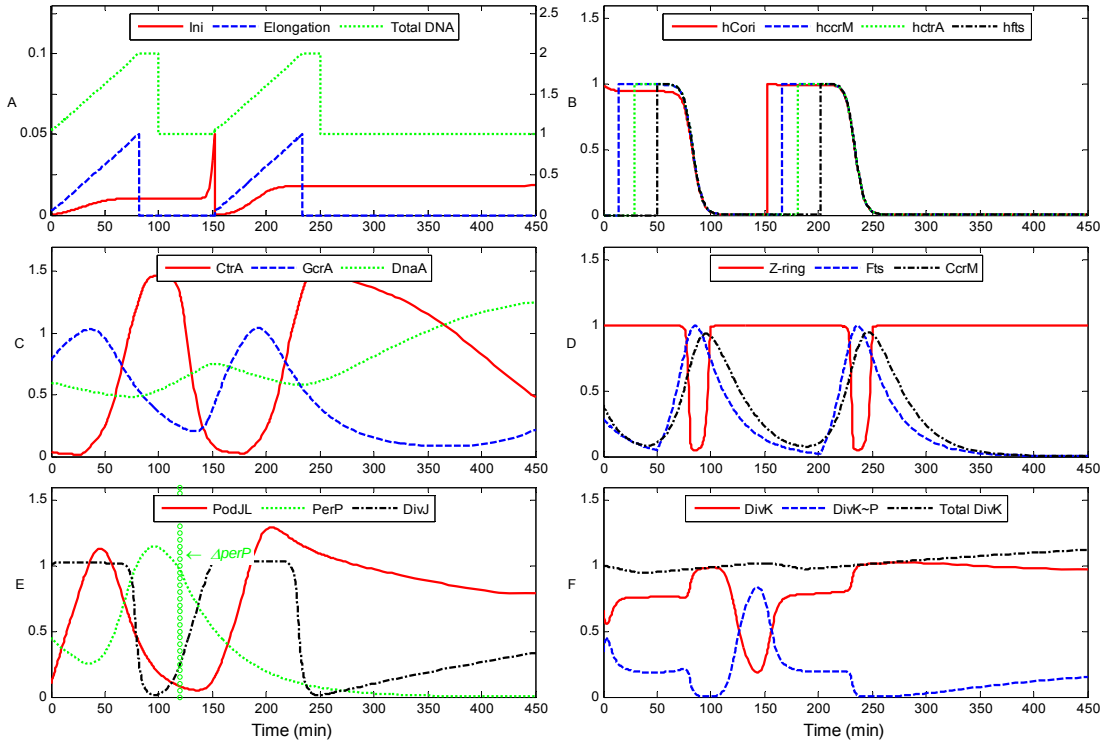

Figure 14. Model simulation of the *ΔperP* mutant.

ΔperP is introduced (set $k_{s,PerP} = 0$) at $t = 120$ min .

perP^{op} mutant

To overexpress *perP,* a chromosomal or plasmid copy of the gene under the control of xylose-inducible promoter (P_{xyl}-*perP*) can be introduced. No $PodJ_L$ is accumulated in a *perP*^{op} mutant (Chen et al., 2006). In our simulation of this mutant (Figure 15) $PodJ_L$ indeed becomes lower when *perP* is constitutively expressed. The lower level of $PodJ_L$ allows for DivJ to be localized and functional. Functional DivJ elevates DivK~P accelerating therefore CtrA degradation (Figure 15A) in the predivisional cell phase. Lower CtrA provides more chances for the initiation of DNA replication but the cell fails to divide (Figure 15B) without sufficient CtrA stimulation for Z-ring constriction.

According to our simulation, a filamentous cell with several copies of chromosomes would be observed in experiments with this mutant.

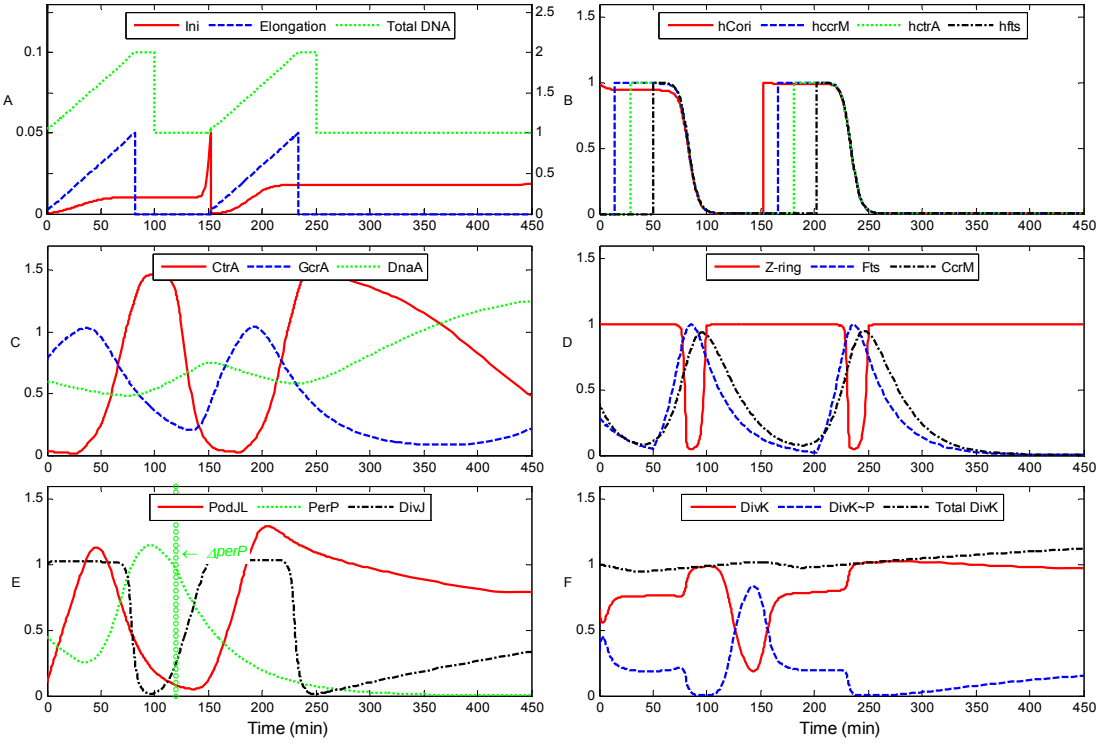

Figure 15. Model simulation of the *perP*^{op} mutant.

perP^{op} is introduced by adding a constitutive production term, $k_{s,PerP} = 0.07$, to [PerP] rate at $t = 120$ min.

2.4.4. Summary of this section

The crucial cellular physiologies, including those we described in the preceding model, as well as the swarmer-to-stalked cell transition, are captured by our current model which covers both the swarmer and stalked cell cycle controls. The major advances of the new model are:

- The model for stalked cell cycle control presented in section 2.3 was extended to describe the swarmer cell cycle based on the assumption that PodJ, PleC, PerP, and DivJ proteins consequently varied and interacted as in this model.
- The characteristics of wild-type cells and mutants were faithfully represented in this model, and the model provides a systematic interpretation of cell cycle progression in both stalked and swarmer cells.
- The assumptions made about the connections among $PodJ_L$, PleC and DivJ, were implemented in our model for the swarmer-to-stalked cell transition phase in simplified way. Currently it is unclear how these interactions actually occur. Therefore, more detailed experimental data are needed to improve this portion.
- These results were partially published in conference proceedings (Brazhnik et al., 2007), and a full version of the model has been prepared and submitted to *PLoS Comp. Biol.*

2.5. Summary of the modeling of cell cycle control of *C. crescentus*

Through our bottom-up modeling process, we reconciled and organized knowledge of cell cycle control in *C. crescentus* into a unified quantitative framework. As a quantitative model, it captures the major temporal dynamical features of cell division and cell differentiation, and it is consistent with the observed average behavior of proliferating cells in the laboratory.

The temporal dynamics of cell cycle control in *C. crescentus*, which are elaborately regulated by an underlying molecular mechanism, are described in our model by variables representing the concentration of interacting proteins and the physiological states of the DNA replication and cell division machinery. G1/S transition, DNA replication, cytokinesis, and other relevant cellular physiologies are governed in our model by these underlying molecular interactions and mechanisms. Available experimental data, including phenotypes of wild-type cells and known mutants, were used to validate the model. The validated (parameterized) model provides predictions of phenotypes of novel mutants requiring further experimental confirmation.

About 1/3 of cell cycle-related genes are regulated by CtrA, GcrA, and DnaA proteins. Our model keeps track of these three regulatory proteins but only a limited number of downstream effects. A number of other proteins and interactions may play important roles in controlling cell cycle of *C. crescentus*. Therefore, what we have presented here is only a starting point. Improvements will make the model more realistic, testable and predictive.

Chapter 3. An extended version of *C. crescentus* cell cycle model

3.1. The purpose of this extension

Our previous model, though well validated by many relevant mutants, cannot account for the phenotypes of mutant cells that express *ctrA* constitutively. The problem is our oversimplification of neglecting the role of phosphorylation in activating CtrA. Furthermore, Z-ring assembly and constriction, also interacting with the progression of DNA replication, can be described in more realistic detail (Figure 16).

1. **CtrA phosphorylation.** In the previous model, CtrA is assumed to be always in its active form (CtrA~P), but in reality this is not the case. So we want to release this assumption and add the processes of CtrA phosphorylation and dephosphorylation into the model. CtrA phosphorylation crosstalks with its proteolysis process (see below).

2. **CtrA proteolysis.** CtrA proteolysis is temporally accelerated by DivK~P. But this is not a sufficient condition for CtrA degradation. Recent reports show that RcdA, ClpXP, CpdR and CckA are also involved into the degradation process. Furthermore, the signaling pathway for degradation has cross-talk with the activation of CtrA (its phosphorylation) via CckA. (See section 2.1.1). Therefore, to take CtrA phosphorylation and its proteolysis during the cell cycle into consideration, the signaling pathway for CtrA degradation should be included into our model.

3. **Z-ring constriction.** Z-ring assembly and constriction in the current model is triggered by the production of Fts proteins (FtsZ, FtsQ, FtsA, FtsW, etc.) which is activated by CtrA~P. However, Z-ring, as a crucial component for cell division, is regulated not only by this CtrA-activated positive feedback, but also through chromosome replication and separation, and other signaling pathways (See section 2.1.5). With these controls, Z-ring assembly and constriction is restricted to happen whenever the cell gets ready for division. Therefore, the complex control of Z-ring constriction in *C. crescentus* should be included in more detail in the model to makes the model more robust.

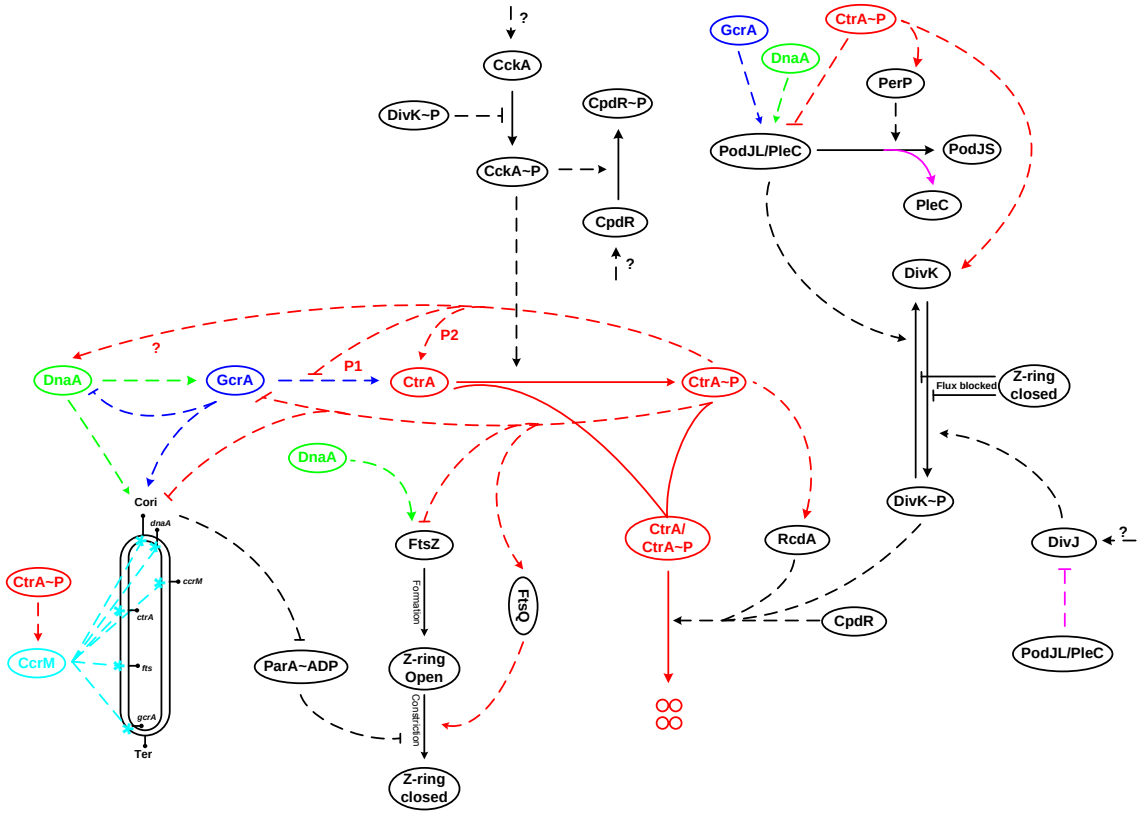

Figure 16. Wiring diagram for the improved version of cell cycle model.

3.2. Implementing the extensions

3.2.1 CtrA phosphorylation and proteolysis

In the model, CtrA phosphorylation is activated by CckA~P only. Other factors for CtrA phosphorylation are neglected at this time.

DivK~P is still the crucial component to trigger degradation of CtrA and CtrA~P. In addition, DivK~P also represses the activation of CtrA by downregulating CckA. Total CckA and ClpXP are stable, but their phosphorylation and localization are regulated and varied throughout the cell cycle. Total CpdR is assumed to be stable but its phosphorylation is regulated by CckA~P. CpdR gets involved in the localization of several proteins, including CtrA and CtrA~P (from here on, we distinguish CtrA and CtrA~P as different species), RcdA, ClpXP, etc. Its total effect seems to recruit CtrA and CtrA~P and accelerate their degradation. However, little is known about how this happens. At this time we simplify this process as a single interaction from CpdR to CtrA/CtrA~P degradation. Other interactions (e.g. CpdR to RcdA) are neglected.

Therefore, in the model CtrA degradation is assumed to require Divk~P, CpdR and RcdA only (assuming ClpXP is always there and ready for CtrA degradation when required).

3.2.2 Z-ring assembly and constriction

Z-ring assembly and constriction have been separated in this new version. ‘Z-ring’ is introduced as a component for the assembly of Z-ring which comes from FtsZ protein. Z

(which is variable 'Zring' in our previous models), now represents the constriction of Z-ring.

We are not clear how FtsQ, FtsA, and FtsW are involved in Z-ring assembly and constriction. Therefore, we simply chose FtsQ as a sufficient representative condition for Z-ring constriction. Little details are available on the role of MipZ and FlbD for Z-ring constriction. At this time we do not include them in our model. ParA and ParB signaling pathway for Z-ring constriction is represented by ParA in this version of the model.

3.3. The model

With the modification above, the model now includes:

- All the components listed in aforementioned model for the whole cell cycle control (Section 2.4).
- CckA~P, CpdR, ParA, FtsQ, FtsZ, Z-ring formation, and Z (Z-ring constriction) were added.

Therefore, our model consists of 28 equations presented in Table S8, including 55 kinetic constants (*k's*), 31 binding constants (*J's*), and 6 thresholds (θ*'s*). The choice of parameter values and initial conditions are given in Table S9.

3.4. Numerical simulation of the model

Similar to the previous simulations (Section 2.3.3 and 2.4.3), this model was simulated for wild-type cells, with the parameter values and initial conditions (Table S9) taken to represent the beginning of a stalked cell cycle in a wild-type cell.

3.4.1. Simulation of wild-type cells

With the modifications described above, our simulations accurately described protein expression patterns during the division cycle of wild-type cells, including the concentration variations of CtrA, CtrA~P, CckA~P, and CpdR (Figure 17). These protein variations in the model also correlate with a correct sequence of cellular physiological events for the cell division cycle in *C. crescentus*.

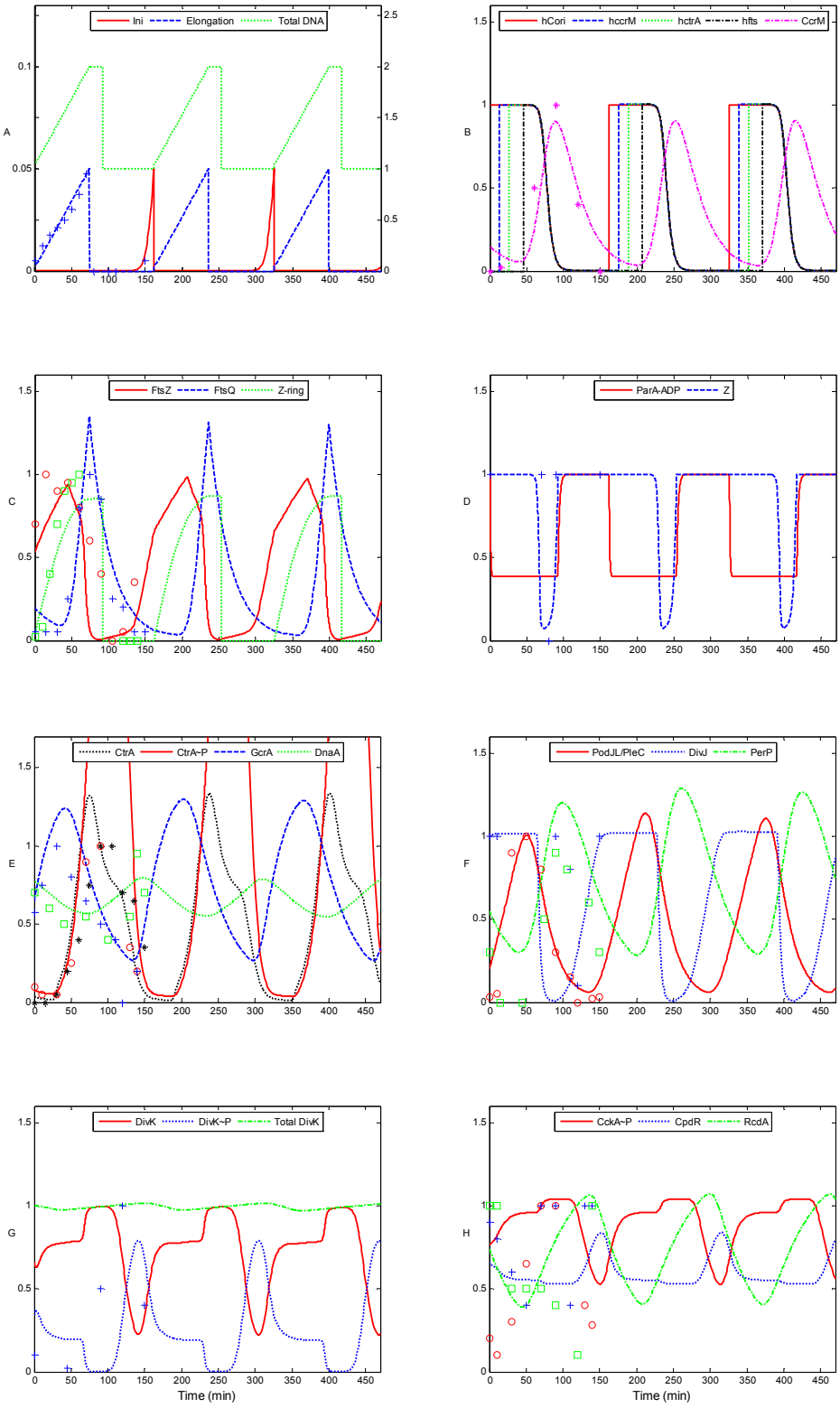
Ini
Elongation
Total DNA
A
hCori
hccrM
hctrA
hfts
CcrM
B
FtsZ
FtsQ
Z-ring
C
ParA-ADP
Z
D
CtrA
CtrA~P
GcrA
DnaA
E
PodJL/PleC
DivJ
PerP
F
DivK
DivK~P
Total DivK
G
CckA~P
CpdR
RcdA
H
Time (min)
Time (min)

Figure 17. Simulated variations of model state variables (curves) during the wild-type *C.crescentus* cell cycle in comparisons to experimental data (symbols).

Most of the experimental data (points in the figures) are replotted from Figure 11, others were collected as follows:

C. FtsZ: Figure 2C in (Martin et al., 2004)

Zring: Figure 3C in (Aaron et al., 2007)

E. CtrA: Figure 3C in (Holtzendorff et al., 2004)

CtrA~P: Figure 3C in (Jacobs et al., 2003)

F. $PodJ_L$/PleC: Figure 1A in (Chen et al., 2006) and Figure 1B in (Viollier et al., 2002)

DivJ: Figure 2B in (Wheeler and Shapiro, 1999)

PerP: Figure 4 in (Chen et al., 2006)

H. CckA~P: Figure 3B in (Jacobs et al., 2003)

CpdR: Figure 5A in (Iniesta et al., 2006)

RcdA: Figure 2C in (McGrath et al., 2006)

3.4.2. Simulation of relevant mutants

Phenotypes of all relevant known mutants were used to validate the model. Also, several novel mutants were simulated and their corresponding phenotypes were predicted as a guide for further experimental tests. To simulate these mutants, parameter values were changed according to the descriptions of the experiments from literature (Table S10).

The simulated mutants were: *ΔctraA-P1, ΔctraA-P2, ΔctrA, ctrA401^{ts}, ctrAD51E*，*ctrA*Δ3Ω，*ctrAD51E*Δ3Ω, *ctrA* constitutively expression, *ctrA^{op} (P_{xylX}-ctrA*Δ3*), ctrA* $^{+}$ + *P_{xylX} – ctrAΔ3, ΔgcrA, gcrA^{op} , ΔdnaA,* rescue of *ΔdnaA, dnaA^{op}*, *ΔftsQ, ΔftsZ, ΔdivK, divK341^{cs},* rescue of *divK341^{cs}, $divK_{D53A}$, $divK_{E9A}$, $divK_{D10A}$, divK^{op}, ΔccrM, ccrM^{op}, Lon*

deletion mutant, *dnaE*^{ts}, *ΔdnaC,* Δ*parA, parA*^{op}, Δ*rcdA,* Δ*rcdA + ctrAD51E, rcdA*^{op}, Δ*cckA (cckATS1),* CckA unphosphorylated, Δ*cpdR, cpdRD51A* (CpdR unphosphorylated), *cpdR*^{op}, CpdR fully phosphorylated, Δ*divJ*, Δ*divJ + divK*^{op}, Δ*pleC* and Δ*podJ, pleC*^{op} and *podJ*^{op} , Δ*perP, perP* constitutive expression .

The full description of these simulation results will be available online at http://mpf.biol.vt.edu/Research/Caulobacter/SWST/PP. Here four *ctrA* mutants were presented to illustrate the importance of CtrA production, phosphorylation, and proteolysis working together as the integrated regulation to control CtrA and CtrA~P variation during the cell cycle in *C. crescentus*.

Constitutive *ctrA* expression mutant has a normal cell cycle (Domian et al., 1997). *ctrAΔ3 Ω* mutant has low degradation rate (15% of wild-type cells) of CtrA and CtrA~P. And in *ctrAD51E* mutant, CtrA is always in active form (CtrA~P) when expressed. Both of them experience almost normal cell cycle (Domian et al., 1997). Only the double mutant *ctrAD51EΔ3 Ω* became filamentous when the mutation is introduced (Figure 18).

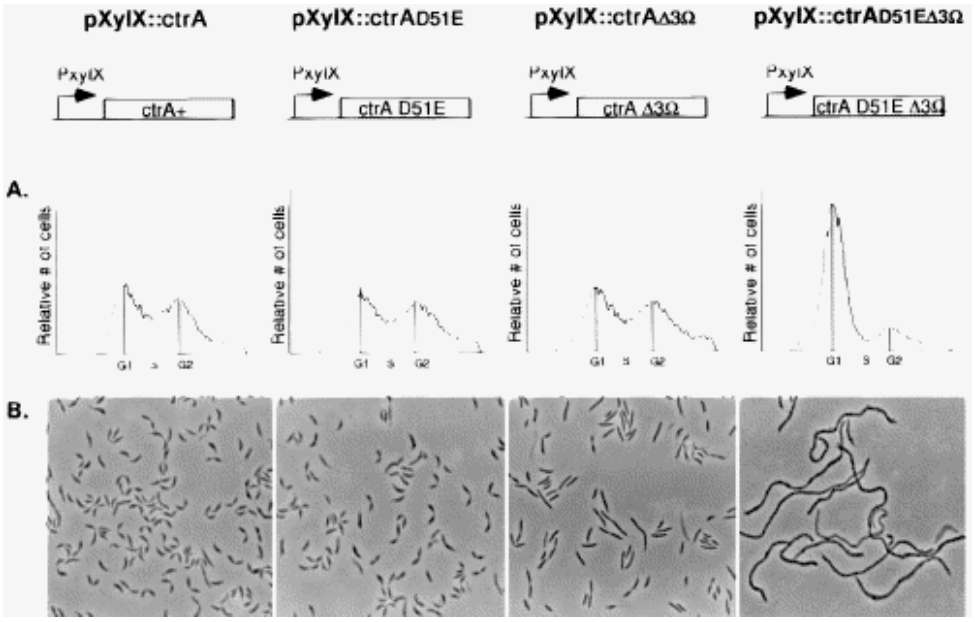

Figure 18. Experimental results of *ctrA* mutants (copied from (Domian et al., 1997))

Our simulations (Figure 19) for these four mutants show that except for *ctrAD51EΔ3 Ω*, all other simulations have periodic variations of protein components (including CtrA~P) and these variations indicate a normal cell division cycle. These results agree well with the observed experimental results we described above.

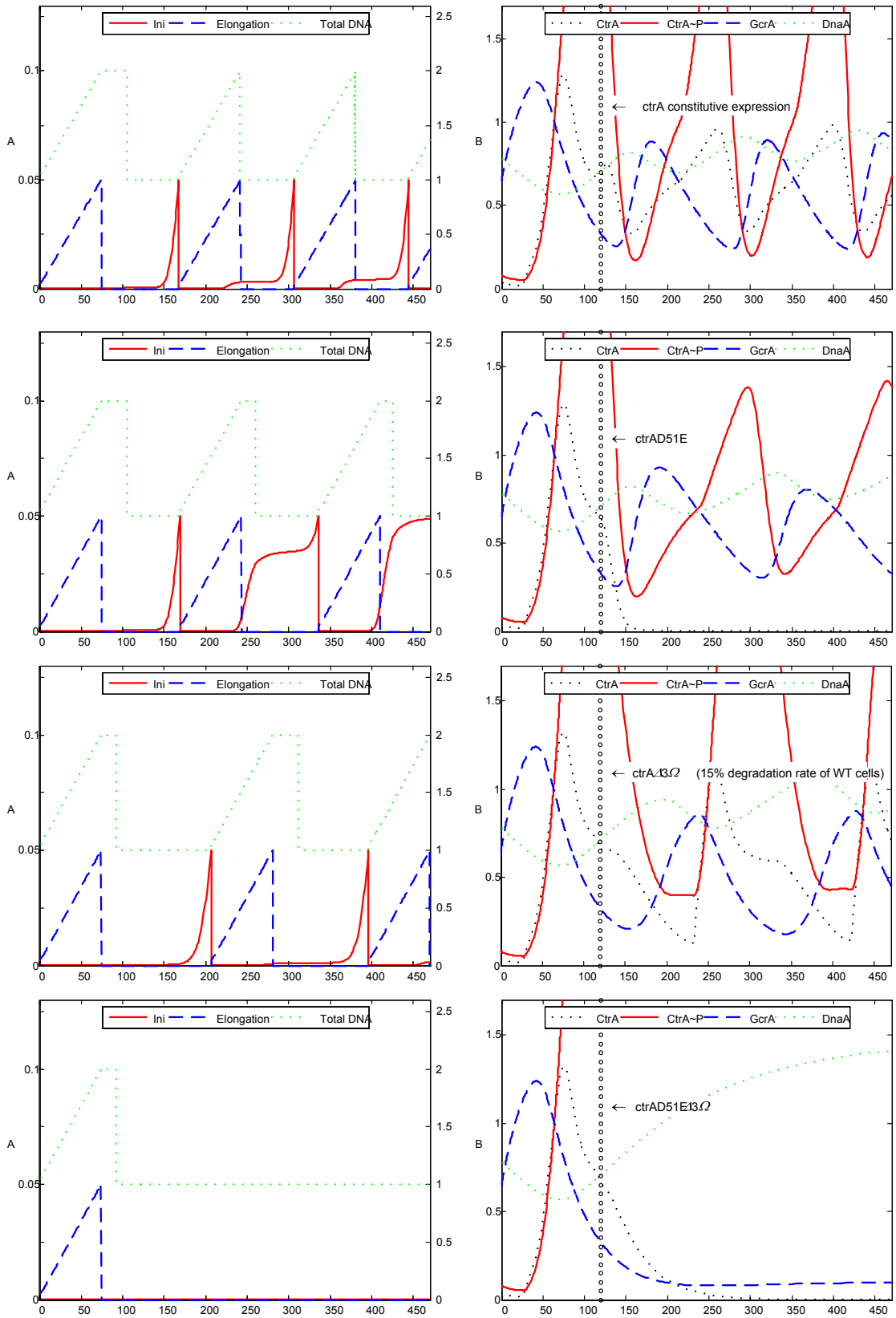

Figure 19. Simulation results for *ctrA* mutants.

3.5. Summary of this chapter

With these modifications, CtrA and CtrA~P were separately described in our model, in agreement with experimental observations. Z-ring assembly and constriction is a key process for cell division in bacteria. Replacing the single positive signaling pathway (via CtrA and Fts in the previous model) with this parallel control more tightly coupled with DNA replication, the current model make Z-ring assembly and constriction more realistic and more robust than before.

As the simulation results of this model are consistent with experimental data and the relevant phenotypes of both wild-type cells and mutant strains, the corresponding predictions of phenotypes for novel mutants are a good reference for experimental designs to test the model's predictions. In addition, further experimental confirmation will provide new data to improve the model into more a validated scenario and systematic framework for the cell cycle research in *C. crescentus*.

This portion of results, together with section 2.5, is organized in an independent paper to be submitted.

Chapter 4. The Web site

4.1. The purpose of the web site

The systematic mathematical model proposed in this work is unique in the details with which it describes the temporal dynamics of cell cycle control in *C. crescentus*. Accompanying with the model, the framework presented through the web site could be a bridge platform to broaden investigations of cell division cycle control among both mathematical modelers and biological experimentalists in a more systematic way.

The web page (http://mpf.biol.vt.edu/Research/Caulobacter/) is designed to accompany the reader in a more in-depth understanding of the mathematical model, and also to get more familiar with the model and the techniques to build it. Experience in building the yeast cell cycle web site (http://mpf.biol.vt.edu/research/budding_yeast_model/pp/) demonstrated the utility of such a platform by providing updated information for both experimentalists and modelers.

Model equations, parameter values, predictions, problems, simulations of wild-type cells and all the mutants, references, and an online simulator are available on the web site as well. Our goal is to help experimental biologists to easily simulate wild-type and relevant mutant scenarios and investigate new experimental designs without getting involved in the mathematical details behind the model.

The online simulator provides for convenient simulation of the model in real time without requiring any expert knowledge of the underlying mathematical techniques.

The publicly available experimental data will also be collected and stored in the online system. This allows mathematical modelers to explore available experimental data in a consistent and convenient format.

4.2. What can be found on the web site?

The web sites http://mpf.biol.vt.edu/research/SWST/Caulobacter/ for the whole cell cycle model (Figure 20) and http://mpf.biol.vt.edu/research/Caulobacter/pp/ for the stalked cell cycle model include the following in-depth information about the model of the cell division cycle in *C. crescentus*.

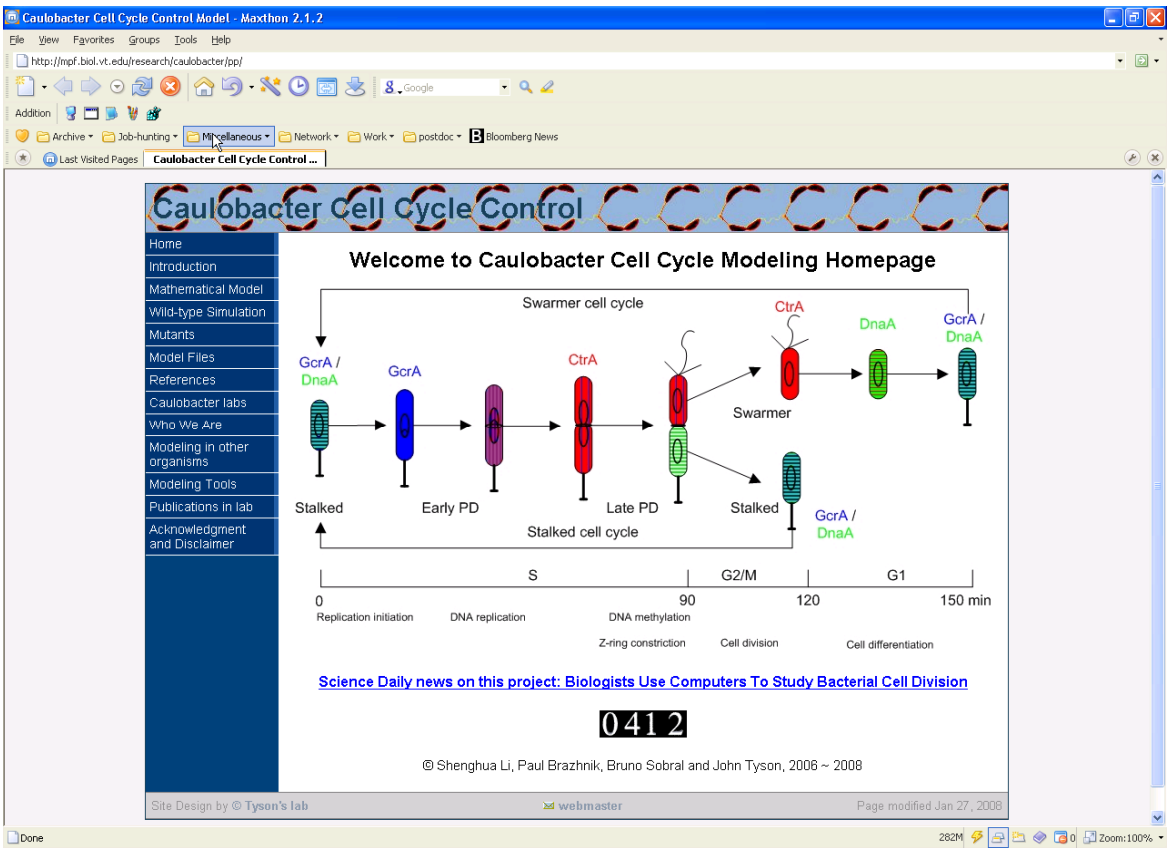

Figure 20. First page of the web site "Modeling the cell division cycle control in *C. crescentus*".

Several sections give in-depth information about the model:

Introduction:

A brief summary of the physiology, biochemistry, genetics and molecular biology of cell division cycle controls in *C. crescentus* are summarized in this section, including a text that walks the reader through the consensus picture. The fundamental mechanism controlling the *C. crescentus* cell cycle (Brazhnik and Tyson, 2006) upon which the full model is based is also summarized in this section.

Mathematical model:

This section is dedicated to the wiring diagram and the mathematical model. Equations,

parameter values and the assumptions used to form these equations are introduced here.

Simulations:

Simulation results for wild-type and mutant cells are listed and classified for reader's convenience. Also, the phenotype description of these mutants and their corresponding original references are listed in detail for easy comparison.

Codes and tools

Scripted codes for models are provided for download in the web pages and their corresponding tools are hyperlinked. The online simulator (see next section) is also linked in these pages.

Online simulator

See Section 4.3.

Others:

Other useful information or links are provided through the web pages for reader's references.

Also, the web page will be updated as the model evolves. As more people will use it, more needs might emerge and many sections will be adapted to meet requests from users.

4.3. The online simulator

For persons unfamiliar with modeling techniques, modifying the model may appear to be a daunting challenge. To help the user in this process, codes for these models are provided for download. Moreover, these codes are compiled into an online simulator system with a user-friendly interface (Figure 21). Both wild-type and mutants can be simulated through this online simulator. The output can be customized to the user's needs. I believe it will be very helpful for experimentalists who do not want to track back to the underlying details of mathematical modeling behind our model. (Thanks to Jason Zwolak for providing the interface script.)

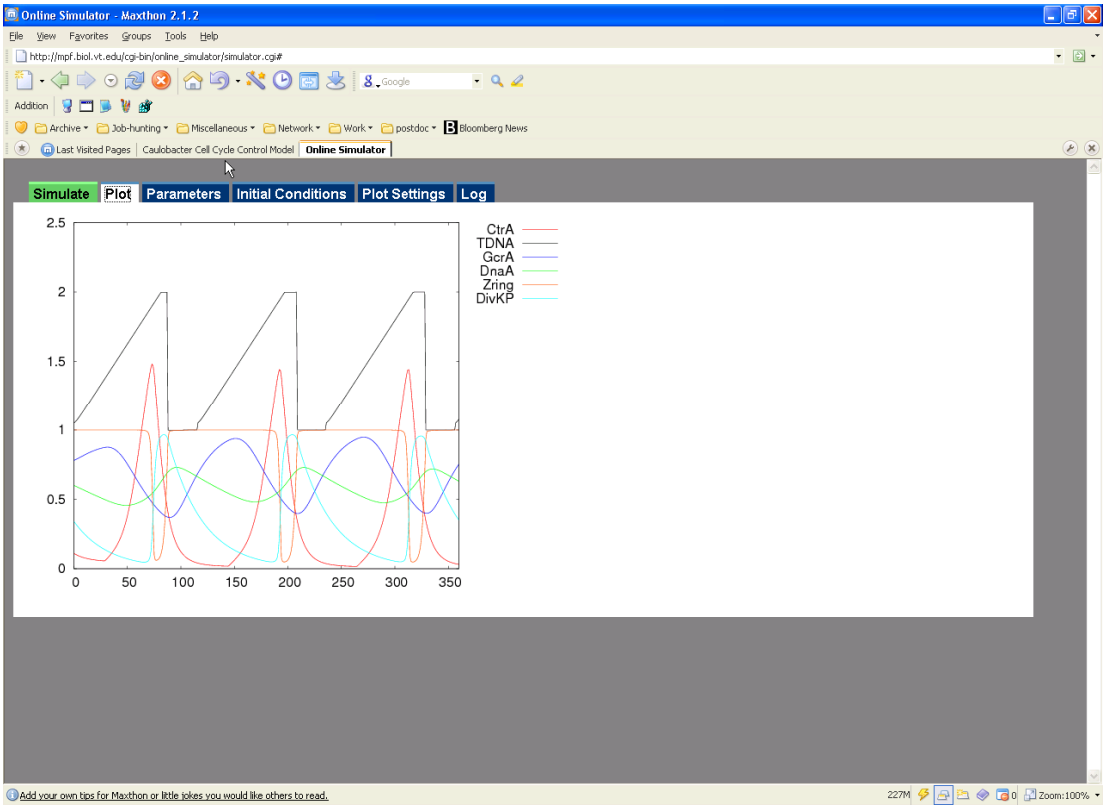

Figure 21.. First page of the online simulator.

Chapter 5. The mechanism of cell division cycle control in *S. meliloti*

C. crescentus is a model organism for cell cycle regulation among alpha-proteobacteria, its mechanism of cell cycle regulation is considered as a generic model to investigate and understand the cell cycle regulation of other species of alpha-proteobacteria (Batut et al., 2004; Hallez et al., 2004). Here, *Sinorhizobium meliloti* is taken to investigate the roles of potential key cell cycle genes (CtrA/CtrA~P, GcrA, and DivK/DivK~P) in the functional transition between free-living cells and symbiotic cells within root nodules of *Medicago truncatula* and other legumes. (This work has been carried out in collaboration with Dr. Bruno Sobral's group at Virginia Bioinformatics Institute.

5.1. The molecular biology of *S. meliloti*

S. meliloti is a rod-shape bacterium that lives in soils or endosymbiotically in nodules of *M. truncatula* and other legumes (Brun and Shimkets, 2000). *S. meliloti* can invade the root of *M. truncatula* and produce a nodule where it functions to fix atmospheric nitrogen into ammonia. *S. meliloti* undergoes symmetric cell division cycle in free-living conditions and in plant root nodules (Figure 22). Recently, several cell cycle-related genes (in particular, *ctrA*, *dnaA*, *divK*, and *ccrM*) where found in *S. meliloti.* Otherwise, little is known on how the cell division cycle in *S. meliloti* is regulated. The free-living bacteria are signaled by flavonoids released from a plant. Bacteria captured by the plant undergo a series of cell divisions and cell differentiation steps to develop into a bacteroid. During this differentiation process, several important genes are expressed or repressed. When a bacteroid is formed, it starts to fix atmospheric nitrogen in a nodule. Most of

bacteriods will die but a few of them might also recover to free-living bacteria (Brun and Shimkets, 2000; Denison, 2000).

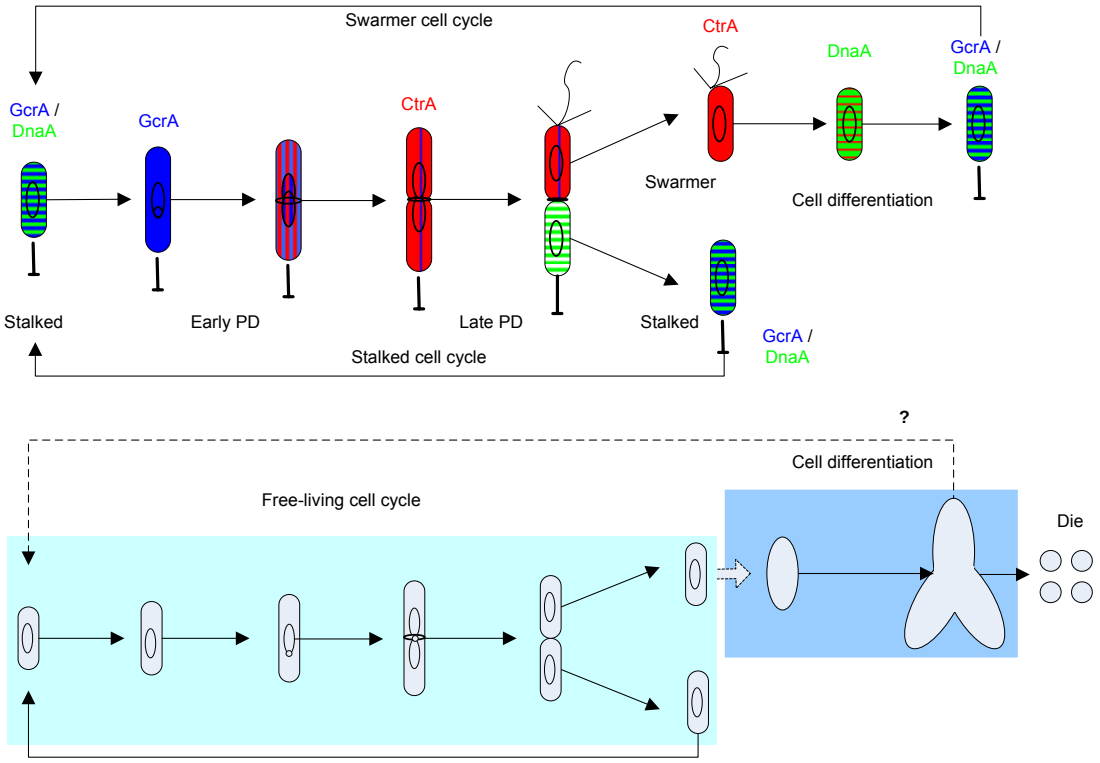

Figure 22.. Physiology of the cell division cycle in *S. meliloti* and *C. crescentus.*

Top. Cell cycle and cell differentiation in *C. crescentus.* Bottom. Cell cycle and cell differentiation (symbiosis) in *S. meliloti.*

Symbiosis of *S. meliloti* and its host has been under intensive investigation for decades. Symbiosis in the host is regarded as a cell differentiation process for *S. meliloti,* where the cell division cycle ceases and specific genes are expressed for nitrogen fixation. Cell cycle control in *S. meliloti* is thought to be tightly connected to its symbiosis, because most cell cycle-related gene expressions vary during the symbiotic process (Capela et al., 2006). However, little is known about regulation of the cell division cycle in *S. meliloti* and what mechanism leads to bacterial differentiation in the host plant.

5.2. The possible genetic similarity of cell cycle controls between *C. crescentus* and *S. meliloti*

S. meliloti, as well as other members of the alpha-proteobacteria family, shares many regulatory proteins of the cell division cycle with *C. crescentus* (Hallez et al., 2004). The genes or their proteins involved into the CtrA control system, including *ctrA*, *dnaA*, *ccrM, pleC, ftsA, ftsZ, cckA, divJ* and *divK,* show high similarity between *C. crescentus* and *S. meliloti* (Table 1). Moreover, CtrA and CcrM proteins are interchangeable between *C. crescentus* and *S. meliloti*, allowing minor modification (Barnett et al., 2001; Reisenauer et al., 1999; Wright et al., 1997). CtrA-dependent regulons are also partially conserved in *S. meliloti* (Hallez et al., 2004). Mutants of *ctrA* and *ccrM* in *C. crescentus* and *S. meliloti* show similar phenotypes of cell cycle deficiency: cell division block and cell filamentation morphology (Barnett et al., 2001; Reisenauer et al., 1999; Wright et al., 1997). In addition, *divK* overexpression mutant in *S. meliloti* has a similar pattern of DivK protein as wild-type cells in *C. crescentus*. As a result, *S. meliloti* mutant cells shown asymmetric cell division as wild-type *C. crescentus* cells (Lam et al., 2003). These homologies and other similarities indicate that the cell division cycle of *C. crescentus* and *S. meliloti* might share a similar regulatory mechanism.

	C.crescentus	*S.meliloti*
ctrA	(Quon et al., 1996)	(Barnett et al., 2001)
gcrA	(Holtzendorff et al., 2004)	
dnaA	(Zweiger and Shapiro, 1994)	(Margolin et al., 1995)
ccrM	(Zweiger et al., 1994)	(Wright et al., 1997)
divL	(Hallez et al., 2004)	(Hallez et al., 2004)
cckA	(Jacobs et al., 1999)	(Hallez et al., 2004)
divK	(Hecht et al., 1995)	(Lam et al., 2003)
divJ	(Wheeler and Shapiro, 1999)	(Hallez et al., 2004)
pleC	(Wheeler and Shapiro, 1999)	(Hallez et al., 2004)
podJ	(Hinz et al., 2003)	
perP	(Chen et al., 2006)	
pleD	(Hecht and Newton, 1995)	
cpdR	(Chen et al., 2006)	
rcdA	(McGrath et al., 2006)	
ftsZ	(Quardokus et al., 1996; Sackett et al., 1998)	(Margolin et al., 1991; Margolin and Long, 1994)
ftsQ	(Sackett et al., 1998)	
ftsA	(Sackett et al., 1998)	(Ma et al., 1997)

Table 1. Experimentally verified homologs of cell cycle-related genes between *C. crescentus* and *S. meliloti.*

5.3. A exploratory model of crucial cell cycle controls in *S. meliloti*

Compared to the details of cell cycle regulation in *C. crescentus*, less is known about the interactions among the cell cycle-related genes and proteins and their functions in controlling the cell cycle of *S. meliloti*. Based on our current knowledge, we proposed a simplified exploratory model of cell cycle control in *S. meliloti*, which only includes CtrA, GcrA and DivK (X and Y introduced for signaling delay between CtrA and DivK) components (Figure 23).

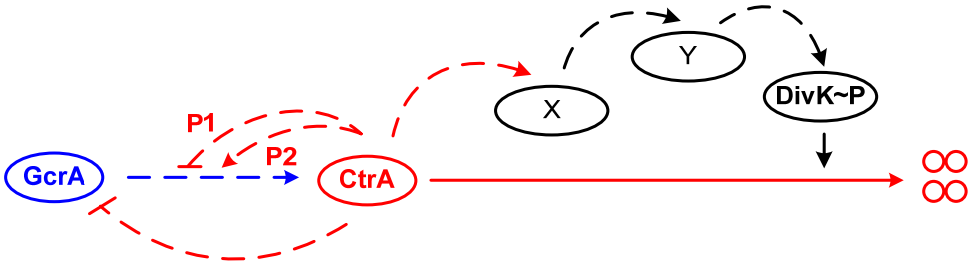

Figure 23. Main feedback loops proposed to control the cell cycle progression in *S.meliloti.*

In the diagram in Figure 23, the production of CtrA protein is regulated by GcrA and CtrA itself, the degradation of CtrA protein is induced by DivK~P (through delayed signaling pathway from X --> Y --> DivK~P). This proposed mechanism is converted into a set of differential equations listed below (Table 2).

$$(1)\ \frac{\mathrm{d}[\mathrm{CtrA}]}{\mathrm{dt}} = k_{\mathrm{s,CtrA\text{-}P1}} \frac{J_{\mathrm{i,CtrA\text{-}CtrA}}{}^{2}}{J_{\mathrm{i,CtrA\text{-}CtrA}}{}^{2} + [\mathrm{CtrA}]^2}[\mathrm{GcrA}] + k_{\mathrm{s,CtrA\text{-}P2}} \frac{[\mathrm{CtrA}]^2}{J_{\mathrm{a,CtrA\text{-}CtrA}}{}^{2} + [\mathrm{CtrA}]^2} - \left(k_{\mathrm{d,CtrA1}} + k_{\mathrm{d,CtrA2}} \frac{[\mathrm{DivK\sim P}]^2}{J_{\mathrm{d,CtrA\text{-}DivK\sim P}}{}^{2} + [\mathrm{DivK\sim P}]^2} \right) \cdot [\mathrm{CtrA}]$$

$$(2)\ \frac{\mathrm{d}[\mathrm{GcrA}]}{\mathrm{dt}} = k_{\mathrm{s,GcrA}} \frac{J_{\mathrm{i,GcrA\text{-}CtrA}}{}^{2}}{J_{\mathrm{i,GcrA\text{-}CtrA}}{}^{2} + [\mathrm{CtrA}]^2} - k_{\mathrm{d,GcrA}}[\mathrm{GcrA}]$$

$$(3)\ \frac{\mathrm{d}[\mathrm{X}]}{\mathrm{dt}} = k_{\mathrm{s,X}}[\mathrm{CtrA}] - k_{\mathrm{d,X}}[\mathrm{X}]$$

$$(4)\ \frac{\mathrm{d}[\mathrm{Y}]}{\mathrm{dt}} = k_{\mathrm{s,Y}}[\mathrm{X}] - k_{\mathrm{d,Y}}[\mathrm{Y}]$$

$$(5)\ \frac{\mathrm{d}[\mathrm{DivK\sim P}]}{\mathrm{dt}} = k_{\mathrm{s,DivK\sim P}}[\mathrm{Y}] - k_{\mathrm{d,DivK\sim P}}[\mathrm{DivK\sim P}]$$

Table 2. Differential equations of the proposed toy model for controlling cell cycle progression in *S.meliloti.*

Numerical simulation of wild-type cells presents us a possible though over-simplified variations of GcrA, CtrA, DivK~P proteins (Figure 24).

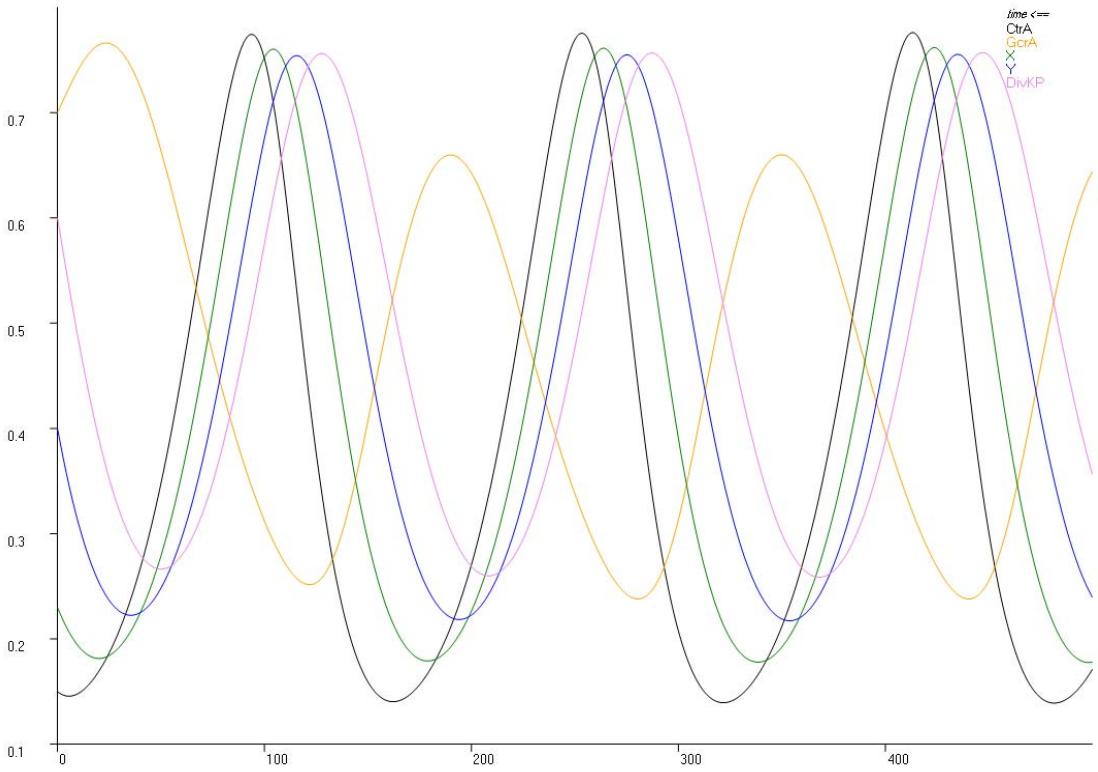

Figure 24. Simulation of wild-type cells in *S.meliloti.*

In this exploratory model, if we introduce *ctrA* deletion or *divK* overexpression mutant, then the cell cycle control system would arrest at a stable steady state with CtrA at a low level and GcrA at a high level. At this state, DNA may be duplicated for several times, if other requirements are satisfied. This scenario might mimic cell differentiation in nature, since during the symbiotic process the cell undergoes several chromosome replications after cell division stops (Brun and Shimkets, 2000).

In another scenario, *gcrA* deletion mutant can lead to a steady state with low level of both GcrA and CtrA. Low GcrA will not satisfy the necessary conditions for DNA replication,

if GcrA is a required component for DNA replication machinery, as we assume in *S. meliloti* from the similar molecular mechanism in *C. crescentus*.

These simple simulations suggest the following experimental design: if *gcrA* deletion mutant introduced experimentally, the variation pattern of GcrA and CtrA proteins could be measured to test the simulation for this scenario. Also, compared with *ctrA* deletion or *divK* overexpression mutants as mentioned above, the differences of variation patterns of these proteins will induce the functional interaction between GcrA and CtrA, if it exists.

5.4. Proposal for investigation of crucial cell cycle control in *S. meliloti*

Based on this model, experiments are being implemented in Dr. Sobral's Lab to investigate the possible interaction between CtrA and GcrA.

The *C. crescentus* model implements a generic pattern of how certain events of the cell cycle are driven by the CtrA-bistable switch (Figure 5). DNA replication, Z-ring closing, cell division and other events in *S. meliloti* cell cycle can also be represented by a mechanism similar to the *C. crescentus* model. Of course, the model assumption needs to be checked specifically for *S. meliloti*.

Chapter 6. Conclusions

6.1. What has the mathematical model accomplished?

The asymmetric cell division cycle in *C. crescentus* is elaborately regulated by an underlying molecular mechanism in time and space (Holtzendorff et al., 2006; McAdams and Shapiro, 2003). The molecular mechanism includes the core regulatory system (DnaA, GcrA and CtrA/CtrA~P), and a delayed feedback system (PodJ, PleC, DivJ, DivK/DivK~P, CckA/CckA~P, CpdR/CpdR~P and other proteins) to differentiate between two different cell development programs (swarmer cell cycle and stalked cell cycle) (Biondi et al., 2006; Goley et al., 2007; Iniesta et al., 2006). The model also includes CcrM and gene methylation state ratchet to govern the DNA replication progression into the cycle (Collier et al., 2007), and Fts proteins for Z-ring assembly and constriction (Harry, 2001). These modular regulatory circuits were organized around a core regulatory mechanism based on a CtrA-bistable switch, as proposed by (Brazhnik and Tyson, 2006). The resulting model of stalked cell cycle control in *C. crescentus* was confirmed by comparing computer simulation to the observed phenotypes of wild-type and mutant *Caulobacter* cells (Li et al., 2008).

In the next step we formulated a model for control of both swarmer and stalked cell cycle in *C. crescentus*. The quantitative schemes consist of rate equations which capture the temporal dynamics of their represented species in Figure 2. The models (the equations and parameters) were fitted to available experimental data (phenotypes of wild-type cells and known mutants, quantitative data points, direct and indirection interactions) from

various literature sources. With these models, we are able to capture (for the first time, to our knowledge) the crucial physiological behaviors of the asymmetric cell division cycle in *C. crescentus* and to illustrate its control in a systematic view.

Our models also provide a wealth of quantitative predictions of the phenotypes of novel mutants as well as the novel phenotypes of known mutants. They provide investigators a zoom-in and zoom-out view of cell cycle control in *C. crescentus* that may guide further experimental designs. Due to *Caulobacter*'s role as a model organism for the investigation of cell division cycle controls in alpha-proteobacteria, the quantitative models presented here can be extended and applied to other species of alpha-proteobacteria (Rhizobia, Brucella spp., Coxiella spp., etc). As an example, the model and results from *C. crescentus* have already been applied in a research project involving *S. meliloti*.

In addition, through our detailed and realistic implementation of the underlying molecular mechanisms using mathematical models, here we confirmed the proposed CtrA-based bistable switch (Brazhnik and Tyson, 2006) as a fundamental core regulatory system for cell cycle control in *C. crescentus*. This confirmation indicates to us that the CtrA-based bistable switch, which shares similarities with the mechanism in yeast and other species, might work as an essential control system not only in *C. crescentus* but also in other bacterial species, even though they might no longer share any conserved genes relevant to cell cycle controls.

The interactive website (http://mpf.biol.vt.edu/research/Caulobacter/SWST/PP/), which includes background information, a description of modeling process, a detailed description of results from our *Caulobacter* model, and the online simulator, provides a useful framework for both mathematical modelers and experimental biologists to get together and communicate more conveniently, sharing experimental data and collaborating on modeling explanations.

6.2. Open problems

Within the mathematical model, we noticed that the dynamic control of asymmetric cell division in *C. crescentus* is not only elaborately coordinated in time, but also deeply dependent on spatial localization of molecules at cell poles. Our model is constrained to general average behavior, ignoring spatial localizations for the most part. However, recent progress on spatial aspects of cell cycle regulation in *Caulobacter* (Ebersbach and Jacobs-Wagner, 2007; Goley et al., 2007) provide useful information on the space-time complexity of this interesting asymmetric cell division control in *C. crescentus*, and we plan to address these issues in a later version of the mathematical model.

Recent measurements of single cell growth and cell division time in *C. crescentus* reveal that the size of single cells exhibits an oscillatory behavior from generation to generation (Siegal-Gaskins and Crosson, 2008). The swarmer cell and the stalked cell exhibit a strong correlation in their generation time and division arrest if they are in the single-cell growth/division scenario. Compared to other bacteria, *Caulobacter* has lower variance in interdivision timing. However, depletion of DivJ increases the variance in interdivision

timing. These facts suggest that a single cell may have its own inheritance in the cell growth and division control from generation to generation. These features can be addressed in the future models.

Moreover, single cells exhibit considerable variation in cell size, even if they are grown under uniform conditions (Siegal-Gaskins and Crosson, 2008). How might intrinsic and extrinsic noise affect progression through the cell cycle for single cells? Future models should address the variability in cell cycle progression exhibited by single cells.

Given that several cell cycle-related gene and proteins are conserved among *C. crescentus* and other species of alpha-proteobacteria, is the core mechanism (the CtrA-based bistable switch) conserved in other alpha-proteobacteria? If so, why might the same core reproductive controls be employed by so many different bacteria, which occupy so many volatile niches in nature?

In this work, several software tools were used to implement the model: XPP, Matlab, Oscill8, PET, Jigcell, etc. Each of them has its own specific advantages compared to others, and thus each one is widely used by the mathematical modelers for different purposes. Most of these software platforms could easily handle all or the majority of requirements for mathematical modeling of cellular signaling network, as we found in this work. Integration of various software tools into a unified interface, which could be convenient for both mathematical modelers and experimental biologists, could be very useful in this field.

6.3. What's next?

1. Incorporate protein localization information into the model, because localization is important for *C. crescentus*'s development, as well as for other bacteria.

2. The model can be used as a basis to investigate the dynamics of flagella, stalk, and Z-ring development during the *C. crescentus* cell cycle, as the development of these components is crucial in the life cycle of *C. crescentus.*

3. Comparative analysis of the molecular regulation of the cell cycle in bacteria and eukaryotes can be insightful for evolutionary biology (Brazhnik and Tyson, 2006). Recent studies have shown that many genes and mechanisms discovered in *C. crescentus* are evolutionarily conserved among other members of the alpha-proteobacteria (Hallez et al., 2004). Thus, the mechanism of cell replication in *C. crescentus* and the mathematical model that we propose may turn out to be extendable to the whole class of alpha-proteobacteria. Working with Dr. Saroj Mohapatra at VBI, we are now trying to explore if a similar molecular mechanism could exist in *Brucella*.

Appendix

A1. Mathematical equations and parameter values

Table S1. Equations of the modified version of minimal model

(Adopted from (Brazhnik and Tyson, 2006))

$$\frac{d[CtrA]}{dt}=\left(k_{s,CtrA\text{-}P1}\frac{J_{i,CtrA\text{-}CtrA}{}^{2}}{J_{i,CtrA\text{-}CtrA}{}^{2}+[CtrA\sim P]^2}[GcrA]+k_{s,CtrA\text{-}P2}\frac{[CtrA\sim P]^2}{J_{a,CtrA\text{-}CtrA}{}^{2}+[CtrA\sim P]^2}\right)$$
$$-\left(k_{d,CtrA1}+k_{d,CtrA2}\frac{[DivK\sim P]^2}{J_{d,CtrA\text{-}DivK\sim P}{}^{2}+[DivK\sim P]^2}\right)\cdot[CtrA]$$
$$-k_{trans,CtrA}[CtrA][CckA\sim P]+k_{trans,CtrA\sim P}[CtrA\sim P]$$

$$\frac{d[CtrA\sim P]}{dt}=-\left(k_{d,CtrA1}+k_{d,CtrA2}\frac{[DivK\sim P]^2}{J_{d,CtrA\text{-}DivK\sim P}{}^{2}+[DivK\sim P]^2}\right)\cdot[CtrA\sim P]$$
$$+k_{trans,CtrA}[CtrA][CckA\sim P]-k_{trans,CtrA\sim P}[CtrA\sim P]$$

$$\frac{d[GcrA]}{dt}=k_{s,GcrA}\frac{J_{i,GcrA\text{-}CtrA}{}^{2}}{J_{i,GcrA\text{-}CtrA}{}^{2}+[CtrA]^2}-k_{d,GcrA}[GcrA]$$

$$\frac{d[Fts]}{dt}=k_{s,Fts}[CtrA][h_{fts}]-k_{d,Fts}[Fts]$$

$$\frac{d[Zring]}{dt}=k_{Zring,open}\frac{1-[Zring]}{J_{a,open}+1-[Zring]}-\left(k_{Zring,closed1}+k_{Zring,closed2}\left(\frac{[Fts]}{J_{Zring\text{-}Fts}}\right)^4\right)\cdot\frac{[Zring]}{J_{a,closed}+[Zring]}$$

$$\frac{d[DivK]}{dt}=k_{s,DivK}[CtrA]+k_{trans,DivK\sim P}[DivK\sim P]-k_{trans,DivK}[DivK](1-[Zring])-k_{d,DivK}[DivK]$$

$$\frac{d[DivK\sim P]}{dt}=-k_{trans,DivK\sim P}[DivK\sim P]+k_{trans,DivK}[DivK](1-[Zring])-k_{d,DivK\sim P}[DivK]$$

$$\frac{d[CckA]}{dt}=k_{s,CckA}-k_{d,CckA}[CckA]+k_{trans,CckA\sim P}[CckA\sim P]-k_{trans,CckA}[CckA]\frac{J_{i,CckA\text{-}DivK\sim P}{}^{2}}{J_{i,CckA\text{-}DivK\sim P}{}^{2}+[DivK\sim P]^2}$$

$$\frac{d[CckA\sim P]}{dt}=-k_{d,CckA}[CckA\sim P]-k_{trans,CckA\sim P}[CckA\sim P]+k_{trans,CckA}[CckA]\frac{J_{i,CckA\text{-}DivK\sim P}{}^{2}}{J_{i,CckA\text{-}DivK\sim P}{}^{2}+[DivK\sim P]^2}$$

Symbols:

k = rate constants, J = binding constants, s = synthesis, d = degradation, a = activation, i = inactivation, trans = transformation (phosphorylation and dephosphorylation in our case).

A. Rate constants, units = min^{-1}

$k_{s,CtrA-P1} = 0.008$, $k_{s,CtrA-P2} = 0.091$	(Domian et al., 1999; Grunenfelder et al., 2001; Holtzendorff et al., 2004)
$k_{d,CtrA1} = 0.002$	(Hung and Shapiro, 2002)
$k_{trams,CtrA} = 0.095$	(Jacobs et al., 2003)
$k_{trams,CtrA\sim P} = 0.025$	(Jacobs et al., 2003)
$k_{d,CtrA2} = 0.15$	(Domian et al., 1997)
$k_{s,GcrA} = 0.046$	(Holtzendorff et al., 2004)
$k_{d,GcrA} = 0.022$	(Collier et al., 2006; Holtzendorff et al., 2004)
$k_{s,Fts} = 0.075$, $k_{d,Fts} = 0.07$	(Martin et al., 2004; Sackett et al., 1998)
$k_{zring,open} = 0.8$	(Judd et al., 2003)
$k_{zring,closed1} = 0.0001$, $k_{zring,closed2} = 0.6$	(Judd et al., 2003)
$k_{s,DivK} = 0.00905$	(Grunenfelder et al., 2001)
$k_{d,DivK} = 0.003$, $k_{d,DivK\sim P} = 0.003$	(Jacobs et al., 2001)
$k_{trans,DivK} = 0.03$, $k_{trans,DivK\sim P} = 0.13$	(Jacobs et al., 2001)
$k_{s,CckA} = 0.0021$	(Jacobs et al., 1999)
$k_{d,CckA} = 0.002$	(Jacobs et al., 1999)
$k_{trans,CckA} = 0.2$	(Jacobs et al., 2003)
$k_{trans,CckA\sim P} = 0.05$	(Jacobs et al., 2003)

B. Binding constants and thresholds (dimensionless)

$J_{i,CtrA-CtrA} = 0.4$	$J_{a,CtrA-CtrA} = 0.4$	$J_{d,CtrA-DivK\sim P} = 0.5$	$J_{i,GcrA-CtrA} = 0.2$
$J_{i,DnaA-GcrA} = 0.5$	$J_{a,DnaA-CtrA} = 0.3$	$J_{a,open} = 0.01$	$J_{a,closed} = 0.1$
$J_{Zring-Fts} = 0.85$	$J_{i,CckA-DivK\sim P} = 0.3$		

C. Initial conditions (dimensionless)

[CtrA] = 0.11	[CtrA~P] = 0.11	[GcrA] = 1.2	[Fts] = 0.23
[Zring] = 1.0	[DivK] = 1.1	[DivK~P] = 0.35	[CckA] = 0.45
[CckA~P] = 0.55			

Table S2. Equations of realistic model for the stalked cell division cycle in *C. crescentus*.

$$\frac{\mathrm{d}[\mathrm{CtrA}]}{\mathrm{dt}}=\left(k_{\mathrm{s,CtrA\text{-}P1}}\frac{{J_{\mathrm{i,CtrA\text{-}CtrA}}}^{2}}{{J_{\mathrm{i,CtrA\text{-}CtrA}}}^{2}+[\mathrm{CtrA}]^2}[\mathrm{GcrA}]+k_{\mathrm{s,CtrA\text{-}P2}}\frac{[\mathrm{CtrA}]^2}{{J_{\mathrm{a,CtrA\text{-}CtrA}}}^{2}+[\mathrm{CtrA}]^2}\right)\cdot[\mathrm{h_{ctrA}}]$$

$$-\left(k_{\mathrm{d,CtrA1}}+k_{\mathrm{d,CtrA2}}\frac{[\mathrm{DivK\sim P}]^2}{{J_{\mathrm{d,CtrA\text{-}DivK\sim P}}}^{2}+[\mathrm{DivK\sim P}]^2}\right)\cdot[\mathrm{CtrA}]$$

$$\frac{\mathrm{d}[\mathrm{GcrA}]}{\mathrm{dt}}=k_{\mathrm{s,GcrA}}\frac{{J_{\mathrm{i,GcrA\text{-}CtrA}}}^{2}}{{J_{\mathrm{i,GcrA\text{-}CtrA}}}^{2}+[\mathrm{CtrA}]^2}[\mathrm{DnaA}]-k_{\mathrm{d,GcrA}}[\mathrm{GcrA}]$$

$$\frac{\mathrm{d}[\mathrm{DnaA}]}{\mathrm{dt}}=k_{\mathrm{s,DnaA}}\frac{{J_{\mathrm{i,DnaA\text{-}GcrA}}}^{2}}{{J_{\mathrm{i,DnaA\text{-}GcrA}}}^{2}+[\mathrm{GcrA}]^2}\cdot\frac{[\mathrm{CtrA}]^2}{{J_{\mathrm{a,DnaA\text{-}CtrA}}}^{2}+[\mathrm{CtrA}]^2}\cdot(2-[\mathrm{h_{cori}}])-k_{\mathrm{d,DnaA}}[\mathrm{DnaA}]$$

$$\frac{\mathrm{d}[\mathrm{Fts}]}{\mathrm{dt}}=k_{\mathrm{s,Fts}}[\mathrm{CtrA}][\mathrm{h_{fts}}]-k_{\mathrm{d,Fts}}[\mathrm{Fts}]$$

$$\frac{\mathrm{d}[\mathrm{Zring}]}{\mathrm{dt}}=k_{\mathrm{Zring,open}}\frac{1-[\mathrm{Zring}]}{\mathrm{J_{a,open}}+1-[\mathrm{Zring}]}-\left(k_{\mathrm{Zring,closed1}}+k_{\mathrm{Zring,closed2}}\left(\frac{[\mathrm{Fts}]}{J_{\mathrm{Zring\text{-}Fts}}}\right)^4\right)\cdot\frac{[\mathrm{Zring}]}{J_{\mathrm{a,closed}}+[\mathrm{Zring}]}$$

$$\frac{\mathrm{d}[\mathrm{DivK}]}{\mathrm{dt}}=k_{\mathrm{s,DivK}}[\mathrm{CtrA}]+k_{\mathrm{trans,DivK\sim P}}[\mathrm{DivK\sim P}]-k_{\mathrm{trans,DivK}}[\mathrm{DivK}](1-[\mathrm{Zring}])-k_{\mathrm{d,DivK}}[\mathrm{DivK}]$$

$$\frac{\mathrm{d}[\mathrm{DivK\sim P}]}{\mathrm{dt}}=-k_{\mathrm{trans,DivK\sim P}}[\mathrm{DivK\sim P}]+k_{\mathrm{trans,DivK}}[\mathrm{DivK}](1-[\mathrm{Zring}])-k_{\mathrm{d,DivK\sim P}}[\mathrm{DivK}]$$

$$\frac{\mathrm{d}[\mathrm{I}]}{\mathrm{dt}}=k_{\mathrm{s,I}}[\mathrm{CtrA}][\mathrm{h_{ccrM}}]-k_{\mathrm{d,I}}[\mathrm{I}]$$

$$\frac{\mathrm{d}[\mathrm{CcrM}]}{\mathrm{dt}}=k_{\mathrm{s,CcrM}}[\mathrm{I}]-k_{\mathrm{d,CcrM}}[\mathrm{CcrM}]$$

$$\frac{\mathrm{d}[\mathrm{h_{cori}}]}{\mathrm{dt}}=-k_{\mathrm{m,cori}}\frac{[\mathrm{CcrM}]^4}{{J_{\mathrm{m,cori}}}^{4}+[\mathrm{CcrM}]^4}[\mathrm{h_{cori}}],\ \text{when } [\mathrm{Elong}]=P_{\mathrm{elong}},\ [\mathrm{h_{cori}}]=1$$

$$\frac{\mathrm{d}[\mathrm{h_{ctrA}}]}{\mathrm{dt}}=-k_{\mathrm{m,ctrA}}\frac{[\mathrm{CcrM}]^4}{{J_{\mathrm{m,ctrA}}}^{4}+[\mathrm{CcrM}]^4}[\mathrm{h_{ctrA}}],\ \text{when } [\mathrm{Elong}]=P_{\mathrm{ctrA}},\ [\mathrm{h_{ctrA}}]=1$$

$$\frac{\mathrm{d}[\mathrm{h_{ccrM}}]}{\mathrm{dt}}=-k_{\mathrm{m,ccrM}}\frac{[\mathrm{CcrM}]^4}{{J_{\mathrm{m,ccrM}}}^{4}+[\mathrm{CcrM}]^4}[\mathrm{h_{ccrM}}],\ \text{when } [\mathrm{Elong}]=P_{\mathrm{ccrM}},\ [\mathrm{h_{ccrM}}]=1$$

$$\frac{\mathrm{d}[\mathrm{h_{fts}}]}{\mathrm{dt}}=-k_{\mathrm{m,fts}}\frac{[\mathrm{CcrM}]^4}{{J_{\mathrm{m,ftsQ}}}^{4}+[\mathrm{CcrM}]^4}[\mathrm{h_{fts}}],\ \text{when } [\mathrm{Elong}]=P_{\mathrm{fts}},\ [\mathrm{h_{fts}}]=1$$

$$\frac{d[Ini]}{dt} = k_{a,Ini} \frac{([DnaA]/\theta_{DnaA})^4 ([GcrA]/\theta_{GcrA})^4}{1 + ([DnaA]/\theta_{DnaA})^4 + ([GcrA]/\theta_{GcrA})^4 + ([CtrA]/\theta_{CtrA})^4 + [h_{cori}]/\theta_{Cori}}$$

When [Ini] reaches [Ini]=0.05, [Ini] is reset to 0.

$$\frac{d[Elong]}{dt} = k_{elong} \frac{[Elong]^4}{[Elong]^4 + P_{elong}{}^4} \cdot Count$$

When [Ini] reaches [Ini] = 0.05, [Elong] is reset as [Elong] = [Elong] + Count · 0.05.

When [Elong] reaches [Elong] = Count/2 – 1, it is reset as [Elong] = 0.

$$\frac{d[DNA]}{dt} = k_{elong} \frac{[Elong]^4}{[Elong]^4 + P_{elong}{}^4} \cdot Count$$

When [Ini] = 0.05, [DNA] = [DNA] + Count · 0.05.

When Z-ring fully constricts, [DNA] = [DNA]/2.

Initially Count = 2. When [Ini] reaches [Ini] = 0.05, Count = Count · 2.

When Z-ring fully constricts, Count = Count/2.

Symbols:

k = rate constants (min^{-1}), J = binding constants (dimensionless), θ = thresholds (dimensionless), P = position of genes relative to origin site (dimensionless). s = synthesis, d = degradation, a = activation, i = inactivation, trans = transformation (phosphorylation and dephosphorylation in our case).

Variables:

1. [I] = activity of an intermediate component or pathway that introduces a time delay between CtrA activation of *ccrM* transcription and the accumulation of CcrM protein.

2. [Fts] = a lumped representation of Fts series proteins as required for Z-ring constriction.

3. [Zring] = state of the Z-ring; for fully open [Zring] = 1 and for fully constricted [Zring] = 0.

4. [Ini] and [Elong] represent the initiation of DNA replication forks and the progression of forks along the DNA molecule, respectively.

5. [DNA] = the total amount of DNA in the cell, scaled to the amount of a full chromosome. The total DNA starts to increase when initiation finishes and is updated with same speed as the elongation [Elong] grows. Both the elongation and the total amount of DNA increase with possible multiple chromosome

replication in specific mutants.

6. Count = a number of chromosomes in the cell. Count is used here in case the multiple initiation happens from several chromosomes when cell does not divide (initiation then is assumed to happen simultaneously on all chromosomes). When initiation is successfully accomplished, 'Count' is doubled. $[h_{cori}]$, $[h_{ccrM}]$, $[h_{ctrA}]$ and $[h_{fts}]$ represent probabilities of hemimethylated states of C_{ori} & *dnaA*, *ccrM*, *ctrA* and *fts* genes, respectively, during the cell division cycle.

7. All other variables represent scaled protein concentrations.

Notes on equations:

1. The rates of protein expression from *ctrA* promoter can be written as a product of the probability of transcription factors to be bound and the probability that the locus is hemimethylated. The same assumption is also adopted for *dnaA*, *fts*, and *ccrM* expression. Specifically, *dnaA* expression is assumed to be half-decreased when the gene is hemimethylated reflecting the experimental facts that *dnaA* has a peak expression only during the swarmer-to-stalked cell transition and that corresponding protein level during the stalked cell cycle is almost constant (Zweiger and Shapiro, 1994). Furthermore, as *dnaA* is very close to C_{ori}, and in order to avoid introducing an extra variable $[h_{dnaA}]$, we use $(2 - [h_{cori}])$ term to describe the methylation effect on DnaA production rate.

2. The rates of $[h_{cori}]$, $[h_{ccrM}]$, $[h_{ctrA}]$ and $[h_{fts}]$ are designed to switch on abruptly when the DNA replication fork passes the gene's position on the chromosome. They switch off as the new DNA strand is methylated by a high concentration of CcrM.

3. Initiation of DNA synthesis is designed to occur when DnaA and GcrA are sufficiently abundant, CtrA concentration is low, and C_{ori} is fully methylated. Protein binding to the origin site is assumed to be cooperative ($n_H = 4$). Hemimethylation, on the other hand, is more likely to inhibit re-licensing in a non-cooperative manner. The rate of DNA elongation is nearly constant after initiation, until the forks reach the termination site, when [Elong] = 1. The total amount of newly synthesized DNA and the number of chromosomes per cell are calculated based on initiation events, DNA elongation, and Z-ring constriction.

Table S3. Basal parameter values for the wild-type stalked-cell division cycle

A. Rate constants, units = min^{-1}	
$k_{s,CtrA-P1} = 0.0083$, $k_{s,CtrA-P2} = 0.073$	(Domian et al., 1999; Grunenfelder et al., 2001; Holtzendorff et al., 2004)
$k_{d,CtrA1} = 0.002$	(Hung and Shapiro, 2002)
$k_{d,CtrA2} = 0.15$	(Domian et al., 1997)
$k_{s,GcrA} = 0.045$	(Holtzendorff et al., 2004)
$k_{d,GcrA} = 0.022$	(Collier et al., 2006; Holtzendorff et al., 2004)
$k_{s,DnaA} = 0.0165$	(Martin et al., 2004; Sackett et al., 1998)
$k_{d,DnaA} = 0.007$	(Judd et al., 2003)
$k_{s,Fts} = 0.063$, $k_{d,Fts} = 0.035$	(Judd et al., 2003)
$k_{zring,open} = 0.8$	(Grunenfelder et al., 2001)
$k_{zring,closed1} = 0.0001$, $k_{zring,closed2} = 0.6$	(Jacobs et al., 2001)
$k_{s,DivK} = 0.0054$	(Jacobs et al., 2001)
$k_{d,DivK} = 0.002$, $k_{d,DivK\sim P} = 0.002$	(Jacobs et al., 2001)
$k_{trans,DivK} = 0.5$, $k_{trans,DivK\sim P} = 0.0295$	(Jacobs et al., 2001)
$k_{s,I} = 0.08$, $k_{d,I} = 0.04$	(Grunenfelder et al., 2001)
$k_{s,CcrM} = 0.072$	(Grunenfelder et al., 2001)
$k_{d,CcrM} = 0.07$	(Stephens et al., 1996)
$k_{m,cori} = 0.4$, $k_{m,ctrA} = 0.4$	(Stephens et al., 1996)
$k_{m,ccrM} = 0.4$, $k_{m,fts} = 0.4$	(Stephens et al., 1996)
$k_{a,Ini} = 0.01$	(Quon et al., 1998)
$k_{elong} = 0.006$	(Dingwall and Shapiro, 1989)

B. Binding constants and thresholds (dimensionless)			
$J_{i,CtrA-CtrA} = 0.4$	$J_{a,CtrA-CtrA} = 0.45$	$J_{d,CtrA-DivK\sim P} = 0.55$	$J_{i,GcrA-CtrA} = 0.2$
$J_{i,DnaA-GcrA} = 0.5$	$J_{a,DnaA-CtrA} = 0.3$	$J_{a,open} = 0.01$	$J_{a,closed} = 0.1$
$J_{Zring-Fts} = 0.78$	$J_{m,cori} = 0.95$	$J_{m,ctrA} = 0.95$	$J_{m,ccrM} = 0.95$

$J_{m,fts}$ = 0.95	θ_{CtrA} = 0.2	θ_{GcrA} = 0.45	θ_{DnaA} = 0.6
θ_{cori} = 0.0002			

C. Gene positions on the chromosome (dimensionless, from http://ecocyc.org)

P_{elong}^{*} = P_{DnaA} =0.05	P_{ccrM} = 0.2	P_{ctrA} = 0.375	P_{fts} = 0.625

*P_{elong} is assumed to be the end point of replication initiation and the starting point of chromosome elongation.

Table S4. Initial values of model variables, for a newborn, wild-type stalked cell

[CtrA] = 0.11	[GcrA] = 0.78	[DnaA] = 0.6	[Fts] = 0.29
[Zring] = 1.0	[DivK] = 0.66	[DivK~P] = 0.34	[I] = 0.11
[CcrM] = 0.5	[h_{ctrA}] = 0	[h_{ccrM}] = 0	[h_{fts}] = 0
[h_{cori}] = 1.0	[Ini] = 0.0	[Elong] = 0.05	[DNA] = 1.05

Table S5. Altered parameter values for mutant simulations

k' represents a constant rate of constitutive synthesis added to the relevant differential equation.

Genotype	Parameter changes
Δ*ctrA*-P1	$k_{s,ctrA\text{-}P1} = 0.001245$ (15% of WT)
Δ*ctrA*	$k_{s,ctrA\text{-}P1} = k_{s,ctrA\text{-}P2} = 0$
ctrA401^{ts}	$k_{s,ctrA\text{-}P1}$, $k_{s,ctrA\text{-}P2}$: 75%, 55% and 15% of WT
ctrA^{op}	$k' = 0.0813$
P_{xylX}-*ctrA*Δ3	$k_{d,ctrA2} = 0.015$ (10% of WT), $k' = 0.0813$
Δ*gcrA*	$k_{s,GcrA} = 0$
Δ*dnaA*	$k_{s,DnaA} = 0$
Δ*ftsQ*	$k_{s,Fts} = 0$
Δ*ftsZ*	Zring = 1 (Z-ring never fully constricts)
Δ*divK*	$k_{s,DivK} = 0$
divK341^{cs}	$k_{d,ctrA2} = 0$
divK$_{D53A}$, etc.	$k_{trans,DivK} = 0$
divK^{op}	$k' = 0.027$ (5 x WT)
Δ*ccrM*	$k_{s,I} = 0$
ccrM^{op}	$k' = 0.08$
Lon null	$k_{d,CcrM} = 0$
Δ*dnaC, dnaE*^{ts}	$k_{elong} = 0$
Δ*ctrA-P2*	$k_{s,ctrA\text{-}P2} = 0$
gcrA^{op}	$k' = 0.0225$ (50% of WT)
dnaA^{op}	$k' = 0.00825$ (50% of WT)

Table S6. Equations of the model for the whole cell division cycle in *C. crescentus*.

To track stalked cell cycle, H = 1; to track swarmer cell cycle, H = 0.

$$\frac{\mathrm{d[CtrA]}}{\mathrm{dt}} = \left(k_{\mathrm{s,CtrA\text{-}P1}} \frac{J_{\mathrm{i,CtrA\text{-}CtrA}}{}^{2}}{J_{\mathrm{i,CtrA\text{-}CtrA}}{}^{2} + [\mathrm{CtrA}]^2} [\mathrm{GcrA}] + k_{\mathrm{s,CtrA\text{-}P2}} \frac{[\mathrm{CtrA}]^2}{J_{\mathrm{a,CtrA\text{-}CtrA}}{}^{2} + [\mathrm{CtrA}]^2} \right) \cdot [\mathrm{h_{ctrA}}] - \left(k_{\mathrm{d,CtrA1}} + k_{\mathrm{d,CtrA2}} \frac{[\mathrm{DivK\sim P}]^2}{J_{\mathrm{d,CtrA\text{-}DivK\sim P}}{}^{2} + [\mathrm{DivK\sim P}]^2} \right) \cdot [\mathrm{CtrA}]$$

$$\frac{\mathrm{d[GcrA]}}{\mathrm{dt}} = k_{\mathrm{s,GcrA}} \frac{J_{\mathrm{i,GcrA\text{-}CtrA}}{}^{2}}{J_{\mathrm{i,GcrA\text{-}CtrA}}{}^{2} + [\mathrm{CtrA}]^2} \cdot [\mathrm{DnaA}] - k_{\mathrm{d,GcrA}} \cdot [\mathrm{GcrA}]$$

$$\frac{\mathrm{d[DnaA]}}{\mathrm{dt}} = \left(k_{\mathrm{s,DnaA1}} \frac{J_{\mathrm{i,DnaA\text{-}GcrA}}{}^{2}}{J_{\mathrm{i,DnaA\text{-}GcrA}}{}^{2} + [\mathrm{GcrA}]^2} + k_{\mathrm{s,DnaA2}} \frac{[\mathrm{CtrA}]^2}{J_{\mathrm{a,DnaA\text{-}CtrA}}{}^{2} + [\mathrm{CtrA}]^2} \right) \cdot (2 - [\mathrm{h_{cori}}]) - k_{\mathrm{d,DnaA}} \cdot [\mathrm{DnaA}]$$

$$\frac{\mathrm{d[Fts]}}{\mathrm{dt}} = k_{\mathrm{s,Fts}} \cdot [\mathrm{CtrA}] \cdot [\mathrm{h_{fts}}] - k_{\mathrm{d,Fts}} \cdot [\mathrm{Fts}]$$

$$\frac{\mathrm{d[Zring]}}{\mathrm{dt}} = k_{\mathrm{Zring,open}} \frac{1 - [\mathrm{Zring}]}{\mathrm{J_{a,open}} + 1 - [\mathrm{Zring}]} - \left(k_{\mathrm{Zring,closed1}} + k_{\mathrm{Zring,closed2}} \left(\frac{[\mathrm{Fts}]}{J_{\mathrm{Zring\text{-}Fts}}} \right)^4 \right) \cdot \frac{[\mathrm{Zring}]}{J_{\mathrm{a,closed}} + [\mathrm{Zring}]}$$

$$\frac{\mathrm{d[DivK]}}{\mathrm{dt}} = k_{\mathrm{s,DivK}} \frac{[\mathrm{CtrA}]^2}{J_{\mathrm{a,DivK\text{-}CtrA}}{}^{2} + [\mathrm{CtrA}]^2} + k_{\mathrm{trans,DivK\sim P}} [\mathrm{DivK\sim P}] \cdot \frac{[\mathrm{PodJL}]^2}{J_{\mathrm{a,DivK\sim P\text{-}PodJL}}{}^{2} + [\mathrm{PodJL}]^2} \cdot (1 + \mathrm{H} \cdot ([\mathrm{Zring}] - 1)) - k_{\mathrm{trans,DivK}} [\mathrm{DivK}] \frac{[\mathrm{DivJ}]^2}{J_{\mathrm{a,DivK\text{-}DivJ}}{}^{2} + [\mathrm{DivJ}]^2} \cdot ([\mathrm{Zring}] + \mathrm{H} \cdot (1 - [\mathrm{Zring}])) - k_{\mathrm{d,DivK}} [\mathrm{DivK}]$$

$$\frac{\mathrm{d[DivK\sim P]}}{\mathrm{dt}} = - k_{\mathrm{trans,DivK\sim P}} [\mathrm{DivK\sim P}] \cdot \frac{[\mathrm{PodJL}]^2}{J_{\mathrm{a,DivK\sim P\text{-}PodJL}}{}^{2} + [\mathrm{PodJL}]^2} \cdot (1 + \mathrm{H} \cdot ([\mathrm{Zring}] - 1)) + k_{\mathrm{trans,DivK}} [\mathrm{DivK}] \cdot \frac{[\mathrm{DivJ}]^2}{J_{\mathrm{a,DivK\text{-}DivJ}}{}^{2} + [\mathrm{DivJ}]^2} \cdot ([\mathrm{Zring}] + \mathrm{H} \cdot (1 - [\mathrm{Zring}])) - k_{\mathrm{d,DivK\sim P}} [\mathrm{DivK}]$$

$$\frac{\mathrm{d[I]}}{\mathrm{dt}} = k_{\mathrm{s,I}} \cdot [\mathrm{CtrA}] \cdot [\mathrm{h_{ccrM}}] - k_{\mathrm{d,I}} \cdot [\mathrm{I}]$$

$$\frac{\mathrm{d[CcrM]}}{\mathrm{dt}} = k_{\mathrm{s,CcrM}} \cdot [\mathrm{I}] - k_{\mathrm{d,CcrM}} \cdot [\mathrm{CcrM}]$$

$$\frac{\mathrm{d[PodJL]}}{\mathrm{dt}} = k_{\mathrm{s,PodJL}} \frac{J_{\mathrm{i,PodJL\text{-}CtrA}}{}^{2}}{J_{\mathrm{i,PodJL\text{-}CtrA}}{}^{2} + [\mathrm{CtrA}]^2} \cdot [\mathrm{GcrA}] \cdot [\mathrm{DnaA}] - \left(k_{\mathrm{d1,PodJL}} \cdot [\mathrm{PodJL}] + k_{\mathrm{d2,PodJL}} \frac{[\mathrm{PerP}]^2}{J_{\mathrm{d,PodJL\text{-}PerP}}{}^{2} + [\mathrm{PerP}]^2} \cdot [\mathrm{PodJL}] \right) - k_{\mathrm{sep,PodJL}} [\mathrm{PodJL}] \cdot \mathrm{H} \cdot \frac{1 - [\mathrm{Zring}]}{J_{\mathrm{sep,PodJL}} + 1 - [\mathrm{Zring}]}$$

$$\frac{\mathrm{d[PerP]}}{\mathrm{dt}} = k_{\mathrm{s,PerP}} \cdot [\mathrm{PodJL}] \cdot [\mathrm{CtrA}] - k_{\mathrm{d,PerP}} [\mathrm{PerP}] - k_{\mathrm{sep,PerP}} [\mathrm{PerP}] \cdot \mathrm{H} \cdot \frac{1 - [\mathrm{Zring}]}{J_{\mathrm{sep,PerP}} + 1 - [\mathrm{Zring}]}$$

$$\frac{\mathrm{d[DivJ]}}{\mathrm{dt}} = k_{\mathrm{s,DivJ1}} + k_{\mathrm{s,DivJ1}} \cdot \frac{(1 - \mathrm{H}) \cdot J_{\mathrm{i,DivJ\text{-}PodJL}}{}^{2}}{J_{\mathrm{i,DivJ\text{-}PodJL}}{}^{2} + [\mathrm{PodJL}]^2} - k_{\mathrm{d1,PDivJ}} [\mathrm{DivJ}] - k_{\mathrm{sep,DivJ}} \cdot \frac{(1 - \mathrm{H}) \cdot (1 - [\mathrm{Zring}])}{J_{\mathrm{sep,DivJ}} + (1 - [\mathrm{Zring}])} \cdot [\mathrm{DivJ}]$$

$$\frac{d[h_{cori}]}{dt} = -k_{m,cori}\frac{[CcrM]^4}{J_{m,cori}^{\ 4} + [CcrM]^4}\cdot[h_{cori}],\ \text{when } [Elong]=P_{elong},\ [h_{cori}]=1$$

$$\frac{d[h_{ctrA}]}{dt} = -k_{m,ctrA}\frac{[CcrM]^4}{J_{m,ctrA}^{\ 4} + [CcrM]^4}\cdot[h_{ctrA}],\ \text{when } [Elong]=P_{ctrA},\ [h_{ctrA}]=1$$

$$\frac{d[h_{ccrM}]}{dt} = -k_{m,ccrM}\frac{[CcrM]^4}{J_{m,ccrM}^{\ 4} + [CcrM]^4}\cdot[h_{ccrM}],\ \text{when } [Elong]=P_{ccrM},\ [h_{ccrM}]=1$$

$$\frac{d[h_{fts}]}{dt} = -k_{m,fts}\frac{[CcrM]^4}{J_{m,ftsQ}^{\ 4} + [CcrM]^4}\cdot[h_{fts}],\ \text{when } [Elong]=P_{fts},\ [h_{fts}]=1$$

$$\frac{d[Ini]}{dt} = k_{a,Ini}\frac{([DnaA]/\theta_{DnaA})^4\cdot([GcrA]/\theta_{GcrA})^4}{1+([DnaA]/\theta_{DnaA})^4+([GcrA]/\theta_{GcrA})^4+([CtrA]/\theta_{CtrA})^4+[h_{cori}]/\theta_{Cori}}$$

When the DNA initiation variable [Ini] reaches [Ini]=0.05, [Ini] is reset to 0.

$$\frac{d[Elong]}{dt} = k_{elong}\frac{[Elong]^4}{[Elong]^4 + P_{elong}^{\ 4}}\cdot Count$$

When [Ini] reaches [Ini] = 0.05, [Elong] is reset as [Elong] = [Elong] + Count · 0.05.

When [Elong] reaches [Elong] = Count/2 − 1, it is reset as [Elong] = 0.

$$\frac{d[DNA]}{dt} = k_{elong}\frac{[Elong]^4}{[Elong]^4 + P_{elong}^{\ 4}}\cdot Count$$

When DNA initiation variable [Ini] = 0.05, [DNA] = [DNA] + Count · 0.05.

When Z-ring fully constricts, [DNA] = [DNA]/2.

Initially Count = 2. When [Ini] reaches [Ini] = 0.05, Count = Count · 2.

When Z-ring fully constricts, Count = Count/2.

Table S7. Parameter values for the wild-type cell division cycle.

A. Rate constants, units = min^{-1}			
$k_{s,CtrA-P1} = 0.0083$	$k_{s,CtrA-P2} = 0.073$	$k_{d,CtrA1} = 0.002$	$k_{d,CtrA2} = 0.15$
$k_{s,GcrA} = 0.055$	$k_{d,GcrA} = 0.022$	$k_{s,DnaA1} = 0.0031$	$k_{s,DnaA2} = 0.0026$
$k_{d,DnaA} = 0.007$	$k_{s,Fts} = 0.068$	$k_{d,Fts} = 0.035$	$k_{zring,open} = 0.8$
$k_{zring,closed1} = 0.0001$	$k_{zring,closed2} = 0.6$	$k_{s,DivK} = 0.0027$	$k_{d,DivK} = 0.002$
$k_{d,DivK\sim P} = 0.002$	$k_{trans,DivK} = 0.15$	$k_{trans,DivK\sim P} = 0.6$	$k_{s,I} = 0.08$
$k_{d,I} = 0.04$	$k_{s,CcrM} = 0.072$	$k_{d,CcrM} = 0.07$	$k_{m,cori} = 0.4$
$k_{m,ctrA} = 0.4$	$k_{m,ccrM} = 0.4$	$k_{m,fts} = 0.4$	$k_{a,Ini} = 0.05$
$k_{elong} = 0.006$	$k_{s,PodJL} = 0.07$	$k_{d,PodJL1} = 0.05$	$k_{d,PodJL2} = 0.002$
$k_{s,PerP} = 0.07$	$k_{d,PerP} = 0.02$	$k_{s,DivJ1} = 0.002$	$k_{s,DivJ2} = 0.03$
$k_{d,DivJ} = 0.002$	$k_{sep,PodJL} = 0.3$	$k_{sep,PerP} = 0..011$	$k_{sep,DivJ} = 0.3$
B. Binding constants and thresholds (dimensionless)			
$J_{i,CtrA-CtrA} = 0.4$	$J_{a,CtrA-CtrA} = 0.45$	$J_{d,CtrA-DivK\sim P} = 0.55$	$J_{i,GcrA-CtrA} = 0.2$
$J_{i,DnaA-GcrA} = 0.6$	$J_{a,DnaA-CtrA} = 0.3$	$J_{a,open} = 0.01$	$J_{a,closed} = 0.1$
$J_{Zring-Fts} = 0.78$	$J_{a,DivK-CtrA} = 0.06$	$J_{a,DivK\sim P-PodJL} = 0.3$	$J_{a,DivK-DivJ} = 0.3$
$J_{m,cori} = 0.95$	$J_{m,ctrA} = 0.95$	$J_{m,ccrM} = 0.95$	$J_{m,fts} = 0.95$
$\theta_{CtrA} = 0.2$	$\theta_{GcrA} = 0.45$	$\theta_{DnaA} = 0.6$	$\theta_{cori} = 0.0002$
$J_{iPodJL-CtrA} = 0.2$	$J_{d,PodJL-PerP} = 0.45$	$J_{a,PerPCtrA} = 0.1$	$J_{i,DivJ-PodJL} = 0.1$
$J_{sep,PodJL} = 0.3$	$J_{sep,PerP} = 0.3$	$J_{sep,DivJ} = 0.3$	
C. Initial values of model variables, for a newborn, wild-type stalked cell			
[CtrA] = 0.04	[GcrA] = 0.78	[DnaA] = 0.6	[Fts] = 0.29
[Zring] = 1.0	[DivK] = 0.66	[DivK~P] = 0.34	[I] = 0.11
[CcrM] = 0.39	$[h_{ctrA}] = 0$	$[h_{ccrM}] = 0$	$[h_{fts}] = 0$
$[h_{cori}] = 1.0$	[Ini] = 0.0	[Elong] = 0.05	[DNA] = 1.05
[PodJL/PleC] = 0.1	[PerP] = 0.45	[DivJ] = 1.0	

Table S8. The improved version of the whole cell division cycle in *C. crescentus*

Tracks of different cell cycles

(1) For stalked cell: $H = 1$; for swarmer cell: $H = 0$.

Three major regulators : DnaA, GcrA, CtrA/CtrA~P

(2) $$\frac{\mathrm{d[CtrA]}}{\mathrm{dt}} = \left(k_{\mathrm{s,CtrA\text{-}P1}} \frac{J_{\mathrm{i,CtrA\text{-}CtrA\sim P}}{}^{2}}{J_{\mathrm{i,CtrA\text{-}CtrA\sim P}}{}^{2} + [\mathrm{CtrA\sim P}]^2} [\mathrm{GcrA}] + k_{\mathrm{s,CtrA\text{-}P2}} \frac{[\mathrm{CtrA\sim P}]^2}{J_{\mathrm{a,CtrA\text{-}CtrA\sim P}}{}^{2} + [\mathrm{CtrA\sim P}]^2} \right) \cdot [\mathrm{h_{ctrA}}]$$

$$- \left(k_{\mathrm{d,CtrA1}} + k_{\mathrm{d,CtrA2}} \frac{[\mathrm{DivK\sim P}]^2}{J_{\mathrm{d,CtrA\text{-}DivK\sim P}}{}^{2} + [\mathrm{DivK\sim P}]^2} \frac{[\mathrm{CpdR}]^4}{J_{\mathrm{d,CtrA\text{-}CpdR}}{}^{4} + [\mathrm{CpdR}]^4} \frac{[\mathrm{RcdA}]^4}{J_{\mathrm{d,CtrA\text{-}RcdA}}{}^{4} + [\mathrm{RcdA}]^4} \right) \cdot [\mathrm{CtrA}]$$

$$+ k_{\mathrm{trans,CtrA\sim P}} [\mathrm{CtrA\sim P}] - k_{\mathrm{trans,CtrA}} [\mathrm{CtrA}][\mathrm{CckA\sim P}]$$

(3) $$\frac{\mathrm{d[CtrA\sim P]}}{\mathrm{dt}} = - \left(k_{\mathrm{d,CtrA1}} + k_{\mathrm{d,CtrA2}} \frac{[\mathrm{DivK\sim P}]^2}{J_{\mathrm{d,CtrA\text{-}DivK\sim P}}{}^{2} + [\mathrm{DivK\sim P}]^2} \frac{[\mathrm{CpdR}]^4}{J_{\mathrm{d,CtrA\text{-}CpdR}}{}^{4} + [\mathrm{CpdR}]^4} \frac{[\mathrm{RcdA}]^4}{J_{\mathrm{d,CtrA\text{-}RcdA}}{}^{4} + [\mathrm{RcdA}]^4} \right) \cdot [\mathrm{CtrA\sim P}]$$

$$- k_{\mathrm{trans,CtrA\sim P}} [\mathrm{CtrA\sim P}] + k_{\mathrm{trans,CtrA}} [\mathrm{CtrA}][\mathrm{CckA\sim P}]$$

(4) $$\frac{\mathrm{d[DnaA]}}{\mathrm{dt}} = \left(k_{\mathrm{s,DnaA1}} \cdot \frac{J_{\mathrm{i,DnaA\text{-}GcrA}}{}^{2}}{J_{\mathrm{i,DnaA\text{-}GcrA}}{}^{2} + [\mathrm{GcrA}]^2} + k_{\mathrm{s,DnaA2}} \cdot \frac{[\mathrm{CtrA\sim P}]^2}{J_{\mathrm{a,DnaA\text{-}CtrA\sim P}}{}^{2} + [\mathrm{CtrA\sim P}]^2} \right) \cdot (2 - [\mathrm{h_{cori}}]) - k_{\mathrm{d,DnaA}} [\mathrm{DnaA}]$$

(5) $$\frac{\mathrm{d[GcrA]}}{\mathrm{dt}} = k_{\mathrm{s,GcrA}} \frac{J_{\mathrm{i,GcrA\text{-}CtrA\sim P}}{}^{2}}{J_{\mathrm{i,GcrA\text{-}CtrA}}{}^{2} + [\mathrm{CtrA\sim P}]^2} [\mathrm{DnaA}] - k_{\mathrm{d,GcrA}} [\mathrm{GcrA}]$$

DNA synthesis

(6) $$\frac{\mathrm{d[Ini]}}{\mathrm{dt}} = k_{\mathrm{a,Ini}} \frac{([\mathrm{DnaA}]/\theta_{\mathrm{DnaA}})^4 \cdot ([\mathrm{GcrA}]/\theta_{\mathrm{GcrA}})^4}{1 + ([\mathrm{DnaA}]/\theta_{\mathrm{DnaA}})^4 + ([\mathrm{GcrA}]/\theta_{\mathrm{GcrA}})^4 + ([\mathrm{CtrA\sim P}]/\theta_{\mathrm{CtrA\sim P}})^4 + ([\mathrm{GcrA}]/\theta_{\mathrm{GcrA}})^4 \cdot ([\mathrm{CtrA\sim P}]/\theta_{\mathrm{CtrA\sim P}})^4 + ([\mathrm{h_{Cori}}]/\theta_{\mathrm{Cori}})^4}$$

When the DNA initiation variable [Ini] reaches [Ini] = Count * 0.05, [Ini] is reset to 0.

(7) $$\frac{\mathrm{d[Elong]}}{\mathrm{dt}} = k_{\mathrm{elong}} \frac{[\mathrm{Elong}]}{[\mathrm{Elong}] + P_{\mathrm{elong}}{}^{4}} * \mathrm{Count}$$

When [Ini] = Count * 0.05, [Elong] = [Elong] + Count * 0.05. When [Elong] = Count/2, [Elong] = 0.

(8) $$\frac{\mathrm{d[DNA]}}{\mathrm{dt}} = k_{\mathrm{elong}} \frac{[\mathrm{Elong}]}{[\mathrm{Elong}] + P_{\mathrm{elong}}{}^{4}} * \mathrm{Count}$$, when [Ini] = Count * 0.05, [DNA] = [DNA] + Count * 0.05.

(9) Count = 1 (The total number of chromosomes).

When [Ini] = Count * 0.05, Count = Count * 2. When Z-ring is constricted, Count = Count/2.

CcrM and DNA methylation

(10) $$\frac{\mathrm{d}[\mathrm{I}]}{\mathrm{dt}} = k_{\mathrm{s,I}} \frac{[\mathrm{CtrA{\sim}P}]^2}{J_{\mathrm{a,I\text{-}CtrA{\sim}P}}{}^2 + [\mathrm{CtrA{\sim}P}]^2} [\mathrm{h}_{\mathrm{ccrM}}] - k_{\mathrm{d,I}}[\mathrm{I}]$$

(11) $$\frac{\mathrm{d}[\mathrm{CcrM}]}{\mathrm{dt}} = k_{\mathrm{s,CcrM}}[\mathrm{I}] - k_{\mathrm{d,CcrM}}[\mathrm{CcrM}]$$

(12) $$\frac{\mathrm{d}[\mathrm{h}_{\mathrm{Cori}}]}{\mathrm{dt}} = -k_{\mathrm{m,Cori}} \frac{[\mathrm{CcrM}]^4}{J_{\mathrm{m,Cori}}{}^4 + [\mathrm{CcrM}]^4} [\mathrm{h}_{\mathrm{Cori}}], \text{ when } [\mathrm{Elong}] = P_{\mathrm{elong}}, [\mathrm{h}_{\mathrm{Cori}}] = 1$$

(13) $$\frac{\mathrm{d}[\mathrm{h}_{\mathrm{ctrA}}]}{\mathrm{dt}} = -k_{\mathrm{m,ctrA}} \frac{[\mathrm{CcrM}]^4}{J_{\mathrm{m,ctrA}}{}^4 + [\mathrm{CcrM}]^4} [\mathrm{h}_{\mathrm{ctrA}}], \text{ when } [\mathrm{Elong}] = P_{\mathrm{ctrA}}, [\mathrm{h}_{\mathrm{ctrA}}] = 1$$

(14) $$\frac{\mathrm{d}[\mathrm{h}_{\mathrm{ccrM}}]}{\mathrm{dt}} = -k_{\mathrm{m,ccrM}} \frac{[\mathrm{CcrM}]^4}{J_{\mathrm{m,ccrM}}{}^4 + [\mathrm{CcrM}]^4} [\mathrm{h}_{\mathrm{ccrM}}], \text{ when } [\mathrm{Elong}] = P_{\mathrm{ccrM}}, [\mathrm{h}_{\mathrm{ccrM}}] = 1$$

(15) $$\frac{\mathrm{d}[\mathrm{h}_{\mathrm{ftsZ}}]}{\mathrm{dt}} = -k_{\mathrm{m,ftsZ}} \frac{[\mathrm{CcrM}]^4}{J_{\mathrm{m,ftsZ}}{}^4 + [\mathrm{CcrM}]^4} [\mathrm{h}_{\mathrm{ftsZ}}], \text{ when } [\mathrm{Elong}] = P_{\mathrm{ftsZ}}, [\mathrm{h}_{\mathrm{ftsZ}}] = 1$$

PodJL/PleC, DivJ localization

$$(16)\ \frac{d[PodJL]}{dt} = k_{s,\,PodJL}\frac{J_{i,\,PodJL\text{-}CtrA\sim P}^{\ 2}}{J_{i,\,PodJL\text{-}CtrA\sim P}^{\ 2} + [CtrA\sim P]^2}[GcrA][DnaA] - k_{d1,\,PodJL}[PodJL]$$
$$- k_{d2,\,PodJL}\frac{[PerP]^2}{J_{d,\,PodJL\text{-}PerP}^{\ 2} + [PerP]^2}[PodJL] - k_{sep,\,PodJL}[PodJL]\cdot H\cdot\frac{(1 - [Z])}{J_{sep,\,PodJL} + (1 - [Z])}$$

$$(17)\ \frac{d[PerP]}{dt} = k_{s,\,PerP}[CtrA\sim P][PodJL] - k_{d,\,PerP}[PerP] - k_{sep,\,PerP}[PerP]\cdot H\cdot\frac{(1 - [Z])}{J_{sep,\,PerP} + (1 - [Z])}$$

$$(18)\ \frac{d[DivJ]}{dt} = k_{s,\,DivJ1} + (1-H)\cdot k_{s,\,DivJ2}\frac{J_{i,\,DivJ\text{-}PodJL}^{\ 2}}{J_{i,\,DivJ\text{-}PodJL}^{\ 2} + [PodJL]^2} - k_{d,\,DivJ}[DivJ] - k_{sep,\,DivJ}[DivJ]\cdot(1-H)\cdot\frac{(1 - [Z])}{J_{sep,\,DivJ} + (1 - [Z])}$$

DivK/DivK~P transformation

$$(19)\ \frac{d[DivK]}{dt} = k_{s,\,DivK}\frac{[CtrA\sim P]^2}{J_{a,\,DivK\text{-}CtrA\sim P}^{\ 2} + [CtrA\sim P]^2} - k_{d,\,DivK}[DivK]$$
$$+ k_{trans,\,DivK\sim P}[DivK\sim P]\cdot\frac{[PodJL]^2}{J_{DivK\sim P\text{-}PodJL}^{\ 2} + [PodJL]^2}\cdot(1 + H\cdot([Z] - 1))$$
$$- k_{trans,\,DivK}[DivK]\cdot\frac{[DivJ]^2}{J_{DivK\text{-}DivJ}^{\ 2} + [DivJ]^2}\cdot([Z] + H\cdot(1 - [Z]))$$

$$(20)\ \frac{d[DivK\sim P]}{dt} = - k_{trans,\,DivK\sim P}[DivK\sim P]\cdot\frac{[PodJL]^2}{J_{DivK\sim P\text{-}PodJL}^{\ 2} + [PodJL]^2}\cdot(1 + H\cdot([Z] - 1))$$
$$+ k_{trans,\,DivK}[DivK]\cdot\frac{[DivJ]^2}{J_{DivK\text{-}DivJ}^{\ 2} + [DivJ]^2}\cdot([Z] + H\cdot(1 - [Z]))$$
$$- k_{d,\,DivK\sim P}[DivK\sim P]$$

RcdA, CckA~P, CpdR, RcdA and ParA-ADP

$$(21)\ \frac{d[CckA\sim P]}{dt} = -k_{trans,CckA\sim P}[CckA\sim P] + k_{trans,CckA}\left([CckA]_{tot} - [CckA]\right)\frac{J_{i,CckA\text{-}DivK\sim P}^{\ 2}}{J_{i,CckA\text{-}DivK\sim P}^{\ 2} + [DivK\sim P]^2}$$

$$(22)\ \frac{d[CpdR]}{dt} = k_{trans,CpdR\sim P}\left([CpdR]_{tot} - [CpdR]\right) - k_{trans,CpdR}[CpdR]\frac{[CckA\sim P]^2}{J_{a,CpdR\text{-}CckA\sim P}^{\ 2} + [CckA\sim P]^2}$$

$$(23)\ \frac{d[ParAADP]}{dt} = k_{trans,ParAATP}\left([ParA]_{tot} - [ParAADP]\right) - k_{trans,ParAADP}\left(Count - 1\right)[ParAADP]$$

$$(24)\ \frac{d[RcdA]}{dt} = k_{s,RcdA}\frac{[CtrA\sim P]^2}{J_{a,RcdA\text{-}CtrA\sim P}^{\ 2} + [CtrA\sim P]^2} - k_{d,RcdA}[RcdA]$$

Z-ring formation, constriction

(25) $\frac{\mathrm{d[FtsQ]}}{\mathrm{dt}} = k_{\mathrm{s,FtsQ}} \frac{[\mathrm{CtrA\sim P}]^2}{J_{\mathrm{a,\ FtsQ\text{-}CtrA\sim P}}{}^2 + [\mathrm{CtrA\sim P}]^2} \frac{[\mathrm{h_{Cori}}]^4}{J_{\mathrm{FtsQ\text{-}DNA}}{}^4 + [\mathrm{h_{Cori}}]^4} - k_{\mathrm{d,FtsQ}}[\mathrm{FtsQ}]$

(26) $\frac{\mathrm{d[FtsZ]}}{\mathrm{dt}} = k_{\mathrm{s,FtsZ}} \frac{J_{\mathrm{i,\ FtsZ\text{-}CtrA\sim P}}{}^2}{J_{\mathrm{i,\ FtsZ\text{-}CtrA\sim P}}{}^2 + [\mathrm{CtrA\sim P}]^2} [\mathrm{DnaA}] \cdot (1 - [\mathrm{h_{ftsZ}}]) - \left(k_{\mathrm{d,FtsZ1}} + k_{\mathrm{d,FtsZ2}}(1 - [\mathrm{Zing}]) + k_{\mathrm{d,FtsZ3}}(1 - [\mathrm{Z}])\right) \cdot [\mathrm{FtsZ}]$

(27) $\frac{\mathrm{d[Zring]}}{\mathrm{dt}} = k_{\mathrm{s,Zring}} \cdot (1 - [\mathrm{Zring}]) \cdot [\mathrm{FtsZ}]$ When DNA replication starts, it grows. When Zring constricts ([Z] = 0), [Zring] = 0.

(28) $\frac{\mathrm{d[Z]}}{\mathrm{dt}} = k_{\mathrm{Z,open}} \frac{1 - [\mathrm{Z}]}{\mathrm{J_{a,open}} + 1 - [\mathrm{Z}]} - \left(k_{\mathrm{Z,closed1}} + k_{\mathrm{Z,closed2}} \frac{[\mathrm{FtsQ}]^4}{1 + [\mathrm{FtsQ}]^4} \frac{\left([\mathrm{Zing}]/\theta_{\mathrm{Zring}}\right)^4}{1 + \left([\mathrm{Zing}]/\theta_{\mathrm{Zring}}\right)^4 + \left([\mathrm{ParAADP}]/\theta_{\mathrm{ParAADP}}\right)^4} \right) \cdot \frac{[\mathrm{Z}]}{J_{\mathrm{a,closed}} + [\mathrm{Z}]}$

Symbols:

k = rate constants ($\mathrm{min^{-1}}$), J = binding constants (dimensionless), θ = thresholds (dimensionless), P = position of genes relative to origin site (dimensionless). s = synthesis, d = degradation, a = activation, i = inactivation, trans = transformation (phosphorylation and dephosphorylation in our case), m = methylation, sep = separation due to Z-ring constriction, tot = total amount of proteins.

Variables:

(1). H is designed to track different cell cycles (for stalked cell cycle H = 1, for swarmer cell cycle H = 0) in the model simulation.

(2) & (3). CtrA and CtrA~P are separately represented here. The phosphorylation of CtrA is assumed to be simply regulated by CckA~P. CtrA~P dephosphorylation is assumed to be at an unknown but constant rate. CtrA/CtrA~P proteolysis is assumed to be equally regulated by a combination of DivK~P, CpdR, and RcdA.

(4) ~ (14). See Table S2 for detailed description.

(15). Here, DNA methylation on the regulation of *fts* genes is explicitly represented by *ftsZ* gene.

(16) ~ (18). PodJ is varied during the cell cycle and contributes to the localization and function of PleC (see detailed description in Section 2.1.3). Due to their similar variation during the cell cycle, we combined them as only one state variable in our model. $\mathrm{PodJ_L}$/PleC, PerP, and DivJ are fully separated into different progeny cells after cell division. To track their difference due to cell division, the separation term, which is triggered by H variable/parameter, is introduced for them. In addition, DivJ is available for function during the swarmer-to-stalked cell cycle transition, once $\mathrm{PodJ_L}$/PleC is truncated/released. This specific event only happens during the swarmer cell cycle and therefore is represented by the trigger of H variable/parameter.

(19) & (20). DivK/DivK~P phosphorylation and dephosphorylation are regulated by PleC and DivJ. In our

formulation, $PodJ_L$/PleC and DivJ are the corresponding state variables for their phosphorylation and dephosphorylation, combined with a signal from Z-ring constriction.

(21) ~ (23). The total amount of CckA, CpdR and ParA are simplified to be constant based on our current known knowledge (see detailed description in Section 2.1). Therefore, their small production and degradation are neglected in our model.

(24). RcdA is produced, localized and contributes to recruiting CtrA/CtrA~P for their proteolysis. Here we describe its production and degradation only, which presents a state variable as a necessary condition for CtrA/CtrA~P degradation.

(25). FtsQ is only produced in the predivisional cell phase where DNA is replicated (Wortinger et al., 2000). In swarmer cell FtsQ is not produced even CtrA/CtrA~P is high. Therefore, in our model, FtsQ only can be produced when it detected that DNA is replicating.

(26). The total decrease of FtsZ protein comes from: a basal background degradation, a rapid degradation after Z-ring constriction, and the component for Z-ring assembly (Zring variable).

(27). Zring variable represents the Ring at the mid-cell plane. It is a structure assembled before it constricts. In our model it disappears immediately when fully constricted (the *Z* variable becomes zero below).

(28). *Z* is a phenomenological variable in our model to represent the Z-ring closure event, which has important consequential effect on the protein separation into different progeny cells. *Z* constriction ($Z = 0$) happens when the combined conditions (Assembled Zring, high FtsQ and low ParA-ADP) are satisfied.

Table S9. Parameter values for the wild-type cell division cycle.

A. Rate constants, units = min^{-1}			
$k_{s,CtrA-P1} = 0.0083$	$k_{s,CtrA-P2} = 0.073$	$k_{d,CtrA1} = 0.002$	$k_{d,CtrA2} = 0.15$
$k_{s,GcrA} = 0.055$	$k_{d,GcrA} = 0.022$	$k_{s,DnaA1} = 0.0031$	$k_{s,DnaA2} = 0.0026$
$k_{d,DnaA} = 0.007$	$k_{s,Fts} = 0.068$	$k_{d,Fts} = 0.035$	$k_{zring,open} = 0.8$
$k_{zring,closed1} = 0.0001$	$k_{zring,closed2} = 0.6$	$k_{s,DivK} = 0.0027$	$k_{d,DivK} = 0.002$
$k_{d,DivK\sim P} = 0.002$	$k_{trans,DivK} = 0.15$	$k_{trans,DivK\sim P} = 0.6$	$k_{s,I} = 0.08$
$k_{d,I} = 0.04$	$k_{s,CcrM} = 0.072$	$k_{d,CcrM} = 0.07$	$k_{m,cori} = 0.4$
$k_{m,ctrA} = 0.4$	$k_{m,ccrM} = 0.4$	$k_{m,fts} = 0.4$	$k_{a,Ini} = 0.05$
$k_{elong} = 0.006$	$k_{s,PodJL} = 0.07$	$k_{d,PodJL1} = 0.05$	$k_{d,PodJL2} = 0.002$
$k_{s,PerP} = 0.07$	$k_{d,PerP} = 0.02$	$k_{s,DivJ1} = 0.002$	$k_{s,DivJ2} = 0.03$
$k_{d,DivJ} = 0.002$	$k_{sep,PodJL} = 0.3$	$k_{sep,PerP} = 0..011$	$k_{sep,DivJ} = 0.3$
B. Binding constants and thresholds (dimensionless)			
$J_{i,CtrA-CtrA} = 0.4$	$J_{a,CtrA-CtrA} = 0.45$	$J_{d,CtrA-DivK\sim P} = 0.55$	$J_{i,GcrA-CtrA} = 0.2$
$J_{i,DnaA-GcrA} = 0.6$	$J_{a,DnaA-CtrA} = 0.3$	$J_{a,open} = 0.01$	$J_{a,closed} = 0.1$
$J_{Zring-Fts} = 0.78$	$J_{a,DivK-CtrA} = 0.06$	$J_{a,DivK\sim P-PodJL} = 0.3$	$J_{a,DivK-DivJ} = 0.3$
$J_{m,cori} = 0.95$	$J_{m,ctrA} = 0.95$	$J_{m,ccrM} = 0.95$	$J_{m,fts} = 0.95$
$\theta_{CtrA} = 0.2$	$\theta_{GcrA} = 0.45$	$\theta_{DnaA} = 0.6$	$\theta_{cori} = 0.0002$
$J_{iPodJL-CtrA} = 0.2$	$J_{d,PodJL-PerP} = 0.45$	$J_{a,PerPCtrA} = 0.1$	$J_{i,DivJ-PodJL} = 0.1$
$J_{sep,PodJL} = 0.3$	$J_{sep,PerP} = 0.3$	$J_{sep,DivJ} = 0.3$	
C. Initial values of model variables, for a newborn, wild-type stalked cell			
[CtrA] = 0.04	[GcrA] = 0.78	[DnaA] = 0.6	[Fts] = 0.29
[Zring] = 1.0	[DivK] = 0.66	[DivK~P] = 0.34	[I] = 0.11
[CcrM] = 0.39	$[h_{ctrA}] = 0$	$[h_{ccrM}] = 0$	$[h_{fts}] = 0$
$[h_{cori}] = 1.0$	[Ini] = 0.0	[Elong] = 0.05	[DNA] = 1.05
[PodJL/PleC] = 0.1	[PerP] = 0.45	[DivJ] = 1.0	

Table S10. Altered parameter values for mutant simulations.

k' represents a constant rate of constitutive synthesis added to the relevant differential equation

Genotype	Parameter changes
ctrA mutants	
Δ*ctrA*-P1	$k_{s,ctrA\text{-}P1} = 0.0024$ (15% of WT)
Δ*ctrA-P2*	$k_{s,ctrA\text{-}P2} = 0$
Δ*ctrA*	$k_{s,ctrA\text{-}P1} = k_{s,ctrA\text{-}P2} = 0$
ctrA401^{ts}	$k_{s,ctrA\text{-}P1}$, $k_{s,ctrA\text{-}P2}$: 75%, 40% and 10% of WT
ctrAD51E	$k_{s,ctrA\text{-}P1} = k_{s,ctrA\text{-}P2} = 0$, $k_{trans,CtrA\sim P} = 0$,
	$k' = 0.16$ was added to [CtrA~P] equation
*ctrA*Δ3Ω	$k_{d,ctrA2} = 0.0375$ (15% of WT)
*ctrAD51E*Δ3Ω	$k_{s,ctrA\text{-}P1} = k_{s,ctrA\text{-}P2} = 0$, $k_{trans,CtrA\sim P} = 0$,
	$k' = 0.16$ was added to [CtrA~P] equation
	$k_{d,ctrA2} = 0.0375$ (15% of WT)
ctrA constitutively expression	$k_{s,ctrA\text{-}P1} = k_{s,ctrA\text{-}P2} = 0$, $k' = 0.048$
ctrA^{op} (*P*$_{xylX}$-*ctrA*Δ3)	$k' = 0.16$
gcrA mutants	
Δ*gcrA*	$k_{s,GcrA} = 0$
gcrA^{op}	$k' = 0.0225$ (50% of WT) or 0.0605 (110% of WT)
dnaA mutants	
Δ*dnaA*	$k_{s,DnaA} = 0$
Δ*dnaA* rescued	$k_{s,DnaA} = 0.05$ at $120 < t < 300$ min
	$k_{s,DnaA} = 0.0$ at $300 < t < 450$ min
	$k_{s,DnaA} = 0.05$ at $t > 450$ min
dnaA^{op}	$k' = 0.0053$ (100% of WT)

divK mutants

Δ*divK*	$k_{s,DivK} = 0$
divK341^{cs}	$k_{d,ctrA2} = 0$
divK341^{cs} rescued	$k_{d,ctrA2} = 0$ at $120 < t < 190$ min
	$k_{d,ctrA2} = 0.25$ (100% of WT) at $t > 190$ min
divK$_{D53A}$, etc.	$k_{trans,DivK} = 0$
divK^{op}	$k' = 0.024$ (10 x WT)

ccrM mutants

Δ*ccrM*	$k_{s,I} = 0$
ccrM^{op}	$k' = 0.09$
Lon null	$k_{d,CcrM} = 0$

DNA mutant

Δ*dnaC, dnaE*^{ts}	$k_{elong} = 0$

Fts mutants

Δ*ftsQ*	$k_{s,FtsQ} = 0$
Δ*ftsZ*	$k_{s,FtsZ} = 0$

parA mutants

Δ*parA*	ParAtot = 0.5, $k_{trans,ParA\text{-}ADP} = 0.0$
parA^{op}	ParAtot = 1.5, $k_{trans,ParA\text{-}ADP} = 0.0$

rcdA mutants

Δ*rcdA*	$k_{s,RcdA} = 0$
Δ*rcdA* + *ctrAD51E*	$k_{s,RcdA} = 0$
	$k_{s,ctrA\text{-}P1} = k_{s,ctrA\text{-}P2} = 0$, $k_{trans,CtrA\sim P} = 0$,
	$k' = 0.16$ was added to [CtrA~P] equation
rcdA^{op}	$k' = 0.023$

cckA mutants

Δ*cckA (cckATS1)*	$CckA_{tot} = 0.1$
CckA unphosphorylated	$k_{trans,CckA} = 0$
cpdR mutants	
Δ*cpdR*	$CpdR_{tot} = 0.0$
cpdRD51A (CpdR unphosphorylated)	$k_{trans,CpdR} = 0$
$cpdR^{op}$	$CpdR_{tot} = 1.5$ (50% overexpression of WT)
CpdR fully phosphorylated	$k_{trans,CpdRP} = 0$
divJ mutants	
Δ*divJ*	$k_{s,DivJ1} = k_{s,DivJ2} = 0$
Δ*divJ* + $divK^{op}$	$k_{s,DivJ1} = 0.0014$, $k_{s,DivJ2} = 0.0175$ (70% of WT, can be lower or higher) $k' = 0.024$ (10 x WT)
pleC/podJ mutants	
Δ*pleC* and Δ*podJ*	$k_{s,PodJL} = 0$
$pleC^{op}$ and $podJ^{op}$	$k_{s,PodJL} = 0$, $k' = 0.043$ (100% of WT)
perP mutants	
Δ*perP*	$k_{s,PerP} = 0$
perP constitutive expression	$k_{s,PerP} = 0$, $k' = 0.04$ (100% of WT)

Bibliography

Aaron, M., Charbon, G., Lam, H., Schwarz, H., Vollmer, W., and Jacobs-Wagner, C. (2007). The tubulin homologue FtsZ contributes to cell elongation by guiding cell wall precursor synthesis in Caulobacter crescentus. MolMicrobiol *64*, 938-952.

Ausmees, N., and Jacobs-Wagner, C. (2003). Spatial and temporal control of differentiation and cell cycle progression in Caulobacter crescentus. AnnuRevMicrobiol *57*, 225-247.

Barnett, M.J., Hung, D.Y., Reisenauer, A., Shapiro, L., and Long, S.R. (2001). A homolog of the CtrA cell cycle regulator is present and essential in Sinorhizobium meliloti. Journal of Bacteriology *183*, 3204-3210.

Bartosik, A.A., and Jagura-Burdzy, G. (2005). Bacterial chromosome segregation. Acta Biochim Pol *52*, 1-34.

Batut, J., Andersson, S.G., and O'Callaghan, D. (2004). The evolution of chronic infection strategies in the alpha-proteobacteria. Nat Rev Microbiol *2*, 933-945.

Bignell, C., and Thomas, C.M. (2001). The bacterial ParA-ParB partitioning proteins. J Biotechnol *91*, 1-34.

Biondi, E.G., Reisinger, S.J., Skerker, J.M., Arif, M., Perchuk, B.S., Ryan, K.R., and Laub, M.T. (2006). Regulation of the bacterial cell cycle by an integrated genetic circuit. Nature.

Brazhnik, P., Li, S., Sobral, B., and Tyson, J.J. (2007). Computational Model of the Division Cycle of Caulobacter crescentus. AIP Conference Proceedings *952*, 219-228.

Brazhnik, P., and Tyson, J.J. (2006). Cell cycle control in bacteria and yeast: a case of convergent evolution? Cell Cycle *5*, 522-529.

Brun, Y.V., and Shimkets, L.J. (2000). Prokaryotic Development (Washington,DC, ASM Press).

Capela, D., Filipe, C., Bobik, C., Batut, J., and Bruand, C. (2006). Sinorhizobium meliloti differentiation during symbiosis with alfalfa: a transcriptomic dissection. Mol Plant Microbe Interact *19*, 363-372.

Chen, J.C., Hottes, A.K., McAdams, H.H., McGrath, P.T., Viollier, P.H., and Shapiro, L. (2006). Cytokinesis signals truncation of the PodJ polarity factor by a cell cycle-regulated protease. EMBO J *25*, 377-386.

Chen, J.C., and Stephens, C. (2007). Bacterial cell cycle: completing the circuit. CurrBiol *17*, R203-R206.

Chen, K.C., Calzone, L., Csikasz-Nagy, A., Cross, F.R., Novak, B., and Tyson, J.J. (2004). Integrative analysis of cell cycle control in budding yeast. Molecular biology of the cell *15*, 3841-3862.

Ciliberto, A., Petrus, M.J., Tyson, J.J., and Sible, J.C. (2003). A kinetic model of the cyclin E/Cdk2 developmental timer in Xenopus laevis embryos. Biophysical chemistry *104*, 573-589.

Collier, J., McAdams, H.H., and Shapiro, L. (2007). A DNA methylation ratchet governs progression through a bacterial cell cycle. Proc Natl Acad Sci U S A *104*, 17111-17116.

Collier, J., Murray, S.R., and Shapiro, L. (2006). DnaA couples DNA replication and the expression of two cell cycle master regulators. EMBO J *25*, 346-356.

Collier, J., and Shapiro, L. (2007). Spatial complexity and control of a bacterial cell cycle. Curr Opin Biotechnol *18*, 333-340.

Cross, F.R., Archambault, V., Miller, M., and Klovstad, M. (2002). Testing a mathematical model of the yeast cell cycle. Molecular biology of the cell *13*, 52-70.

Cross, F.R., Schroeder, L., Kruse, M., and Chen, K.C. (2005). Quantitative characterization of a mitotic cyclin threshold regulating exit from mitosis. Molecular biology of the cell *16*, 2129-2138.

Denison, R.F. (2000). Legume sanctions and the evolution of symbiotic cooperation by rhizobia. American Naturalist *156*, 567-576.

Dingwall, A., and Shapiro, L. (1989). Rate, Origin, and Bidirectionality of Caulobacter Chromosome-Replication As Determined by Pulsed-Field Gel-Electrophoresis. Proceedings of the National Academy of Sciences of the United States of America *86*, 119-123.

Domian, I.J., Quon, K.C., and Shapiro, L. (1996). The control of temporal and spatial organization during the Caulobacter cell cycle. CurrOpinGenetDev *6*, 538-544.

Domian, I.J., Quon, K.C., and Shapiro, L. (1997). Cell type-specific phosphorylation and proteolysis of a transcriptional regulator controls the G1-to-S transition in a bacterial cell cycle. Cell *90*, 415-424.

Domian, I.J., Reisenauer, A., and Shapiro, L. (1999). Feedback control of a master bacterial cell-cycle regulator. ProcNatlAcadSciUSA *96*, 6648-6653.

Easter, J., and Gober, J.W. (2002). ParB-stimulated nucleotide exchange regulates a switch in functionally distinct ParA activities. Molecular Cell *10*, 427-434.

Ebersbach, G., and Jacobs-Wagner, C. (2007). Exploration into the spatial and temporal mechanisms of bacterial polarity. Trends Microbiol *15*, 101-108.

Goldbeter, A., and Koshland, D.E. (1981). An Amplified Sensitivity Arising from Covalent Modification in Biological Systems. PNAS *78*, 6840-6844.

Goley, E.D., Iniesta, A.A., and Shapiro, L. (2007). Cell cycle regulation in Caulobacter: location, location, location. J Cell Sci *120*, 3501-3507.

Gorbatyuk, B., and Marczynski, G.T. (2001). Physiological consequences of blocked Caulobacter crescentus dnaA expression, an essential DNA replication gene. MolMicrobiol *40*, 485-497.

Gorbatyuk, B., and Marczynski, G.T. (2005). Regulated degradation of chromosome replication proteins DnaA and CtrA in Caulobacter crescentus. MolMicrobiol *55*, 1233-1245.

Grunenfelder, B., Rummel, G., Vohradsky, J., Roder, D., Langen, H., and Jenal, U. (2001). Proteomic analysis of the bacterial cell cycle. ProcNatlAcadSciUSA *98*, 4681-4686.

Hallez, R., Bellefontaine, A.F., Letesson, J.J., and De Bolle, X. (2004). Morphological and functional asymmetry in alpha-proteobacteria. Trends in Microbiology *12*, 361-365.

Harry, E.J. (2001). Bacterial cell division: regulating Z-ring formation. MolMicrobiol *40*, 795-803.

Hecht, G.B., Lane, T., Ohta, N., Sommer, J.M., and Newton, A. (1995). An essential single domain response regulator required for normal cell division and differentiation in Caulobacter crescentus. EMBO J *14*, 3915-3924.

Hecht, G.B., and Newton, A. (1995). Identification of a novel response regulator required for the swarmer-to-stalked-cell transition in Caulobacter crescentus. JBacteriol *177*, 6223-6229.

Hillson, N.J., Hu, P., Andersen, G.L., and Shapiro, L. (2007). Caulobacter crescentus as a whole cell uranium biosensor. Appl Environ Microbiol.

Hinz, A.J., Larson, D.E., Smith, C.S., and Brun, Y.V. (2003). The Caulobacter crescentus polar organelle development protein PodJ is differentially localized and is required for polar targeting of the PleC development regulator. Molecular Microbiology *47*, 929-941.

Holtzendorff, J., Hung, D., Brende, P., Reisenauer, A., Viollier, P.H., McAdams, H.H., and Shapiro, L. (2004). Oscillating global regulators control the genetic circuit driving a bacterial cell cycle. Science *304*, 983-987.

Holtzendorff, J., Reinhardt, J., and Viollier, P.H. (2006). Cell cycle control by oscillating regulatory proteins in Caulobacter crescentus. Bioessays *28*, 355-361.

Hottes, A.K., Shapiro, L., and McAdams, H.H. (2005). DnaA coordinates replication initiation and cell cycle transcription in Caulobacter crescentus. MolMicrobiol *58*, 1340-1353.

Hung, D.Y., and Shapiro, L. (2002). A signal transduction protein cues proteolytic events critical to Caulobacter cell cycle progression. ProcNatlAcadSciUSA *99*, 13160-13165.

Iniesta, A.A., McGrath, P.T., Reisenauer, A., McAdams, H.H., and Shapiro, L. (2006). A phospho-signaling pathway controls the localization and activity of a protease complex critical for bacterial cell cycle progression. ProcNatlAcadSciUSA *103*, 10935-10940.

Jacobs, C., Ausmees, N., Cordwell, S.J., Shapiro, L., and Laub, M.T. (2003). Functions of the CckA histidine kinase in Caulobacter cell cycle control. MolMicrobiol *47*, 1279-1290.

Jacobs, C., Domian, I.J., Maddock, J.R., and Shapiro, L. (1999). Cell cycle-dependent polar localization of an essential bacterial histidine kinase that controls DNA replication and cell division. Cell *97*, 111-120.

Jacobs, C., Hung, D., and Shapiro, L. (2001). Dynamic localization of a cytoplasmic signal transduction response regulator controls morphogenesis during the Caulobacter cell cycle. ProcNatlAcadSciUSA *98*, 4095-4100.

Jenal, U. (2000). Signal transduction mechanisms in Caulobacter crescentus development and cell cycle control. Fems Microbiology Reviews *24*, 177-191.

Jenal, U., and Fuchs, T. (1998). An essential protease involved in bacterial cell-cycle control. EMBO J *17*, 5658-5669.

Judd, E.M., Ryan, K.R., Moerner, W.E., Shapiro, L., and McAdams, H.H. (2003). Fluorescence bleaching reveals asymmetric compartment formation prior to cell division in Caulobacter. ProcNatlAcadSciUSA *100*, 8235-8240.

Justesen, U.S., Holt, H.M., Thiesson, H.C., Blom, J., Nielsen, X.C., Dargis, R., Kemp, M., and Christensen, J.J. (2007). Report of the first human case of Caulobacter sp infection. Journal of Clinical Microbiology *45*, 1366-1369.

Kohn, K.W., and Pommier, Y. (2005). Molecular interaction map of the p53 and Mdm2 logic elements, which control the Off-On switch of p53 in response to DNA damage. Biochemical and biophysical research communications *331*, 816-827.

Lam, H., Matroule, J.Y., and Jacobs-Wagner, C. (2003). The asymmetric spatial distribution of bacterial signal transduction proteins coordinates cell cycle events. Developmental Cell *5*, 149-159.

Laub, M.T., Chen, S.L., Shapiro, L., and McAdams, H.H. (2002). Genes directly controlled by CtrA, a master regulator of the Caulobacter cell cycle. Proceedings of the National Academy of Sciences of the United States of America *99*, 4632-4637.

Laub, M.T., McAdams, T.H., Feldblyum, T., Fraser, C.M., and Shapiro, L. (2000). Global analysis of the genetic network controlling a bacterial cell cycle. Science *290*, 2144-2148.

Li, S., Brazhnik, P., Sobral, B., and Tyson, J.J. (2008). A quantitative study of the division cycle of Caulobacter crescentus stalked cells. PLoS Comput Biol *4*, e9.

Ma, X., Sun, Q., Wang, R., Singh, G., Jonietz, E.L., and Margolin, W. (1997). Interactions between heterologous FtsA and FtsZ proteins at the FtsZ ring. J Bacteriol *179*, 6788-6797.

Marczynski, G.T., and Shapiro, L. (1992). Cell-Cycle Control of A Cloned Chromosomal Origin of Replication from Caulobacter-Crescentus. Journal of Molecular Biology *226*, 959-977.

Marczynski, G.T., and Shapiro, L. (2002). Control of chromosome replication in Caulobacter crescentus. Annual Review of Microbiology *56*, 625-656.

Margolin, W. (2006). Bacterial division: another way to box in the ring. CurrBiol *16*, R881-R884.

Margolin, W., Bramhill, D., and Long, S.R. (1995). The dnaA gene of Rhizobium meliloti lies within an unusual gene arrangement. JBacteriol *177*, 2892-2900.

Margolin, W., Corbo, J.C., and Long, S.R. (1991). Cloning and characterization of a Rhizobium meliloti homolog of the Escherichia coli cell division gene ftsZ. J Bacteriol *173*, 5822-5830.

Margolin, W., and Long, S.R. (1994). Rhizobium meliloti contains a novel second homolog of the cell division gene ftsZ. J Bacteriol *176*, 2033-2043.

Martin, M.E., Trimble, M.J., and Brun, Y.V. (2004). Cell cycle-dependent abundance, stability and localization of FtsA and FtsQ in Caulobacter crescentus. MolMicrobiol *54*, 60-74.

Matroule, J.Y., Lam, H., Burnette, D.T., and Jacobs-Wagner, C. (2004). Cytokinesis monitoring during development: Rapid pole-to-pole shuttling of a signaling protein by localized kinase and phosphatase in Caulobacter. Cell *118*, 579-590.

McAdams, H. (2005). Personal communication.

McAdams, H.H., and Arkin, A. (1998). Simulation of prokaryotic genetic circuits. AnnuRevBiophysBiomolStruct *27*, 199-224.

McAdams, H.H., and Shapiro, L. (2003). A bacterial cell-cycle regulatory network operating in time and space. Science *301*, 1874-1877.

McGrath, P.T., Iniesta, A.A., Ryan, K.R., Shapiro, L., and McAdams, H.H. (2006). A dynamically localized protease complex and a polar specificity factor control a cell cycle master regulator. Cell *124*, 535-547.

McGrath, P.T., Viollier, P., and McAdams, H.H. (2004). Setting the pace: mechanisms tying Caulobacter cell-cycle progression to macroscopic cellular events. CurrOpinMicrobiol *7*, 192-197.

Milo, R., Shen-Orr, S., Itzkovitz, S., Kashtan, N., Chklovskii, D., and Alon, U. (2002). Network motifs: simple building blocks of complex networks. Science *298*, 824-827.

Mohl, D.A., Easter, J., and Gober, J.W. (2001). The chromosome partitioning protein, ParB, is required for cytokinesis in Caulobacter crescentus. Molecular Microbiology *42*, 741-755.

Mohl, D.A., and Gober, J.W. (1997). Cell cycle-dependent polar localization of chromosome partitioning proteins in Caulobacter crescentus. Cell *88*, 675-684.

Nierman, W.C., Feldblyum, T.V., Laub, M.T., Paulsen, I.T., Nelson, K.E., Eisen, J.A., Heidelberg, J.F., Alley, M.R., Ohta, N., Maddock, J.R., *et al.* (2001). Complete genome sequence of Caulobacter crescentus. ProcNatlAcadSciUSA *98*, 4136-4141.

Novak, B., and Tyson, J.J. (2004). A model for restriction point control of the mammalian cell cycle. Journal of theoretical biology *230*, 563-579.

Ohta, N., Ninfa, A.J., Allaire, A., Kulick, L., and Newton, A. (1997). Identification, characterization, and chromosomal organization of cell division cycle genes in Caulobacter crescentus. JBacteriol *179*, 2169-2180.

Osteras, M., Stotz, A., Schmid, N.S., and Jenal, U. (1999). Identification and transcriptional control of the genes encoding the Caulobacter crescentus ClpXP protease. JBacteriol *181*, 3039-3050.

Poindexter, J.S., and Hagenzieker, J.G. (1981). Constriction and septation during cell division in caulobacters. CanJMicrobiol *27*, 704-719.

Pomerening, J.R., Kim, S.Y., and Ferrell, J.E., Jr. (2005). Systems-level dissection of the cell-cycle oscillator: bypassing positive feedback produces damped oscillations. Cell *122*, 565-578.

Qu, Z., Weiss, J.N., and MacLellan, W.R. (2003). Regulation of the mammalian cell cycle: a model of the G1-to-S transition. American journal of physiology *284*, C349-364.

Quardokus, E., Din, N., and Brun, Y.V. (1996). Cell cycle regulation and cell type-specific localization of the FtsZ division initiation protein in Caulobacter. Proceedings of the National Academy of Sciences of the United States of America *93*, 6314-6319.

Quon, K.C., Marczynski, G.T., and Shapiro, L. (1996). Cell cycle control by an essential bacterial two-component signal transduction protein. Cell *84*, 83-93.

Quon, K.C., Yang, B., Domian, I.J., Shapiro, L., and Marczynski, G.T. (1998). Negative control of bacterial DNA replication by a cell cycle regulatory protein that binds at the chromosome origin. Proceedings of the National Academy of Sciences of the United States of America *95*, 120-125.

Radhakrishnan, S.K., Thanbichler, M., and Viollier, P.H. (2008). The dynamic interplay between a cell fate determinant and a lysozyme homolog drives the asymmetric division cycle of Caulobacter crescentus. Genes Dev *22*, 212-225.

Reisenauer, A., Kahng, L.S., McCollum, S., and Shapiro, L. (1999). Bacterial DNA methylation: a cell cycle regulator? JBacteriol *181*, 5135-5139.

Reisenauer, A., and Shapiro, L. (2002). DNA methylation affects the cell cycle transcription of the CtrA global regulator in Caulobacter. EMBO J *21*, 4969-4977.

Reisinger, S.J., Huntwork, S., Viollier, P.H., and Ryan, K.R. (2007). DivL performs critical cell cycle functions in Caulobacter crescentus independent of kinase activity. J Bacteriol.

Ryan, K.R., Huntwork, S., and Shapiro, L. (2004). Recruitment of a cytoplasmic response regulator to the cell pole is linked to its cell cycle-regulated proteolysis. ProcNatlAcadSciUSA *101*, 7415-7420.

Ryan, K.R., and Shapiro, L. (2003). Temporal and spatial regulation in prokaryotic cell cycle progression and development. AnnuRevBiochem *72*, 367-394.

Sackett, M.J., Kelly, A.J., and Brun, Y.V. (1998). Ordered expression of ftsQA and ftsZ during the Caulobacter crescentus cell cycle. MolMicrobiol *28*, 421-434.

Sha, W., Moore, J., Chen, K., Lassaletta, A.D., Yi, C.S., Tyson, J.J., and Sible, J.C. (2003). Hysteresis drives cell-cycle transitions in Xenopus laevis egg extracts. Proc Natl Acad Sci U S A *100*, 975-980.

Shapiro, L., McAdams, H.H., and Losick, R. (2002). Generating and exploiting polarity in bacteria. Science *298*, 1942-1946.

Sible, J.C., and Tyson, J.J. (2007). Mathematical modeling as a tool for investigating cell cycle control networks. Methods *41*, 238-247.

Siegal-Gaskins, D., and Crosson, S. (2008). Tightly-Regulated and Heritable Division Control in Single Bacterial Cells. Biophys J.

Skerker, J.M., and Laub, M.T. (2004). Cell-cycle progression and the generation of asymmetry in Caulobacter crescentus. NatRevMicrobiol *2*, 325-337.

Stephens, C. (2004). Prokaryotic development: a new player on the cell cycle circuit. CurrBiol *14*, R505-R507.

Stephens, C., Reisenauer, A., Wright, R., and Shapiro, L. (1996). A cell cycle-regulated bacterial DNA methyltransferase is essential for viability. ProcNatlAcadSciUSA *93*, 1210-1214.

Stephens, C.M., Zweiger, G., and Shapiro, L. (1995). Coordinate Cell-Cycle Control of A Caulobacter Dna Methyltransferase and the Flagellar Genetic Hierarchy. Journal of Bacteriology *177*, 1662-1669.

Sveiczer, A., Tyson, J.J., and Novak, B. (2004). Modelling the fission yeast cell cycle. Briefings in functional genomics & proteomics *2*, 298-307.

Swat, M., Kel, A., and Herzel, H. (2004). Bifurcation analysis of the regulatory modules of the mammalian G1/S transition. Bioinformatics (Oxford, England) *20*, 1506-1511.

Thanbichler, M., and Shapiro, L. (2006). MipZ, a spatial regulator coordinating chromosome segregation with cell division in Caulobacter. Cell *126*, 147-162.

Thornton, B.R., Chen, K.C., Cross, F.R., Tyson, J.J., and Toczyski, D.P. (2004). Cycling without the cyclosome: modeling a yeast strain lacking the APC. Cell cycle (Georgetown, Tex *3*, 629-633.

Tyson, J.J., Chen, K., and Novak, B. (2001). Network dynamics and cell physiology. NatRevMolCell Biol *2*, 908-916.

Viollier, P.H., Sternheim, N., and Shapiro, L. (2002). A dynamically localized histidine kinase controls the asymmetric distribution of polar pili proteins. EMBO J *21*, 4420-4428.

Wagner, J., Brun, Y.V., Vicente, M., Tamames, J., Valencia, A., and Mingorance, J. (2004). Regulation and utilization of cell division for bacterial cell differentiation. In Molecules in Time and Space: Bacterial Shape, Division and Phylogeny (New York, Kluwer Academic/Plenum Publishers), pp. 103-132.

Wheeler, R.T., and Shapiro, L. (1999). Differential localization of two histidine kinases controlling bacterial cell differentiation. MolCell *4*, 683-694.

Williams, K.P., Sobral, B.W., and Dickerman, A.W. (2007). A robust species tree for the alphaproteobacteria. J Bacteriol *189*, 4578-4586.

Wortinger, M., Sackett, M.J., and Brun, Y.V. (2000). CtrA mediates a DNA replication checkpoint that prevents cell division in Caulobacter crescentus. Embo Journal *19*, 4503-4512.

Wright, R., Stephens, C., and Shapiro, L. (1997). The CcrM DNA methyltransferase is widespread in the alpha subdivision of proteobacteria, and its essential functions are conserved in Rhizobium meliloti and Caulobacter crescentus. Journal of Bacteriology *179*, 5869-5877.

Wright, R., Stephens, C., Zweiger, G., Shapiro, L., and Alley, M.R.K. (1996). Caulobacter Lon protease has a critical role in cell-cycle control of DNA methylation. Genes & Development *10*, 1532-1542.

Wu, J.G., Ohta, N., Zhao, J.L., and Newton, A. (1999). A novel bacterial tyrosine kinase essential for cell division and differentiation. Proceedings of the National Academy of Sciences of the United States of America *96*, 13068-13073.

Zweiger, G., Marczynski, G., and Shapiro, L. (1994). A Caulobacter DNA methyltransferase that functions only in the predivisional cell. JMolBiol *235*, 472-485.

Zweiger, G., and Shapiro, L. (1994). Expression of Caulobacter-Dnaa As A Function of the Cell-Cycle. Journal of Bacteriology *176*, 401-408.